Award Number: W81XWH-08-2-0018

TITLE: "Brain Vulnerability to Repeated Blast Overpressure and Polytrauma"

PRINCIPAL INVESTIGATOR: Joseph B. Long, PhD

CONTRACTING ORGANIZATION: The Geneva Foundation
Tacoma, WA 98402

REPORT DATE: November 2014

TYPE OF REPORT: Annual

PREPARED FOR: U.S. Army Medical Research and Materiel Command
Fort Detrick, Maryland 21702-5012

REPORT DOCUMENTATION PAGE

Form Approved
OMB No. 0704-0188

1. REPORT DATE	2. REPORT TYPE	3. DATES COVERED
November 2014	Annual	1 Nov 2013 - 31 Oct 2014

4. TITLE AND SUBTITLE

"Brain Vulnerability to Repeated Blast Overpressure and Polytrauma"

5a. CONTRACT NUMBER

5b. GRANT NUMBER
W81XWH-08-2-0018

5c. PROGRAM ELEMENT NUMBER

6. AUTHOR(S)

Joseph B. Long, Ph.D.

E-Mail: joseph.b.long.civ@mail.mil

5d. PROJECT NUMBER

5e. TASK NUMBER

5f. WORK UNIT NUMBER

7. PERFORMING ORGANIZATION NAME(S) AND ADDRESS(ES) AND ADDRESS(ES)

The Geneva Foundation
917 Pacific Ave, Suite 600
Tacoma, WA 98402

8. PERFORMING ORGANIZATION REPORT NUMBER

9. SPONSORING / MONITORING AGENCY NAME(S) AND ADDRESS(ES)
U.S. Army Medical Research and Materiel Command
Fort Detrick, Maryland 21702-5012

10. SPONSOR/MONITOR'S ACRONYM(S)

11. SPONSOR/MONITOR'S REPORT NUMBER(S)

12. DISTRIBUTION / AVAILABILITY STATEMENT
Approved for Public Release; Distribution Unlimited

13. SUPPLEMENTARY NOTES

14. ABSTRACT

It is likely that the mild TBI and cognitive impairments observed among many of the troops returning from OIF and OEF result from repeated exposures to blast overpressure. Although the clinical symptoms of concussion are typically transient, there is both a cumulative risk for persistent damage due to repeated concussions, and a post-concussion period of greatest vulnerability to a second impact. Specific risk assessments and guidelines should be established for exposure to blast overpressure. We are using a preclinical model of blast overpressure in rats to investigate the cumulative effects of multiple blast exposures on neurologic status, neurobehavioral function, and brain histopathological endpoints. Repeated exposures to blast overpressure with varied inter-blast intervals are used to characterize and define the temporal window of brain vulnerability to repeated blast overpressure. We anticipate that these data will provide a critical first step in establishing rational risk guidelines and developing mitigation strategies.

15. SUBJECT TERMS
Traumatic Brain Injury (TBI), blast exposure, blast overpressure

16. SECURITY CLASSIFICATION OF:			17. LIMITATION OF ABSTRACT	18. NUMBER OF PAGES	19a. NAME OF RESPONSIBLE PERSON
a. REPORT	b. ABSTRACT	c. THIS PAGE			USAMRMC
U	U	U	UU	67	19b. TELEPHONE NUMBER *(include area code)*

Standard Form 298 (Rev. 8-98)
Prescribed by ANSI Std. Z39.18

Table of Contents

INTRODUCTION

It is likely that the mild TBI and cognitive impairments observed among many of the troops returning from OIF and OEF result from repeated exposures to blast overpressure. Although the clinical symptoms of concussion are typically transient, mild concussive brain injury can also result in persistent alterations in cognitive and emotional status. Based upon observations among athletes in contact sports, there is both a cumulative risk for persistent damage due to repeated concussions, and a post-concussion period of greatest vulnerability to a second impact, which may elicit subdural hematoma, vasospasm, brain swelling, elevated intracranial pressure, and occasionally death. Specific guidelines have been developed and periodically revised to establish when an athlete can resume their sport, based upon concussion severity and number. Similar risk assessments and guidelines should be established for exposure to blast overpressure.

We are using a preclinical model of blast overpressure in rats to investigate the cumulative effects of multiple blast exposures on neurologic status, neurobehavioral function, and brain histopathological endpoints. Repeated exposures to blast overpressure with varied inter-blast intervals are used to characterize and define the temporal window of brain vulnerability to repeated blast overpressure. Along with vestibulomotor assessments on a rotating pole, spatial learning and memory is assessed using the Morris water maze (MWM) on days 1-10 post-BOP. Following training, latencies to find the submerged platform are recorded along with swim patterns while doing so. Following injury, the platform is repositioned to a new location on each test day to increase the challenge of the test and its sensitivity to distinguish impairments. Brains are then prepared for histopathological analysis to establish the extent of brain injury and to determine whether the brain injury severity increases with repeated exposure to blast, and diminishes with increased inter-blast overpressure (BOP) intervals. We anticipate that these data will provide a critical first step in establishing rational risk guidelines and developing mitigation strategies.

BODY

Overview

An air-driven shock tube is used to simulate BOP and study the cumulative effects of repeated blast exposures on neurological status, neurobehavioral function, visual acuity, and brain histopathological endpoints. Varied inter-BOP intervals are used to identify the temporal window of brain vulnerability to repeated BOP. We failed to consistently observe the hypothesized vulnerabilities and associated worsened outcomes with blast overpressure exposures repeated with 1, 3, or 5 day intervals as was proposed in the initial statement of work. From our own ongoing observations in related projects, and from discussions with other investigators, we conclude that the hypothesized vulnerabilities and worsened outcomes will be readily apparent with the outcome measures we are employing, but require much shorter interblast intervals.

Consequently, we revised our milestones to expose rats to repeated blasts separated by 1, 4, or 24 h intervals. Furthermore, since beginning this project, we discovered that injury-induced deficits are often more pronounced at later stages (e.g. >30 days post-injury) than acutely (e.g. < 14 days post-injury) (Kovesdi et al., 2011). Consequently, we plan to extend our post-injury evaluations over a longer timeframe. In addition to neurobehavioral assessments, EEG is telemetrically recorded pre- and post-BOP to distinguish electrophysiological consequences of blast and repeated blast. EEG evaluations were initially focused on analysis and quantification of seizures and epileptiform activity which are seen prominently in other preclinical models of TBI. Although they were occasionally detected immediately after blast exposure, seizures were neither prominent nor persistent in this injury model, so different EEG parameters have been established to better capture disruptions resulting from blast.

Over the course of this project, modifications in blast exposure conditions were implemented to improve the fidelity of blast simulation in the cylindrical shock tube. In particular, artefactual biomechanical loading associated with end jet effects were eliminated along uncontrolled acceleration and displacement occurring with limited movement restriction. Nevertheless, we have learned that cylindrical shock tubes are inherently and universally limited for blast simulation. Notably, in the absence of an end wave eliminator, negative phase and recompression waves are artefacts of the rarefaction from the end of the open tube and the secondary shock is moving in the reverse direction (upstream not downstream). Additionally, without a reflection eliminator, waves reverberate throughout the length of the tube after the passage of the initial shock front (Ritzel et al., 2011). Finally, rather than the sharp peak positive pressures associated with the Friedlander waveform, cylindrical shock tubes typically produce plateau or flat-top waveforms with relatively long durations (6-12 msec).

With a divergent transition section and an end wave eliminator, a recently acquired advanced blast simulator (ABS) eliminates these artefacts along with the positional heterogeneity in pressures and flow conditions encountered in cylindrical shock tubes (Ritzel et al., 2011). In the ABS (fig 1), positive pressure durations can be reduced to 1-2 msec, which may better represent waveforms resulting from IEDs. We strongly believe that it is important to perform several key experiments using the new ABS to confirm results, particularly since the flow conditions are quite different between the two devices (fig 2) and the means by which rats were secured in the old shock tube and exposed to blast overpressure evolved substantially over the duration of the project as we became more aware of the impact of set-up variables on experimental measures and outcomes. Confirmation of results obtained with the cylindrical shock tube by blast simulations in the ABS will validate the findings and also provide valuable insights for their interpretation. As noted previously, bad blast simulations have confounded much of the preclinical biomedical blast literature to date, and we strongly desire to correct that situation.

Task 1: Using rats pretrained on neurological and neurobehavioral procedures, determine if re-exposure to a mild BOP 24 hrs following the first BOP exposure significantly worsens acute physiological responses, visual acuity, and neurobehavioral and histopathological outcome measures relative to those seen in shams and in single insult subjects.

No additional animal experiments were performed during this reporting period as we prepared to confirm results using the advanced blast simulator (fig 1). An animal use protocol was written to conduct these experiments and to evaluate rats with shortened interblast intervals. Neurobiological and neurochemical analyses were performed using previously collected tissue samples. In addition, analyses of telemetric EEG recordings have shifted from detection of post-traumatic seizure activity, which proved to be infrequent and variable, to longer-term spectral shifts to monitor for other EEG anomalies over a more prolonged timeframe.

Ongoing light microscopic evaluations continue to reveal that neuropathological changes resulting from a single BOP exposure are modest and largely consist of limited fiber degeneration that is evident in silver-stained sections and is most prominent in the cerebellum, optic tracts, and in the internal capsule. Collaborative DTI imaging of brains exposed to BOP has corroborated the light microscopic observations and has provided a powerful tool to comprehensively and quantitatively compare these subtle neuropathological features across treatment groups.

Task 2: Determine if vulnerability to worsened outcome diminishes with the inter-BOP interval extended to 3 days.

Not initiated due to the absence of worsened outcome with a 1 day inter-BOP interval. New inter-BOP intervals have been defined to evaluate vulnerabilities at 4 h post-blast.

Task 3: Determine if vulnerability to worsened outcome diminishes with the inter-BOP interval extended to 5 days.

Not initiated due to the absence of worsened outcome with a 1 day inter-BOP interval. New inter-BOP intervals have been defined to evaluate vulnerabilities at 24 h post-blast.

KEY RESEARCH ACCOMPLISHMENTS

- BOP exposure conditions have been greatly refined to create a high fidelity simulation of blast TBI in the advanced blast simulator to confirm and extend findings generated in a cylindrical shock tube.
- A battery of sensitive neurobehavioral assessments have been carefully developed to distinguish functional disruptions resulting from single or repeated BOP exposures.
- Neuropathological features and neurobiological underpinnings of blast TBI have been carefully assessed in the rodent brain.
- Telemetric EEG recordings have been established to distinguish electrophysiological consequences of single and repeated blast exposures independent of post-traumatic epilepsy.

REPORTABLE OUTCOMES

Based in part upon the work supported by this award, funding was sought through research preproposals and proposals submitted to the CDMRP and DMRP. Two proposals were selected for funding during this reporting period:

"Assessment and Treatment of Blast-Induced Auditory and Vestibular Injuries" was selected for funding as a Clinical Rehabilitative Medicine Research Program (CRMRP) Neurosensory Research Award within the Defense Health Program/Defense Medical Research Development Program.

"Elucidation of Inflammation Processes Exacerbating Neuronal Cell Damage to the Retina and Brain Visual Centers, as a Quest for Therapeutic Drug Targets, in a Rat Model of Blast Over Pressure Wave Exposure" was selected for funding as a CDMRP Clinical and Rehabilitative Medicine Research Program (CRMRP) Vision Research Program - Hypothesis Development Award.

Presentations:

P. Arun, R. Abu-Taleb, S. Oguntayo, A. Edwards, C. Riccio, S. VanAlbert, I. Gist, Y. Wang, M.P. Nambiar, J.B. Long. Tissue non-specific alkaline phosphatase in the etiology of tauopathy and chronic traumatic encephalopathy after traumatic brain injury. USUHS Research Day held at Bethesda, MD – May 13, 2013

Y. Wang, Y Wei, L. Tang, Oguntayo, A. Edwards, C. Riccio, I. Gist, P. Arun, Van Albert and J. Long. Comparison of Combined Primary and Tertiary Blast Traumatic Brain Injury in Young and Middle Age Rats. Military Health Sciences Research Symposium (MHSRS), Fort Lauderdale, FL, August 2013.

P. Arun, R. Abu-Taleb, S. Oguntayo, A. Edwards, C. Riccio, S. VanAlbert, I. Gist, Y. Wang, M.P. Nambiar, J.B. Long. Tissue non-specific alkaline phosphatase in the etiology and diagnosis of tauopathy and chronic traumatic encephalopathy. Advanced Technology Applications for Combat Casualty Care / Military Health Sciences Research Symposium (ATACCC / MHSRS), Fort Lauderdale, FL, – August 2013

J. DeMar - Exposure to Primary Blast Waves Causes Traumatic Injury to the Visual System, in Rats. MHSRS meeting, held in Ft. Lauderdale, FL on 12 -15 August, 2013.

P. Arun, D. Wilder, A. Edwards, Y. Wang, I. Gist, J. B. Long. Blast exposure phosphorylates Tau preferentially at serine396, which can trigger Alzheimer's-like pathology. National Neurotrauma Symposium held at San Francisco, CA- July 2014

James C. DeMar, Stephen A. VanAlbert, Miya I. Hill, Robert B. Gharavi, Joseph R. Andrist, Andrea A. Edwards, Cory A. Riccio, and Joseph B. Long. Exposure to Primary Blast Waves Causes Traumatic Injury to the Visual System, in Rats. 32nd National Neurotrauma Society Symposium; San Francisco CA, held on June 29th - July 2nd, 2014.

Keith M. Sharrow, James C. DeMar, Miya I. Hill, Andrea A. Edwards, Joseph B. Long, and Thomas G. Oliver. Characterization of a Blast-Induced Brain and Eye Injury Model in Rats. National Capital Area Traumatic Brain Injury Research Symposium; NIH - Bethesda MD, held on March 3rd - 4th, 2014.

Ying Wang, Yanling Wei, Lawrence Tong, Peethambaran Arun, Andrea Edwards, Samuel Oguntayo, Irene Gist and Joseph B. Long. Characterization of Blast-

Induced Vestibular Injury in Rats. The Annual Symposium for Neurotrauma Society San Francisco, CA June 2014

Publications

Ahmed, F.A., Kamnaksh, A., Kovesdi, E., Long, J.B., Agoston, D.V. Long-term consequences of single and multiple mild blast exposure on select physiological parameters and blood-based biomarkers. Electrophoresis. 2013 Aug; 34(15):2229-33.

Arun, P., Abu-Taleb, R., Oguntayo, S., Wang, Y., Valiyaveettil, M., Long, J.B., Nambiar, M.P. Acute mitochondrial dysfunction after blast exposure: potential role of mitochondrial glutamate oxaloacetate transaminase. J Neurotrauma. 2013 Oct 1; 30(19):1645-51.

Arun, P., Abu-Taleb, R., Valiyaveettil, M., Wang, Y., Long, J.B., Nambiar, M.P. Extracellular cyclophilin A protects against blast-induced neuronal injury. Neurosci Res. 2013 May-Jun; 76(1-2):98-100.

Arun. P, Abu-Taleb. R, Oguntayo, S., Wang, Y., Valiyaveettil, M., Long, J.B., Nambiar, M.P. Distinct patterns of expression of traumatic brain injury biomarkers after blast exposure: Role of compromised cell membrane integrity. Neuroscience Letters. 2013 Sept 27; 552: 87-91.

Ahmed FA, Kamnaksh A, Kovesdi E, Long JB, Agoston DV. Long-term consequences of single and multiple mild blast exposure on select physiological parameters and blood-based biomarkers. Electrophoresis. 2013 Aug;34(15):2229-33. doi: 10.1002/elps.201300077. Epub 2013 Jul 8.

Kamnaksh A, Budde MD, Kovesdi E, Long JB, Frank JA, Agoston DV. Diffusion tensor imaging reveals acute subcortical changes after mild blast-induced traumatic brain injury. Sci Rep. 2014 May 2;4:4809. doi: 10.1038/srep04809.

Calabrese E, Du F, Garman RH, Johnson GA, Riccio C, Tong LC, Long JB. Diffusion tensor imaging reveals white matter injury in a rat model of repetitive blast-induced traumatic brain injury. J Neurotrauma. 2014 May 15;31(10):938-50. doi: 10.1089/neu.2013.3144. Epub 2014 Mar 27.

CONCLUSION

As the result of substantial refinement, under carefully controlled experimental conditions, the biomechanical perturbations of the brain that yield blast-induced mild TBI in injured Warfighters can be recreated with reasonable fidelity to reproduce characteristic sequelae of blast-induced mild TBI. Results to date are consistent with the hypothesis that BOP generates a mild insult to the brain (and other organs as well). With the refined exposure conditions used to date, the severity of these disruptions has not been consistently worsened with repeated blasts with a 24 hr interblast interval. These findings point to a need to alter our experimental plan and examine consequences of BOP repeated with shorter intervals (1, 4, and 24 h). The end-product repeated BOP model will provide an invaluable tool to define underlying neurobiological mechanisms and rationally establish effective guidelines (e.g. return-to-duty) and

countermeasures to lessen short-term impairments as well as chronic debilitation (e.g. chronic traumatic encephalopathy).

REFERENCES

Kovesdi E, Gyorgy AB, Kwon SK, Wingo DL, Kamnaksh A, Long JB, Kasper CE, Agoston DV. The effect of enriched environment on the outcome of traumatic brain injury; a behavioral, proteomics, and histological study. Front Neurosci. 2011 Apr 1;5:42. doi: 10.3389/fnins.2011.00042. eCollection 2011.

Ritzel, D.V., Parks, S.A., Roseveare, J., Rude, G. Sawyer, T., "Experimental Blast Simulation for Injury Studies", NATO/RTO HFM-207 Symposium, Halifax, Canada, 3-5 Oct 2011.

APPENDIX

1. Supporting Data
2. Presentations and Publications

SUPPORTING DATA

Using the cylindrical shock tube, we observed that repeated BOP exposures separated by 24 hrs do not appreciably and consistently worsen outcomes relative to a single BOP exposure, but combined effects are greater when the interblast interval is shortened to 1, 10, or 60 min. These heightened responses to repeated blast exposures were clearly evident using neurobehavioral, neurochemical, and morphological outcome measures and have prompted us to revise our approach to evaluate shifts in vulnerability to a second BOP exposure at 1, 4 and 24 hr intervals.

Fig1. MCP-1 in CSF after repeated blast exposures

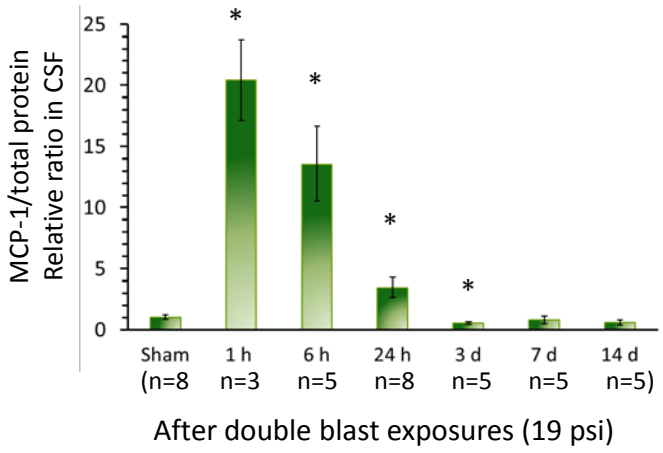

Fig 2. CCL2 in CSF after single or repeated blast exposures

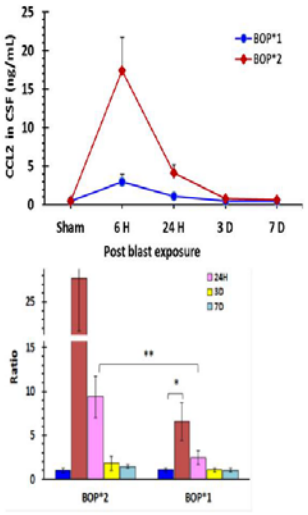

We have established several important neurobiological responses to blast during this reporting period. It is well known that cytokines including chemokines (CC), interferons, interleukins (IL) and tumor necrosis factor (TNF) play crucial roles in inflammatory development. Chemokine ligand 2 (CCL2) exhibits a chemotactic activity for monocytes and basophils. It is primarily secreted by monocytes, macrophages, dendritic cells in peripheral and also expressed by neurons, astrocytes and microglia. CCL2 is also referred to as monocyte chemotactic protein-1 (MCP-1) and small inducible cytokine A2. MCP-1/CCL2 recruits monocytes, memory T cells, and dendritic cells to the sites of inflammation produced by either tissue injury or infection.

To explore neuroinflammation after BOP exposures, we have measured changes in levels of MCP-1 in CSF, plasma and brain tissue, and we see sizeable increases that are appreciably larger with two blast exposures than with one (fig 1-3).

Fig 3. Plasma CCL2 changes after blast exposure

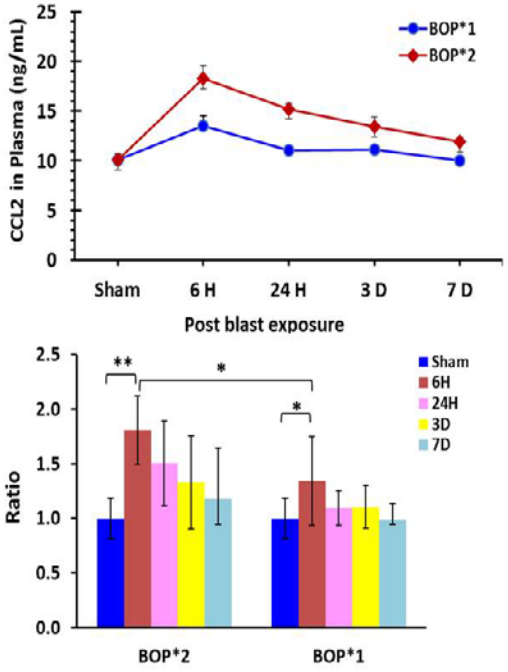

Blast exposure also caused phosphorylation of Tau protein in different brain regions in a time dependent manner. Maximum phosphorylation of Tau proteins occurs at early stages of injury. The phosphorylation of Tau protein was found to increase with repeated blast exposures in many brain regions (fig 4). The degree of phosphorylation of Tau protein after blast exposure varied in different regions of the brain. The phosphorylation of Tau protein at Serine396 was found to be higher than that at Threonine231. The preferential phosphorylation of Tau protein at Serine396 may be playing a role in Alzheimer's-like pathology observed in TBI victims. Blast exposure also results in the accumulation of APP in different brain regions in a time-dependent manner with maximum accumulation at chronic stages (fig 5). Similar to pTau, accumulation of APP was found to increase with the number of blast exposures. Phosphorylation of Tau protein didn't show a positive correlation with the accumulation of APP in different brain regions suggesting a distinct pathological mechanism leading to Alzheimer's-like neuropathology after blast exposure.

Fig 4. Changes in brain pTau after blast exposure

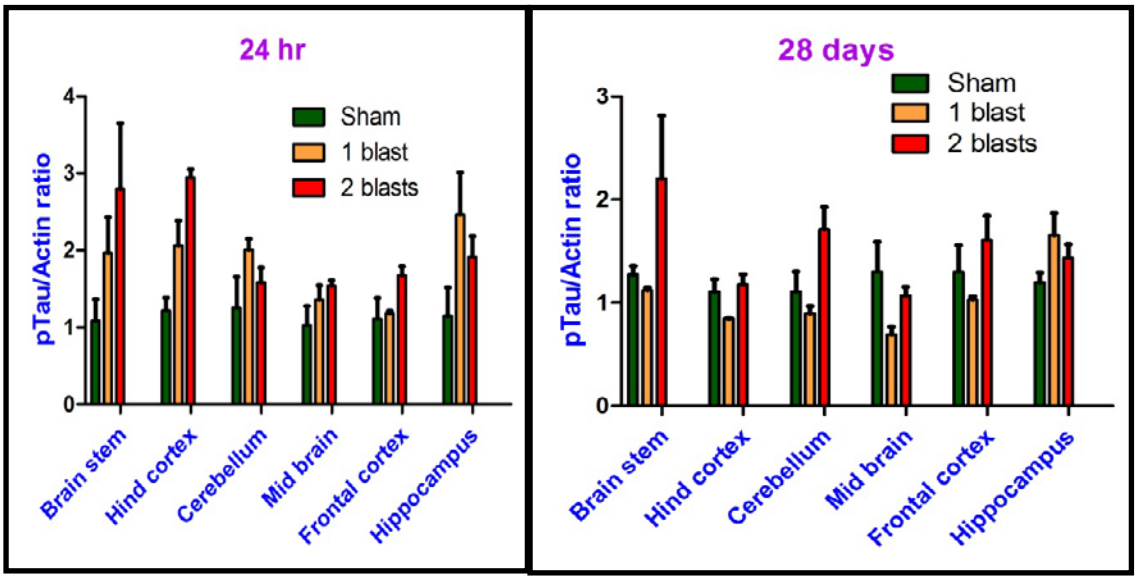

Fig 5. Changes in brain APP after blast exposure

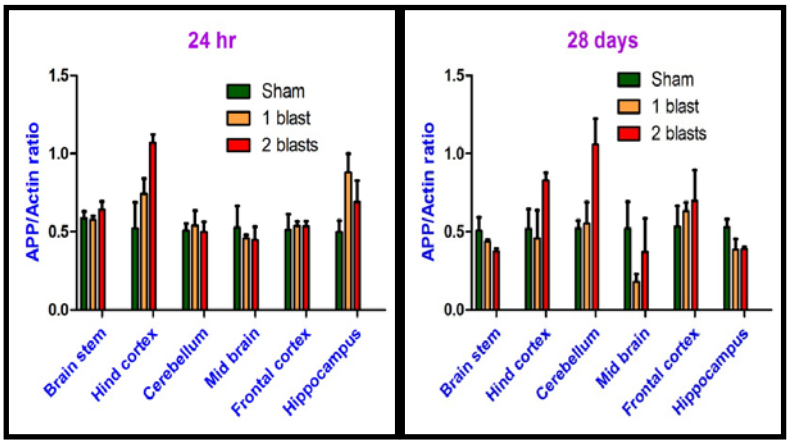

We recently acquired an advanced blast simulator (ABS, fig 6), which generates a high fidelity Friedlander waveforms closely resembling that produced by explosives in the open field. Comparison of these pressure tracings highlights the contrast between the “Friedlander-like” sharp peak positive pressures produced in the

Fig 6. Advanced blast simulator.

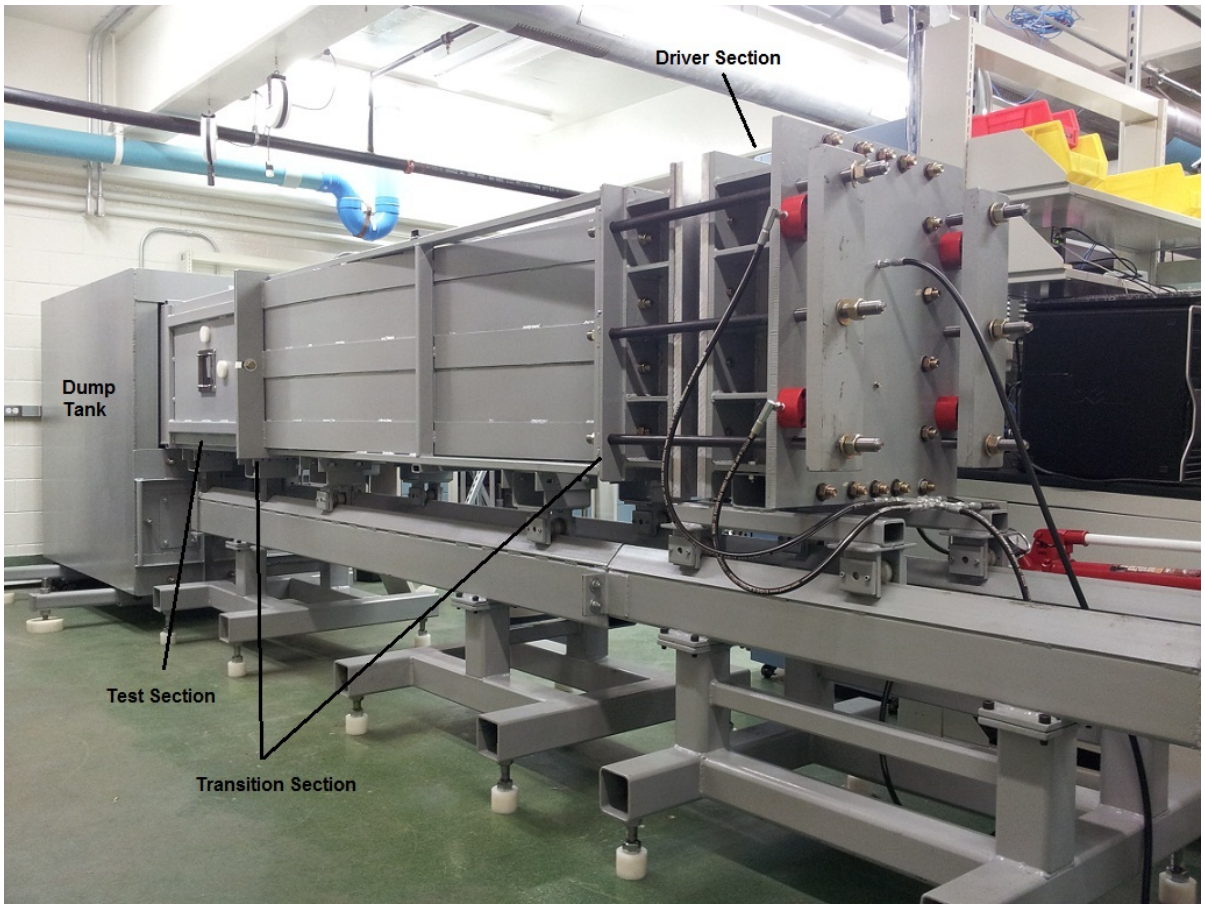

ABS (fig 7) and the plateau waveforms with relatively long durations (6-12 msec) produced in this and other cylindrical shock tubes (fig 8), which will yield unscaled drag forces greatly exceeding those occurring with an explosion in the free field. In addition,

the difference between the total and static pressure recordings (blue vs green tracings in figs 7 and 8) is much less in the ABS than in the cylindrical shock tube. This difference between total and static pressure is the dynamic pressure which gives rise to blast wind resulting from the kinetic energy imparted to the air as it is traversed by the shock wave. In addition to creating a higher fidelity shock wave, the ABS is equipped with optical windows and gauge ports which allow high speed video and pressure recordings to capture the flow conditions and response of the test subject (i.e. translation, acceleration, deformation, etc.).

Fig 7. ABS pressure trace

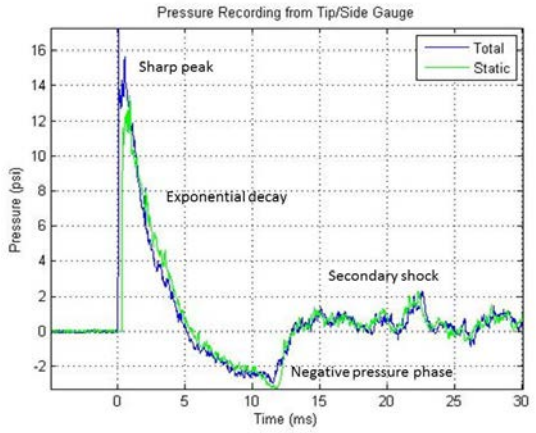

Fig 8. Cylindrical shock tube pressure trace

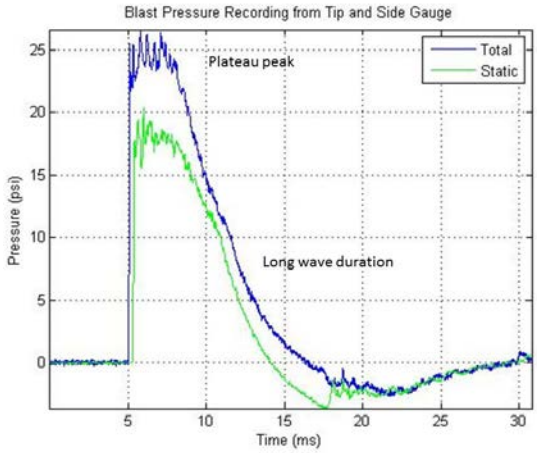

Comparison of Combined Primary and Tertiary Blast Traumatic Brain Injury in Young and Aged Rats

Ying Wang, Yanling Wei, Lawrence Tong, Samuel Oguntayo, Andrea Edwards, Cory Riccio, Irene Gist, Peethambaran Arun, Stephen Van Albert, Joseph B. Long

Blast-Induced Neurotrauma Branch, Center for Military Psychiatry and Neuroscience, Walter Reed Army Institute of Research, Silver Spring, MD 20910

Age-dependent variations in the pathophysiology of blast-induced traumatic brain injury (bTBI) may influence efficacy of therapies for mitigation of damage. Since Warfighters who sustain bTBI are typically exposed to a combination of blast overpressure (BOP) and a biomechanical perturbation related to acceleration and/or impact, BOP and weight drop injury were combined into a dual insult model to compare bTBI in different age rats. Anesthetized 3 and 6 month old rats were exposed to BOP in a shock tube (19 psi total) followed immediately by weight-drop (500 g, 150 cm). Brain and plasma were collected through 14 d postinjury. Axonal degeneration and inflammation were revealed in both groups by silver stained or anti-Iba1 immunostained sections, respectively. MAP2 increased at 6 h post TBI in frontal cortex with both ages, whereas GFAP increased at 6 h and 14 d in older rats but decreased at 6 h in younger rats. Contactin-associated protein-2 increased in older rats at 14 d postinjury, but was unchanged in younger rats. In both age groups, MCP-1 increased in plasma and CSF at 6 h postinjury. Cdc25A and p21 increased in younger rats at 6 h postinjury, whereas only p21 increased in older injured rats. These biomarkers revealed time-dependent brain injury and neuroinflammatory processes which varied by age. They further indicate that the molecular responses directing DNA repair and regulation of cell proliferation after bTBI may also differ in an age-dependent manner.

Characterization of Blast-Induced Vestibular Injury in Rats

Ying Wang, Yanling Wei, Lawrence Tong, Peethambaran Arun, Andrea Edwards, Samuel Oguntayo, Irene Gist and Joseph B. Long

Blast-Induced Neurotrauma Branch, Center for Military Psychiatry and Neuroscience, Walter Reed Army Institute of Research, Silver Spring, MD 20910

Blast exposure is the most common cause of traumatic brain injury (TBI) in warfighters. Nearly 60% of blast TBI victims exhibit hearing loss, tinnitus, dizziness and balance disorders. To date, the etiologies of these injuries are largely undefined. A high fidelity animal model is critical to define the mechanism(s) of injury and develop therapeutic strategies for blast-induced neurobehavioral deficits. In this study, we used an air-driven shock tube to simulate primary blast and investigated the pathological effects of blast exposures on central and peripheral auditory/vestibular systems.

Method: Anesthetized SD rats (male, 350 g) were tautly secured in a transverse prone position 2.5 ft within the mouth of a 1 ft diameter shock tube with the right side facing the oncoming shockwave. Rats were exposed to two closely coupled shockwaves (peak total pressures of 5, 12 or 19 psi) separated by 30 sec. Rats were euthanized at varied intervals (6 h, 24 h, 7 d and 14 d) post injury and tissues underwent histological and RNA analyses.

Results: All rats received rotarod training prior to and testing after blast exposures for evaluation of motor coordination and balance. Compared to a single blast insult, repeated blast exposures significantly impaired motor coordination. Intensity-dependent blast-induced damage to middle and inner ears was evident with no significant differences between left and right ears. Labyrinthine hemorrhage was prominent at 24 h up to 14 days after blast exposure, but was not observed at 6 h post injury. Repeated blast exposures caused significant axonal degeneration and glial cell proliferation in the central vestibular signal processing regions of the brain. Repeated blast exposures also triggered multiple gene expression changes in the inner ear and cerebellum which are associated with DNA repair, neural growth, inflammation and pain. These data indicate that both peripheral and central vestibular systems are vulnerable to blast injuries, and are particularly disrupted by closely coupled repeated blasts. Neuroinflammation, which occurred during the early phase post injury, could be a major factor leading to secondary neuronal damage.

Keywords: Modeling

Indexing Kewords: Blast TBI, Vestibular system, Motor coordination, Pathology, Inflammation

Tissue non-specific alkaline phosphatase in the etiology and diagnosis of tauopathy and chronic traumatic encephalopathy

Peethambaran Arun, Rania Abu-Taleb, Samuel Oguntayo, Andrea Edwards, Cory Riccio, Stephen VanAlbert, Irene Gist, Ying Wang, Madhusoodana P. Nambiar, Joseph B. Long

Blast-Induced Neurotrauma Branch, Center for Military Psychiatry and Neuroscience, Walter Reed Army Institute of Research, Silver Spring, MD 20910

Dephosphorylation of *pTau* is essential for the preservation of neuronal microtubule assemblies and for protection against trauma-induced tauopathy and chronic traumatic encephalopathy (CTE). Tissue non-specific alkaline phosphatase (TNAP) serves this role in the brain by dephosphorylating *pTau*. Paired helical filaments (PHFs) and *Tau* isolated from Alzheimer's disease (AD) patients' brains formed microtubule assemblies with tubulin only after treatment with TNAP or protein phosphatase-2A, 2B and -1, suggesting that *Tau* protein in the PHFs of neurons in AD brain is hyperphosphorylated, which prevents microtubule assembly. Our studies using blast and impact acceleration models of traumatic brain injury in rats revealed *pTau* accumulation in the brain as early as 6 h post-injury and further accumulation by 24 h which varied in different brain regions. The *pTau* accumulation was accompanied by reduced TNAP expression/activity in the brain at 6 h after blast/impact acceleration and the activity remained suppressed through 14 days. Plasma alkaline phosphatase activity also decreased as early as 3 h after these insults and remained low at 14 days. These results reveal that blast/impact acceleration decreases the level/activity of TNAP in the brain, which likely contributes to trauma-induced accumulation of *pTau* and the resultant tauopathy associated with CTE and decreased levels/activities of TNAP in the plasma after brain injury might be useful biomarkers for early diagnosis.

Tissue non-specific alkaline phosphatase in the etiology of tauopathy and chronic traumatic encephalopathy after traumatic brain injury

Peethambaran Arun, Rania Abu-Taleb, Samuel Oguntayo, Andrea Edwards, Cory Riccio, Stephen VanAlbert, Irene Gist, Ying Wang, Madhusoodana P. Nambiar, Joseph B. Long

Blast-Induced Neurotrauma Branch, Center for Military Psychiatry and Neuroscience, Walter Reed Army Institute of Research, Silver Spring, MD 20910

Studies indicate that chronic traumatic encephalopathy (CTE), a *tau* protein-linked neurodegenerative disorder observed in athletes with multiple concussions, shares clinical symptoms and neuropathological characteristics with those seen in victims of blast. Prevention of *Tau* phosphorylation and facilitation of the dephosphorylation of *pTa*u are critical to prevent tauopathy and preserve/restore microtubule assembly. Tissue non-specific alkaline phosphatase (TNAP) serves this major role in the brain by dephosphorylating *pTau*. Paired helical filaments and *Tau* protein isolated from Alzheimer's disease (AD) patients' brains formed microtubule assembly with tubulin *in vitro* only after treatment with TNAP or protein phosphatase-2A, 2B and -1, suggesting that *Tau* protein in the paired helical filaments of neurons in AD brain is hyperphosphorylated which prevents microtubule assembly. TNAP showed higher activity in dephosphorylating *pTau* compared to other protein phosphatases. Our preliminary studies using blast and impact acceleration models of traumatic brain injury (TBI) in rats reveal significant *pTau* accumulation in the brain as early as 6 h post-injury and further increased accumulation by 24 h. The extent of *pTau* accumulation varied in different brain regions after the insults. The *pTau* accumulation was accompanied by reduced TNAP activity, which decreased significantly in the brain at 6 h after blast exposure and/or impact acceleration and remained low through 14 days. Western blotting showed decreased TNAP expression in the brain at 6 h after blast exposure and impact acceleration. Plasma alkaline phosphatase activity also decreased significantly as early as 3 h after these insults and remained low at 14 days. These results reveal that blast exposure/impact acceleration decrease the levels/activity of TNAP in the brain, which likely contributes to accumulation of *pTau* and the resultant tauopathy and CTE. Additionally, decreased levels/activities of TNAP in the cerebrospinal fluid (CSF) and plasma after blast exposure might be useful biomarkers for the early diagnosis of tauopathy/CTE.

Exposure to Primary Blast Waves Causes Traumatic Injury to the Visual System, in Rats

James C. DeMar, Ph.D., Stephen A. VanAlbert, Miya I. Hill, Robert B. Gharavi, Joseph R. Andrist, Andrea A. Edwards, Cory A. Riccio, and Joseph B. Long

Blast-Induced Neurotrauma Branch, Center for Military Psychiatry and Neuroscience, Walter Reed Army Institute of Research, Silver Spring, MD 20910

Blast injury has emerged as arguably the greatest threat to warfighters in current theaters of operation, and is a leading cause of vision loss due to non-penetrating traumatic injuries to the eyes or brain, likely caused by blast shock waves. In light of the difficult lifelong disability that permanent loss of vision represents, we propose there is a dire need to determine the degree of injury occurring specifically to the retina (e.g., photoreceptors) and brain visual processing centers (e.g., optic tracts), as result of exposure to blast waves. Using an adult rat model of blast wave exposure, we have now quantified the cellular and functional damage to the retina and brain, by electroretinography (ERG), visual discrimination behavioral testing, and histopathology. Blast wave injury was carried out by placing rats in a compressed air driven shock tube and exposing them once to a 20 psi (260 Hz) blast over pressure wave. Animals were then assessed at 1, 7, and 14 days post-injury. By 2 weeks out, blasted rats versus shams showed significantly decreased ERG waveform amplitudes, impaired ability to visually discern a cue light of variable intensity to earn food rewards, and severe neuronal cell degeneration within the retina and most brain visual processing centers (H&E and silver stains). Our research is an important contribution to providing the pathophysiological knowledge needed for developing therapies for blast related injuries and to advancing military medicine.

SUPPORT: This work is supported by a USAMRMC/ TATRC Vision Research Program grant award, #: W81XWH-12-2-0082.

Exposure to Primary Blast Waves Causes Traumatic Injury to the Visual System in Rats

[1,2]James C. DeMar, Ph.D., [1,2]Miya I. Hill, [1]Robert B. Gharavi, [1]Joseph R. Andrist, [1]Andrea A. Edwards, [1,2]Cory A. Riccio, [1,2]Stephen A. VanAlbert, and [1]Joseph B. Long

[1]Blast-Induced Neurotrauma Branch, Center for Military Psychiatry and Neuroscience, Walter Reed Army Institute of Research, Silver Spring, MD 20910;
[2]As Contracted Through The Geneva Foundation, Tacoma, WA 98402

Background

Blast injury has emerged as arguably the greatest threat to War fighters in current theaters of operation, and is a leading cause of vision loss due to non-penetrating traumatic injuries to the eyes or brain, likely caused by blast shock waves. In light of the difficult lifelong disability that permanent loss of vision represents, we propose there is a dire need to determine the degree of injury occurring specifically to the retina (e.g., photoreceptors) and brain visual processing centers (e.g., optic tracts), as result of exposure to blast waves. Using an adult rat model of blast wave exposure, we have now quantified the cellular and functional damage to the retina and brain, by electroretinography (ERG), visual discrimination behavioral testing, and histopathology. Blast wave injury was carried out by placing rats in a compressed air driven shock tube and exposing them once to a 20 psi (260 Hz) blast over pressure wave. Animals were then assessed at 1, 7, and 14 days post-injury. By 2 weeks out, blasted rats versus shams showed significantly decreased ERG waveform amplitudes, impaired ability to visually discern a cue light of decreasing intensity to earn food rewards, and severe neuronal cell degeneration within the retina and most brain visual processing centers (H&E and silver stains). Our research is an important contribution to providing the pathophysiological knowledge for developing therapies for blast related injuries and to advancing military medicine.

SUPPORT: USAMRMC / TATRC Vision Research Program grant, award #: W81XWH-12-2-0082.

Introduction

❑ In recent theaters of operation (OIF and OEF), 80% of the neurotrauma cases in U.S. soldiers resulted from attacks using improvised explosive devices (Warden, 2006).

❑ Blast injuries are a leading cause of loss of visual function in War fighters, due to trauma to the eyes and brain visual processing enters (Capó-Aponte, 2012; Cockerham, 2011).

❑ Of these afflicted patients, 43% display closed-eye injuries (Cockerham, 2011).

❑ Of the ocular injuries, 26% involve the retina, consistent with a blast wave displacement of fragile tissues (Cockerham, 2011).

❑ Despite the serious life-long disability loss of vision represents, relatively few animal studies have been done to characterize neurotrauma to the visual system resulting from blast wave exposure (Petras, 2007; Hines-Beard, 2012; Jiang, 2013; Mohan, 2013; and Zou, 2013).

References:

Capó-Aponte et al., 2012; Mil. Med. 177(7): 804-813.
Cockerham et al., 2011; N. Engl. J. Med. 364(22): 2172-2173.
Hines-Beard et al., 2012; Exp. Eye Res. 99: 63-70.
Jiang et al., 2013; J. Neuroinflammation. 10: 96-102.
Mohan et al., 2013; Invest. Ophthalmol. Vis. Sci. 54(5): 3440-3450.
Petras et al., 1997; Toxicology. 121(1): 41-49.
Warden, 2006; J. Head Trauma Rehabil. 21(5): 398-402.
Zou et al., 2013; J. Neuroinflammation. 10: 79-99.

Aim of Study

Rigorously, characterize in rats exposed to high fidelity simulated blast overpressure waves the cellular, neuronal signaling, behavioral pathology of injuries to the eyes – specifically retina – and brain visual processing centers, as by:

1) Electroretinography (ERG).

2) Visual discrimination (operant conditioning).

3) Histopathology (H&E and silver stains).

Materials and Methods

Simulation of Primary Blast Wave Injuries:

❑ Adult male Sprague Dawley rats (6 wk-old) are exposed under isoflurane to blast over pressure waves, in a right-side on orientation, using a compressed air driven shock tube.

❑ Single air blast of ~20 psi is applied to the rat, via rupture of a Mylar membrane of predetermined thickness.

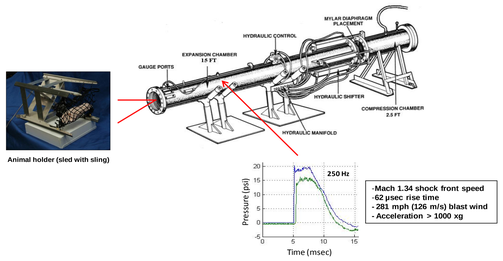

Figure 1. Diagrammatic view of the WRAIR shock tube.

Electroretinography (ERG):

❑ Rats are dark adapted for 5 h; and then kept under red lights.

❑ Under isoflurane, pupils are drug-dilated; and electrodes put on eyes (recording), cheeks (reference), and tail (ground).

❑ Eyes are flashed with light (0.1 – 25 cd.s/m^2; 5 msec); and evoked retina potentials are recorded (a- and b- waveforms).

❑ Tested at baseline (1 d prior) and 1, 7, and 14 d post-blast.

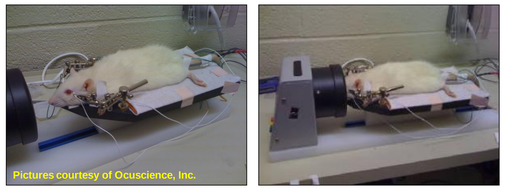

Figure 2. Rat mounted in an ERG instrument (Ocuscience, Inc.).

Visual Discrimination (Operant Conditioning):

❑ Rats are trained in operant conditioning boxes over 7 d to press a lever when a cue light shines to gain food rewards.

❑ Cue light is then varied in brightness (13 random levels) over next 2 d to challenge visual response, as a baseline prior to blast.

❑ Those having a ≥ 60% correct response are continued on.

❑ Retested at 2, 5, 7, 12, and 14 d after blast; and data is reported as total, correct, and incorrect lever responses.

Figure 3. Views of an operant conditioning box (Med Associates, Inc.).

Histopathology (H&E and Silver Stains):

❑ Rats are transcardial perfused with paraformaldehyde; and eyes and brains are removed and then post-fixed.

❑ Tissue samples are submitted (FD Neurotechnologies, Inc.) for processing into H&E (eyes) and silver (brains) stained slides.

❑ Examined under microscope for damage to retina and brain visual processing centers; where H&E stains for general cell morphology (pink to purple) and sliver for axonal fiber tract degeneration (brown to black). Assigned relative damage scores on a scale of 1 – 6.

Results

Electroretinography (ERG):

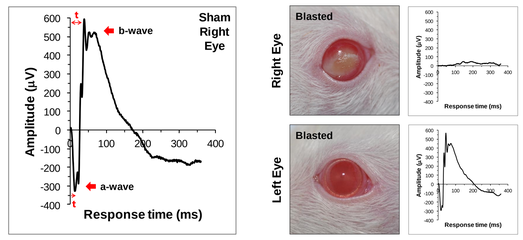

Figure 4. Electroretinogram (ERG) trace showing a- and b-wave responses (1 cd.s/m^2 flash), from retina photoreceptor and bipolar cell neurons, respectively; t = implicit time. Right and left eyes of a rat at 7 d post-blast, as shown along side their respective ERG traces.

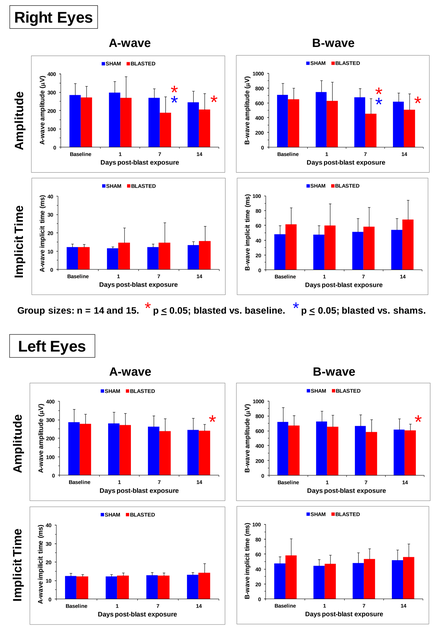

Figure 5. ERG amplitudes and implicit times for a- and b-wave signal responses (3 cd.s/m^2 flash) of sham and blasted rats (right and left eyes) at baseline and 1, 7, and 14 d after exposure. * p ≤ 0.05, for blasted rats vs. their baseline or shams, as determined by t-test.

Visual Discrimination (Operant Conditioning):

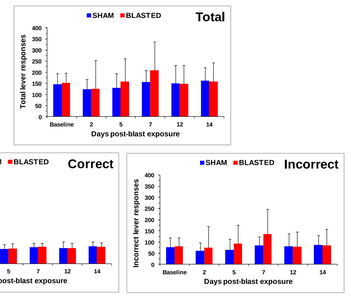

Group sizes: n = 11 and 10. No significant differences.

Figure 6. Visual discrimination test data for total, correct, and incorrect lever responses to a cue light in attempt to gain food rewards, as taken at baseline and 2, 5, 7, 12, and 14 d post-blast.

Histopathology (H&E and Silver Stains):

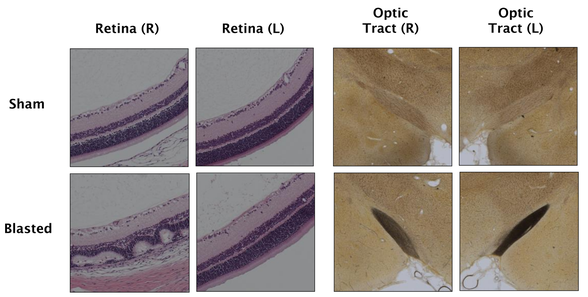

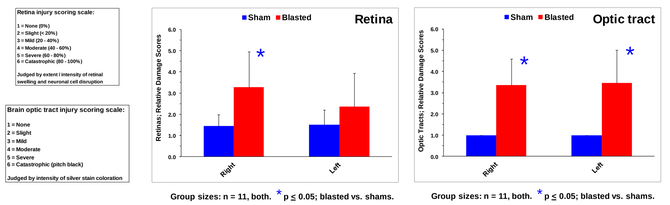

Figure 7. Histopathology of eyes (retina) and brains (optic tract) for sham and blasted rats; H&E and silver stains with relative damage scores, respectively. Magnifications are 4 – 10x. R = right; L = left.

Summary and Conclusions

❑ Blasted rats had significantly lower ERG exam a- and b-wave amplitudes at 7 and 14 d post-exposure, versus their baseline and sham values, which is a clear sign of retinal dysfunction.

❑ Visual discrimination testing showed a trend for the blasted rats to "guess" more for food rewards, over time similar to the ERG results.

❑ Histopathology showed cell damage to be present in the blasted rat retinas (degeneration) and brain optic tracts (axonal shearing).

Characterization of a Blast-Induced Brain and Eye Injury Model in Rats.

Authors: Keith M. Sharrow[1*], James C. DeMar[2*], Miya I. Hill[2], Andrea Edwards[2], Joseph Long[2] , Thomas G. Oliver[1]

[1] Department of Clinical Pharmacology, Walter Reed Army Institute of Research (WRAIR), Silver Spring, MD 20910; [2] Division of Blast Neurotrauma, Center of Excellence for Military Psychiatry and Neurosciences, WRAIR, Silver Spring, MD 20910, *Both authors contributed equally to this work

BACKGROUND

Blast injury has emerged as arguably the greatest threat to War fighters in current theaters of operation, and is a leading cause of vision loss due to non-penetrating traumatic injuries to the eyes or brain, likely caused by blast shock waves. In light of the difficult lifelong disability that permanent loss of vision represents, we propose there is a dire need to determine the degree of injury occurring specifically to the retina (e.g., photoreceptors) and brain visual processing centers (e.g., optic tracts), as result of exposure to blast waves. Using an adult rat model of blast wave exposure, we have now characterized the cellular and functional damage to the retina and brain, by electroretinography (ERG) and histopathology. Blast wave injury was carried out by placing rats in a compressed air driven shock tube and exposing them once to a 20 psi (260 Hz) blast over pressure wave either in a head on or right side head orientation. Animals were then assessed at 1, 7, and 14 days post-injury. By 2 weeks out, blasted rats versus shams showed significantly decreased ERG waveform amplitudes, impaired ability to visually discern a cue light of decreasing intensity to earn food rewards, and severe neuronal cell degeneration within the retina and most brain visual processing centers (H&E and silver stains). Our research is an important contribution to providing the pathophysiological knowledge for developing therapies for blast related injuries and to advancing military medicine.

AIMS OF THE STUDY

Characterize in rats exposed at various head orientations to high fidelity simulated blast overpressure waves the cellular, neuronal signaling, behavioral pathology of injuries to the eyes - specifically retina - and brain visual processing centers, as by:

1) Electroretinography (ERG).

2) Histopathology (H&E and silver stains).

METHODS

Simulation of Primary Blast Wave Injuries:

❑ Adult male Sprague Dawley rats (6 wk-old) are exposed under isoflurane to blast over pressure waves, in a right-side on or face on orientation, using a compressed air driven shock tube.

❑ Single air blast of ~20 psi is applied to the rat, via rupture of a Mylar membrane of predetermined thickness.

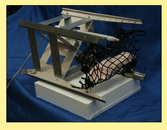

Animal holder (sled with sling)

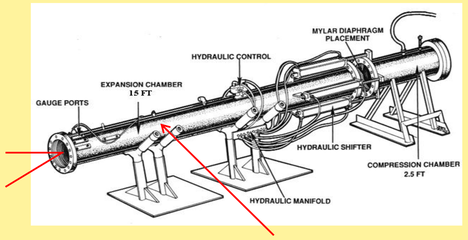

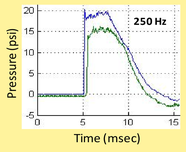

- Mach 1.34 shock front speed
- 62 µsec rise time
- 281 mph (126 m/s) blast wind
- Acceleration > 1000 xg

Figure 1. Diagrammatic view of the WRAIR shock tube.

METHODS (Cont.)

Electroretinography (ERG):

❑ Rats are dark adapted for 5 h; and then kept under red lights.

❑ Under isoflurane, pupils are drug-dilated; and electrodes put on eyes (recording), cheeks (reference), and tail (ground).

❑ Eyes are flashed with light (0.1 - 25 cd.s/m^2; 5 msec); and evoked retina potentials are recorded (a- and b- waveforms).

❑ Tested at baseline (1 d prior) and 1, 7, and 14 d post-blast.

Histopathology (H&E and Silver Stains):

❑ Rats are transcardial perfused with paraformaldehyde; and eyes and brains are removed and then post-fixed.

❑ Tissue samples are submitted (FD Neurotechnologies, Inc.) for processing into H&E (eyes) and silver (brains) stained slides.

❑ Examined under microscope for damage to retina and brain visual processing centers; where H&E stains for general cell morphology (pink to purple) and sliver for axonal fiber tract degeneration (brown to black). Assigned relative damage scores on a scale of 1 - 6.

RESULTS

Electroretinography (ERG):

FACE ON

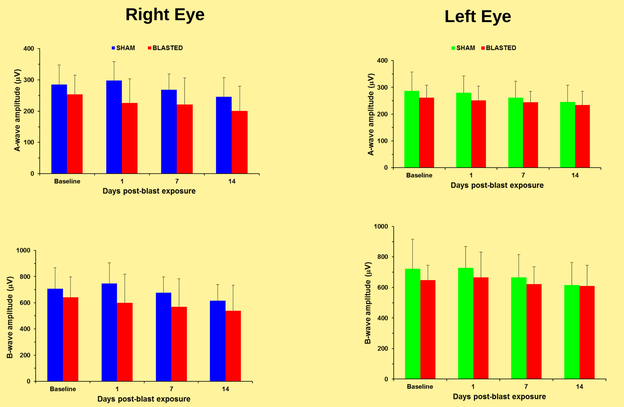

RIGHT SIDE ORIENTATION

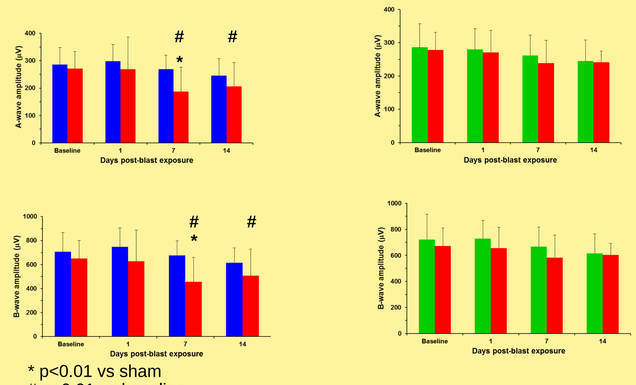

* p<0.01 vs sham
\# p<0.01 vs baseline

RESULTS (Cont.)

FACE ON HISTOPATHOLOGY

RETINAS

OPTIC TRACTS

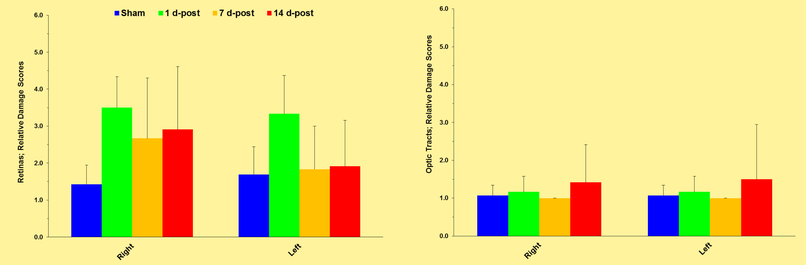

RIGHT SIDE HISTOPATHOLOGY

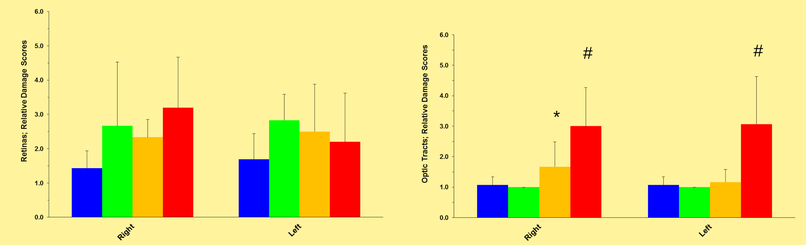

* p<0.05 vs sham
\# p<0.01 vs sham

Retina injury scoring scale:	Brain optic tract injury scoring scale:
1 = None (0%)	1 = None
2 = Slight (< 20%)	2 = Slight
3 = Mild (20 - 40%)	3 = Mild
4 = Moderate (40 - 60%)	4 = Moderate
5 = Severe (60 - 80%)	5 = Severe
6 = Catastrophic (80 - 100%)	6 = Catastrophic (pitch black)
Judged by extent / intensity of retinal swelling and neuronal cell disruption	Judged by intensity of silver stain coloration

CONCLUSION

We have demonstrated a reproducible method of studying BOP-induced eye and brain injuries in rats. Differences in eye and brain injury between the side-on and face-on orientation might be due to deflection of the shock wave away from the eyes in the face-on animals, owing, in part, to the conical morphology of the rodent skull. We conclude that the side-on orientation offers a reproducible model of BOP-induced eye and visual processing center brain injury in the rat and that it is suitable for further preventive and treatment paradigms.

SUPPORT: This work is supported in part by a USAMRMC/ TATRC Vision Research Program grant award, #: W81XWH-12-2-0082 and by the U.S. Army Clinical Pharmacology Fellowship Program.

DISCLAIMER: The views, opinions and/or findings contained in this presentation are those of the author and do not necessarily reflect the views of the Department of Defense and should not be construed as an official DoD/Army position, policy or decision unless so designated by other documentation. No official endorsement should be made.

Acknowledgements: Thanks to Robert Gharavi for sample preparation and data analysis.

REFERENCES

Capó-Aponte et al., 2012; Mil. Med. 177(7): 804-813.
Cockerham et al., 2011; N. Engl. J. Med. 364(22): 2172-2173.
Hines-Beard et al., 2012; Exp. Eye Res. 99: 63-70.
Jiang et al., 2013; J. Neuroinflammation. 10: 96-102.
Mohan et al., 2013; Invest. Ophthalmol. Vis. Sci. 54(5): 3440-3450.
Petras et al., 1997; Toxicology. 121(1): 41-49.
Warden, 2006; J. Head Trauma Rehabil. 21(5): 398-402.
Zou et al., 2013; J. Neuroinflammation. 10: 79-99.

Blast exposure phosphorylates *Tau* preferentially at serine396, which can trigger Alzheimer's-like pathology

Peethambaran Arun, Donna Wilder, Andrea Edwards, Ying Wang, Irene Gist, Joseph B. Long
Blast-Induced Neurotrauma Branch, Center for Military Psychiatry and Neuroscience,
Walter Reed Army Institute of Research, Silver Spring, MD 20910

Abstract

Blast-induced traumatic brain injury (TBI) is one of the major disabilities in service members returning from recent military operations. Blast-induced TBI is associated with acute and chronic neuropathological and neurobehavioral deficits. Epidemiological studies indicate that brains of 30% of victims who die acutely following TBI have Aβ plaques, a pathological feature of Alzheimer's disease (AD), which suggests that TBI may predispose to AD, although to date this notion remains somewhat speculative. *Tau* protein, phosphorylated at Serine396 (S396), is rich in paired helical filaments which form neurofibrillary tangles (NFTs) observed in the brains of patients with AD. The number of NFTs is tightly linked to the degree of dementia, indicating that the formation of NFTs may underlie and contribute to neuronal dysfunction. Preliminary studies carried out in our laboratory using shock tube models of single and repeated blast-induced TBI in rats indicate that phosphorylation of *Tau* protein occurs preferentially at S396. Phosphorylation of *Tau* varied in different regions of the brain and the degree of phosphorylation increased with number of blast exposures in many of the brain regions. Increased phosphorylation of *Tau* occurred acutely after blast exposures and chronically returned towards normal levels which at this stage did not positively correlate with the accumulation of amyloid precursor protein (APP) that occurred chronically. These results indicate that acute *Tau* protein phosphorylation at S396 and chronic accumulation of APP in the brain after blast exposure may predispose to Alzheimer's-like neuropathology.

Background

The complex biochemical and molecular mechanisms of blast-induced TBI and how they trigger subsequent secondary pathological processes and behavioral deficits are not well understood. Brain injury severity after blast exposure was found to increase with number of blast exposures. Studies indicate accumulation of Aβ plaques in the brains of TBI victims suggesting that TBI may predispose to Alzheimer's-like pathology. The NFTS present in the brains of patients with AD is rich in *pTau*(S396) indicating a potential role of phosphorylation of *Tau* at Serine396 in the pathology of AD. In the present study, we explored the phosphorylation of *Tau* protein and accumulation of APP in the brain after single and double blast exposures using the shock tube model of blast-induced TBI in rats.

Methods

Animals: Male Sprague Dawley rats (300-350g)

Blast TBI: After anesthesia (isoflurane, 4%), animals were secured in a prone position in the shock tube and exposed to single (19psi) or double (two 19psi blasts within 1 min) blast exposures.

Shock tube

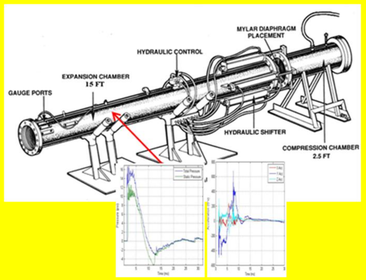

Animal holder

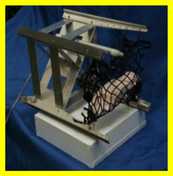

Western blotting: At different intervals after blast exposures, brain tissues were collected for Western blotting for total *pTau,* APP, *pTau*(S396), *pTau*-T231 *and* β-actin. Band intensities were determined by densitometry.

Results

Blast exposure increased the phosphorylation of *Tau* protein in most of the brain regions in a time dependent manner with maximum increase at early stages. The degree of phosphorylation varied in different brain regions. The phosphorylation of *Tau* protein increased with number of blast exposures.

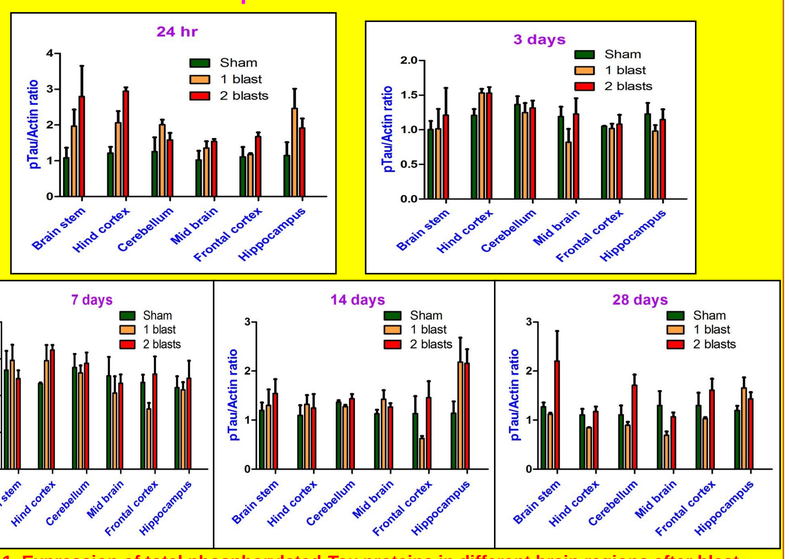

Fig.1. Expression of total phosphorylated *Tau* proteins in different brain regions after blast exposure

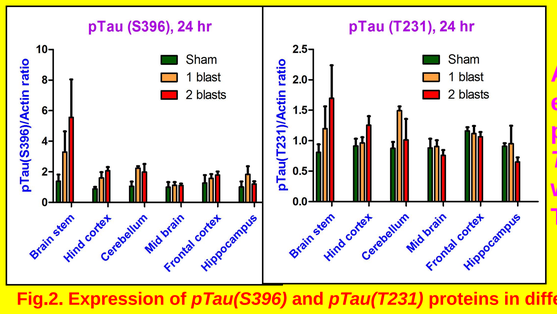

After blast exposure, phosphorylation of *Tau* at Serine396 was higher than at Threonine231

Fig.2. Expression of *pTau(S396)* and *pTau(T231)* proteins in different brain regions after blast exposure

Results continued…..

Blast exposure increased the accumulation of APP in most of the brain regions in a time-dependent manner with maximum accumulation at chronic stages. APP accumulation varied in different regions of the brain. The accumulation of APP increased with the number of blast exposures in most of the brain regions.

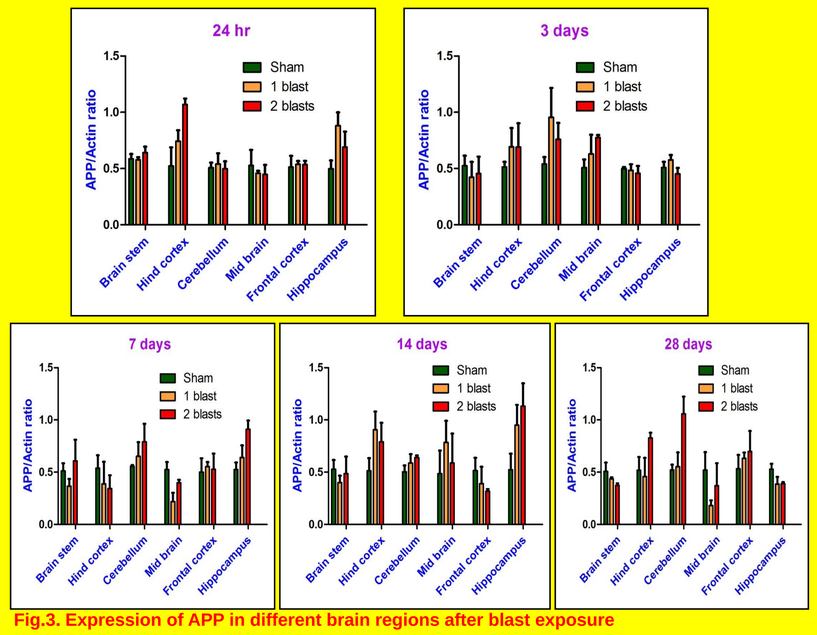

Fig.3. Expression of APP in different brain regions after blast exposure

Summary/Discussion

- Blast exposure caused phosphorylation of *Tau* protein in different brain regions in a time dependent manner. Maximum phosphorylation of *Tau* proteins occurs at early stages of injury. The phosphorylation of *Tau* protein was found to increase with repeated blast exposures in many brain regions. The degree of phosphorylation of *Tau* protein after blast exposure varied in different regions of the brain.
- The phosphorylation of *Tau* protein at Serine396 was found to be higher than that at Threonine231. The preferential phosphorylation of *Tau* protein at Serine396 may be playing a role in Alzheimer's-like pathology observed in TBI victims.
- Blast exposure results in the accumulation of APP in different brain regions in a time-dependent manner with maximum accumulation at chronic stages. Accumulation of APP was found to be increasing with the number of blast exposures.
- Phosphorylation of *Tau* protein didn't show a positive correlation with the accumulation of APP in different brain regions suggesting a distinct pathological mechanism leading to Alzheimer's-like neuropathology after blast exposure.

Acknowledgements

This study was supported by the CDMRP grants (W81XWH-11-2-0127 and W81XWH-08-2-0018)

Validation of a Blast-Induced Brain and Eye Injury Model in Rats

Keith M. Sharrow[1]*, James C. DeMar[2]*, Miya I. Hill[2], Andrea A. Edwards[2], Joseph B. Long[2] and Thomas G. Oliver[1]

Department of Clinical Pharmacology and Translational Medicine, Division Of Experimental Therapeutics[1] and Blast-Induced Neurotrauma Branch, Center for Military Psychiatry and Neuroscience[2], Walter Reed Army Institute of Research, Silver Spring, MD 20910 * Both authors contributed equally to work

Background: Non-penetrating eye (retina) and brain injury, most likely caused by blast shock waves, has emerged as a significant threat to warfighters in current theatres of operation. Expanding upon previous research in the field using rodent models of blast pressure demonstrated to cause reproducible injury to the brain and eyes, as assessed by Electroretinography (ERG) and histopathology, we validated our blast-induced injury model by examining the effect of various head orientations in relation to the oncoming blast overpressure wave on the extent of eye injury in the rat.

Methods: In these studies, adult male rats were placed into a compressed air driven shock tube with either their right eye (side-on) or their snout (face-on) facing toward the oncoming shock wave and then exposed to a single 20 psi (260 Hz) blast over pressure wave. The animals were then assessed at 1, 7 and 14 days post-blast along with non-blasted sham animals utilizing ERG measurements as well as histopathological assessments.

Results: At 2 weeks post-blast, side-on blasted rats versus sham animals showed significantly decreased ERG waveform amplitudes (approximately 30% from shams) and severe neuronal degradation within the retina and brain visual processing centers which could indicate functional visual deficits in the blasted animals. However, the face-on blasted rats showed little in any visual impairment from sham animals.

Conclusion: This study was conducted to validate the most reproducible method for this blast injury animal model. The difference in eye and brain damage between the side-on and face-on rats could be due to a deflection of the shock wave away from the eyes in the face-on animals. Based upon the results of these studies, future studies of preventative and treatment paradigms for blast induced eye and brain injury will use the side-on head orientation in this animal model.

SUPPORT: This work is supported in part by a USAMRMC/ TATRC Vision Research Program grant award, #: W81XWH-12-2-0082 and by the U.S. Army Clinical Pharmacology Fellowship Program.

Tissue non-specific alkaline phosphatase in the etiology and diagnosis of tauopathy and chronic traumatic encephalopathy

Peethambaran Arun, Rania Abu-Taleb, Samuel Oguntayo, Andrea Edwards, Cory Riccio, Stephen VanAlbert, Irene Gist, Ying Wang, Madhusoodana P. Nambiar, Joseph B. Long
Blast-Induced Neurotrauma Branch, Center for Military Psychiatry and Neuroscience,
Walter Reed Army Institute of Research, Silver Spring, MD 20910

Abstract

Dephosphorylation of *pTau* is essential for the preservation of neuronal microtubule assemblies and for protection against trauma-induced tauopathy and chronic traumatic encephalopathy (CTE). Tissue non-specific alkaline phosphatase (TNAP) serves this role in the brain by dephosphorylating *pTau*. Paired helical filaments (PHFs) and *Tau* isolated from Alzheimer's disease (AD) patients' brains formed microtubule assemblies with tubulin only after treatment with TNAP or protein phosphatase-2A, 2B and -1, suggesting that *Tau* protein in the PHFs of neurons in AD brain is hyperphosphorylated, which prevents microtubule assembly. Our studies using blast and impact acceleration models of traumatic brain injury in rats revealed *pTau* accumulation in the brain as early as 6 h post-injury and further accumulation by 24 h which varied in different brain regions. The *pTau* accumulation was accompanied by reduced TNAP expression/activity in the brain at 6 h after blast/impact acceleration and the activity remained suppressed through 14 days. Plasma alkaline phosphatase activity also decreased as early as 3 h after these insults and remained low at 14 days. These results reveal that blast/impact acceleration decreases the level/activity of TNAP in the brain, which likely contributes to trauma-induced accumulation of *pTau* and the resultant tauopathy associated with CTE and decreased levels/activities of TNAP in the plasma after brain injury might be useful biomarkers for early diagnosis.

Background

Battlefield blast exposures and TBI have been described as the 'signature injury' of the wars in Iraq and Afghanistan. The complex biochemical and molecular mechanisms of blast TBI and how they trigger subsequent secondary pathological processes and behavioral deficits are not well understood. Blast victims have been shown to share with professional football players with multiple concussions similar neuropathological changes which include tauopathy and CTE, suggesting convergent pathological mechanisms of injury in these 2 patient populations. In the present study, we evaluated the role of TNAP in the development of tauopathy and CTE using rat models of 1) blast-induced TBI using a shock tube and 2) impact acceleration induced head injury using weight drop and explored the possibility of utilizing the activity of TNAP as a biomarker of tauopathy and CTE.

Methods

Animals: Male Sprague Dawley rats (300-350g)

Blast TBI: After anesthesia (isoflurane, 4%), animals were kept in prone position in the shock tube and exposed to single blast exposure at 19 psi.

Shock tube

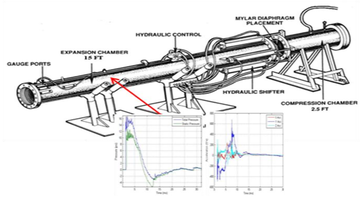

Animal holder

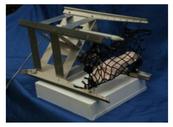

Head impact acceleration injury: After the anesthesia (isoflurane, 4%), rats were positioned on a foam cushion and a 500g weight was dropped from a 125cm height onto a 10 mm stainless steel disc positioned on the rat's head by a flexible Mylar headpiece. The disc prevented direct impact and skull fracture.

Weight drop model

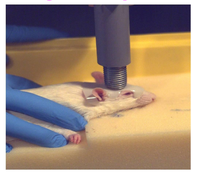

Activity of TNAP in the brain regions: Homogenates of different brain regions were prepared in T-Per Tissue protein extraction buffer containing protease inhibitors. Activity of TNAP in the homogenates was measured using alkaline phosphatase assay kit from Randox Laboratories according to manufacturer's instructions.

Activity of alkaline phosphatase in the plasma: The activity of alkaline phosphatase in the plasma was determined using alkaline phosphatase assay kit from Randox Laboratories according to manufacturer's instructions

Western blotting: Western blotting for *pTau* and TNAP in the tissue homogenates was carried out using monoclonal antibodies raised in rabbit and mouse respectively.

Results

Blast exposure and head impact acceleration increase accumulation of *pTau* in brain regions

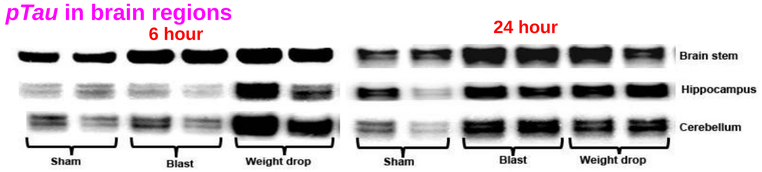

Blast exposure and head impact acceleration decrease activity of TNAP in brain regions

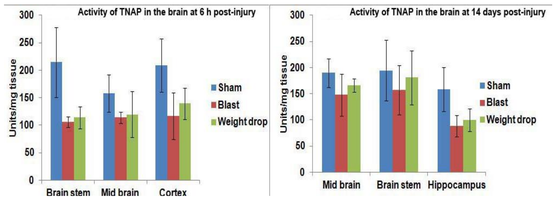

Results continued…..

Expression of TNAP in the brain regions after 6 h

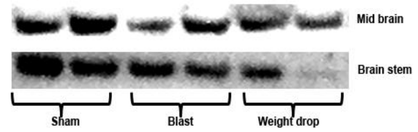

Level of TNAP decreases in the brain regions after blast exposure and after head impact acceleration

Activity of alkaline phosphatase decreases in the plasma after blast exposure and after head impact acceleration

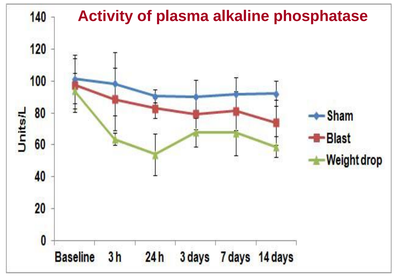

Proposed hypothesis

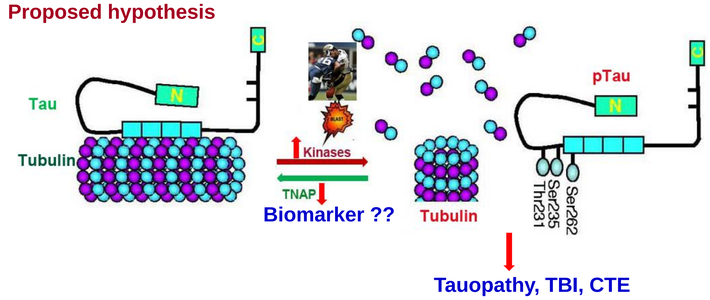

Summary/Discussion

- Phosphorylation of *Tau* inhibits microtubule assembly in the neurons leading to neurofibrillary tangle formation, neurodegeneration, tauopathy and CTE.
- TNAP is a critical enzyme involved in the dephosphorylation of *pTau*. Decrease in its activity can lead to accumulation of *pTau*, tauopathy and CTE.
- Blast exposure as well as head impact acceleration in rats leads to decreased expression and activity of TNAP in different regions of the brain. The decrease in TNAP activity was associated with accumulation of *pTau* in different regions of the brain.
- The decreased activity of TNAP in the brain after blast exposure as well as after head impact in rats was associated with a decreased activity of alkaline phosphatase in the plasma which can potentially be used as a biomarker of taupathy/CTE

Tissue non-specific alkaline phosphatase in the etiology of tauopathy and chronic traumatic encephalopathy after traumatic brain injury

Peethambaran Arun, Rania Abu-Taleb, Samuel Oguntayo, Andrea Edwards, Cory Riccio, Stephen VanAlbert, Irene Gist, Ying Wang, Madhusoodana P. Nambiar, Joseph B. Long
Blast-Induced Neurotrauma Branch, Center for Military Psychiatry and Neuroscience,
Walter Reed Army Institute of Research, Silver Spring, MD 20910

Abstract

Studies indicate that chronic traumatic encephalopathy (CTE), a *tau* protein-linked neurodegenerative disorder observed in athletes with multiple concussions, shares clinical symptoms and neuropathological characteristics with those seen in victims of blast. Prevention of *Tau* phosphorylation and facilitation of the dephosphorylation of *pTau* are critical to prevent tauopathy and preserve/restore microtubule assembly. Tissue non-specific alkaline phosphatase (TNAP) serves this major role in the brain by dephosphorylating *pTau*. Paired helical filaments and *Tau* protein isolated from Alzheimer's disease (AD) patients' brains formed microtubule assembly with tubulin *in vitro* only after treatment with TNAP or protein phosphatase-2A, 2B and -1, suggesting that *Tau* protein in the paired helical filaments of neurons in AD brain is hyperphosphorylated which prevents microtubule assembly. TNAP showed higher activity in dephosphorylating *pTau* compared to other protein phosphatases. Our preliminary studies using blast and impact acceleration models of traumatic brain injury (TBI) in rats reveal significant *pTau* accumulation in the brain as early as 6 h post-injury and further increased accumulation by 24 h. The extent of *pTau* accumulation varied in different brain regions after the insults. The *pTau* accumulation was accompanied by reduced TNAP activity, which decreased significantly in the brain at 6 h after blast exposure and/or impact acceleration and remained low through 14 days. Western blotting showed decreased TNAP expression in the brain at 6 h after blast exposure and impact acceleration. Plasma alkaline phosphatase activity also decreased significantly as early as 3 h after these insults and remained low at 14 days. These results reveal that blast exposure/impact acceleration decrease the levels/activity of TNAP in the brain, which likely contributes to accumulation of *pTau* and the resultant tauopathy and CTE. Additionally, decreased levels/activities of TNAP in the cerebrospinal fluid (CSF) and plasma after blast exposure might be useful biomarkers for the early diagnosis of tauopathy/CTE.

Background

Battlefield blast exposures and TBI have been described as the 'signature injury' of the wars in Iraq and Afghanistan. The complex biochemical and molecular mechanisms of blast TBI and how they trigger subsequent secondary pathological processes and behavioral deficits are not well understood. Blast victims have been shown to share with professional football players with multiple concussions similar neuropathological changes which include tauopathy and CTE, suggesting convergent pathological mechanisms of injury in these 2 patient populations. In the present study, we evaluated the role of TNAP in the development of tauopathy and CTE using rat models of 1) blast-induced TBI using a shock tube and 2) impact acceleration induced head injury using weight drop and explored the possibility of utilizing the activity of TNAP as a biomarker of tauopathy and CTE.

Methods

Animals: Male Sprague Dawley rats (300-350g)

Blast TBI: After anesthesia (isoflurane, 4%), animals were kept in prone position in the shock tube and exposed to single blast exposure at 19 psi.

Shock tube

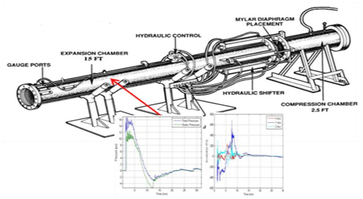

Animal holder

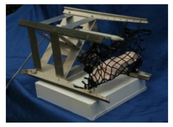

Head impact acceleration injury: After the anesthesia (isoflurane, 4%), rats were positioned on a foam cushion and a 500g weight was dropped from a 125cm height onto a 10 mm stainless steel disc positioned on the rat's head by a flexible Mylar headpiece. The disc prevented direct impact and skull fracture.

Weight drop model

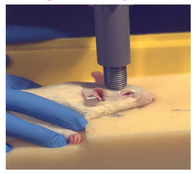

Activity of TNAP in the brain regions: Homogenates of different brain regions were prepared in T-Per Tissue protein extraction buffer containing protease inhibitors. Activity of TNAP in the homogenates was measured using alkaline phosphatase assay kit from Randox Laboratories according to manufacturer's instructions.

Activity of alkaline phosphatase in the plasma: The activity of alkaline phosphatase in the plasma was determined using alkaline phosphatase assay kit from Randox Laboratories according to manufacturer's instructions

Western blotting: Western blotting for *pTau* and TNAP in the tissue homogenates was carried out using monoclonal antibodies raised in rabbit and mouse respectively.

Results

Blast exposure and head impact acceleration increase accumulation of *pTau* in brain regions

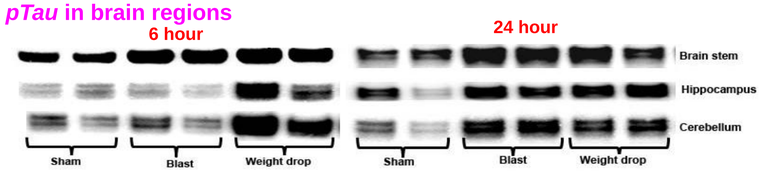

Blast exposure and head impact acceleration decrease activity of TNAP in brain regions

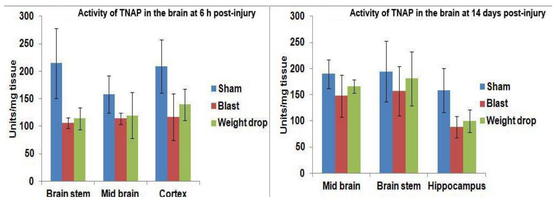

Results continued…..

Expression of TNAP in the brain regions after 6 h

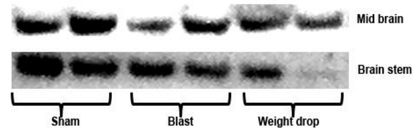

Level of TNAP decreases in the brain regions after blast exposure and after head impact acceleration

Activity of alkaline phosphatase decreases in the plasma after blast exposure and after head impact acceleration

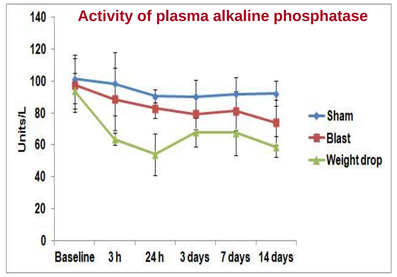

Proposed hypothesis

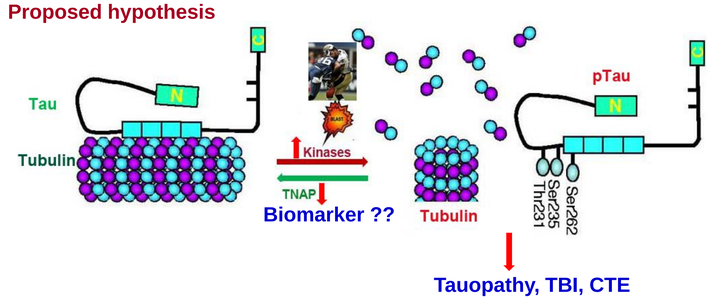

Summary/Discussion

- Phosphorylation of *Tau* inhibits microtubule assembly in the neurons leading to neurofibrillary tangle formation, neurodegeneration, tauopathy and CTE.
- TNAP is a critical enzyme involved in the dephosphorylation of *pTau*. Decrease in its activity can lead to accumulation of *pTau*, tauopathy and CTE.
- Blast exposure as well as head impact acceleration in rats leads to decreased expression and activity of TNAP in different regions of the brain. The decrease in TNAP activity was associated with accumulation of *pTau* in different regions of the brain.
- The decreased activity of TNAP in the brain after blast exposure as well as after head impact in rats was associated with a decreased activity of alkaline phosphatase in the plasma which can potentially be used as a biomarker of taupathy/CTE

Comparison of Combined Primary and Tertiary Blast Traumatic Brain Injury in Young and Middle Age Rats

Ying Wang, Yanling Wei, Lawrence Tong, Samuel Oguntayo, Andrea Edwards, Cory Riccio, Irene Gist, Peethambaran Arun, Stephen Van Albert, Joseph B. Long

Blast-Induced Neurotrauma Branch, Center for Military Psychiatry and Neuroscience, Walter Reed Army Institute of Research, Silver Spring, MD 20910

ABSTRACT

Age-dependent variations in the pathophysiology of blast-induced traumatic brain injury (bTBI) may influence efficacy of therapies for mitigation of damage. Since War fighters who sustain bTBI are typically exposed to a combination of blast overpressure (BOP) and a biomechanical perturbation related to acceleration and/or impact, BOP and weight drop injury were combined into a dual insult model to compare bTBI in different age rats. Anesthetized 10-wks and 24-wks old rats were exposed to BOP in a shock tube (19 psi total) followed immediately by weight-drop (500 g, 150 cm). Brain and plasma were collected through 14 d post-injury. Axonal degeneration and inflammation were revealed in both groups by silver stained or anti-Iba1 immunostained sections, respectively. GFAP increased at 6 h and 14 d in older rats but decreased at 6 h in younger rats. Contactin-associated protein-2 (Caspr2) increased in older rats at 14 d post-injury, but was unchanged in younger rats. In both age groups, MCP-1 increased in the CSF and plasma at 6 h post-injury. Cdc25A and p21 increased in younger rats at 6 h post-injury, whereas only p21 increased in older injured rats. These biomarkers revealed time-dependent brain injury and neuroinflammatory processes which varied by age. They further indicate that the molecular responses directing DNA repair and regulation of cell proliferation after bTBI may also differ in an age-dependent manner.

METHODS

Animals and TBI model:

Male Sprague Dawley rats, the age of 10 weeks (10-wks) and 24 weeks (24-wks) old (Charles River Laboratories), were housed with free access to food and water *ad libitum*. After anesthetized with isofluorane, animal were exposed to blast overpressure in a shock tube (19 psi peak amplitude) followed immediately by weight-drop (500 g, 150 cm). Brain, CSF and plasma were collected at 6 h or 14 days post-injury and were analyzed using histopathology, immunohistochemistry, ELISA and immunoblotting.

Enzyme-linked immunosorbent assay:

ELISA for MCP-1 was performed using commercially available kit (Pierce) in accordance with the manufacturer's instructions.

Histopathological Analysis:

At the indicated post-injury time points, the animals were fully anesthetized and perfused with saline followed by 4% paraformaldehyde. Serial coronal sections were cut through the cerebrum and brain stem/cerebellum. The sections were processed using FD Neurosilver kit (FD Neurotechnologies). Neuronal degeneration was indicated by dense silver precipitates when images were examined under a light microscope with bright field. The coronal brain sections were stained with Iba-1 antibody (Wako chemicals) and images were examined under a fluorescent microscope for the determination of neuronal inflammation.

Immunoblot Analyses:

Tissues were homogenized in TPER buffer containing protease and phosphatase inhibitors. Equal quantities of proteins were subjected to SDS-PAGE and western blot analysis using antibodies to GFAP and Caspr2 (Cell Signaling Technology); Cdc25A and p21 (Abcam), as well as actin (Sigma).

RESULTS

1 Decreased mortality in middle age rats treated with blast and weight-drop TBI compared to younger rats

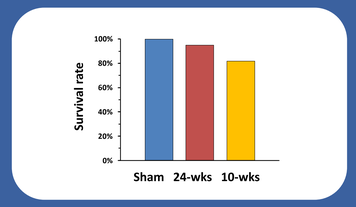

2 The combination of blast and weight-drop impact induced axonal degeneration at 14 d after injury

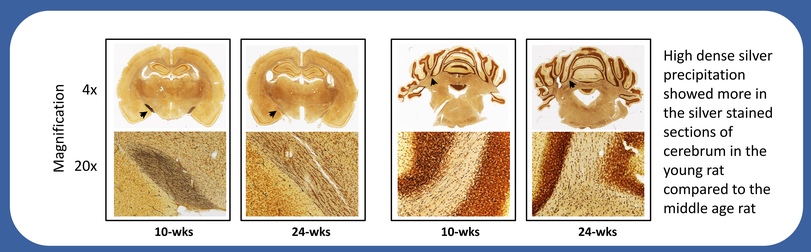

High dense silver precipitation showed more in the silver stained sections of cerebrum in the young rat compared to the middle age rat

3 Increased expression of GFAP and Caspr2 in the frontal cortex at 6 h and 14 d after TBI in young and middle age rats

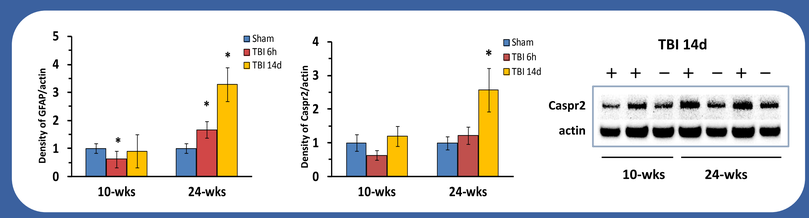

4 The combination TBI increases MCP-1 in the cerebrospinal fluid (CSF) and serum at 6 h post-injury

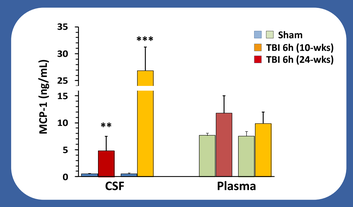

5 Increased expression of Iba-1, a microglia marker in multiple brain regions at 14 d post-injury

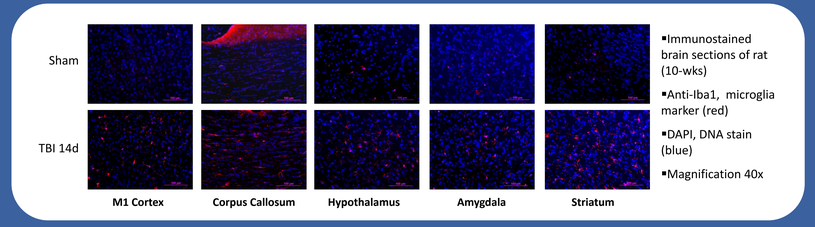

6 Increased expression of GFAP and Caspr2 in the frontal cortex at 6 h and 14 d after TBI in young and aged rats

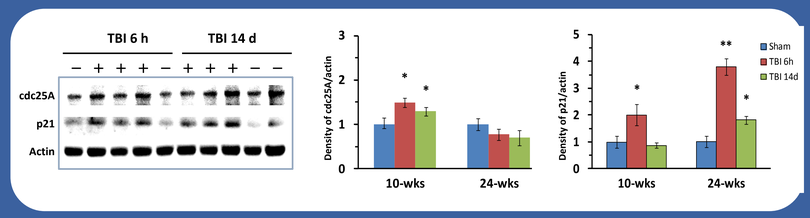

CONCLUSIONS

- Compared to the 10-wks age rat, the lower mortality rate in 24-wks old rat probably was due to a stronger thicker skull.
- Widespread time-dependent changes in astrocytic and microglial biomarkers revealed brain injury accompanied by neuroinflammation in both younger and older rats (Iba-1 data was not shown for 24-wks old rats) , although these changes varied by age.
- Double-strand DNA damage and cell-cycle activity have recently been shown to be tightly associated and to precede neuronal death. Thus, cell-cycle regulators may play a critical role directing apoptotic responses.
- Our findings suggest that the molecular changes directing DNA damage repair and regulation of cell proliferation after bTBI may differ in an age-dependent manner.

There is no objection to its presentation. The opinions or assertions contained herein are the private views of the author, and are not to be construed as official, or as reflecting true views of the Department of the Army or the Department of Defense. Research was conducted in compliance with the Animal Welfare Act and other federal statues and regulations relating to animals.

Characterization of Blast-Induced Auditory and Vestibular Injury in Rats

Ying Wang, Yanling Wei, Lawrence Tong, Andrea Edwards, Irene Gist, Peethambaran Arun, Joseph B. Long

Blast-Induced Neurotrauma Branch, Center for Military Psychiatry and Neuroscience, Walter Reed Army Institute of Research, Silver Spring, MD 20910

ABSTRACT Blast exposure is the most common cause of traumatic brain injury (TBI) in warfighters. Nearly 60% of blast TBI victims exhibit hearing loss, tinnitus, dizziness and balance disorders. To date, the etiologies of these injuries are largely undefined. A high fidelity animal model is critical to define the mechanism(s) of injury and develop therapeutic strategies for blast-induced neurobehavioral deficits. In this study, we used an air-driven shock tube to simulate primary blast and investigated the pathological effects of blast exposures on central and peripheral auditory/vestibular systems. Anesthetized rats were tautly secured in a transverse prone position 2.5 ft within the mouth of a 1 ft diameter shock tube with the right side facing the oncoming shockwave. Rats were exposed to two closely coupled shockwaves (peak total pressures of 5, 12 or 19 psi) separated by 30 sec. Rats were euthanized at varied intervals (6 h, 24 h, 7 d and 14 d) post injury and tissues underwent histological and RNA analyses. All rats received rotarod training prior to and testing after blast exposures for evaluation of motor coordination and balance. Compared to a single blast insult, repeated blast exposures significantly impaired motor coordination. Intensity-dependent blast-induced damage to middle and inner ears was evident with no significant differences between left and right ears. Labyrinthine hemorrhage was prominent at 24 h up to 14 days after blast exposures. Repeated blast exposures caused significant axonal degeneration and glial cell proliferation in the central vestibular signal processing regions of the brain, also triggered multiple gene expression changes that are associated with DNA repair, neural growth, inflammation and pain. These findings indicate that both peripheral and central vestibular systems are vulnerable to blast injuries, and are particularly disrupted by closely coupled repeated blasts. Neuroinflammation, which occurred during the early phase post injury, could be a major factor leading to secondary neuronal damage.

METHODS

Animals and TBI model: Sprague Dawley rats, male, 350 ± 25 g (Charles River Laboratories), were anesthetized with isofluorane and were tautly secured in a transverse prone position 2.5 ft within the mouth of a 1 ft diameter shock tube with the right side of the animal facing the oncoming shockwave. Rats were exposed to two closely coupled shockwaves (peak total pressures of 5, 12 or 19 psi) separated by 30 sec. Rats were euthanized at varied intervals post-injury and tissues underwent histological and RNA analyses.

Neurobehavioral Assessment: Rotarod balance testing was used to assess the ability of an animal to balance on a rotating rod. Rats received fixed speed and accelerating-speed rotarod training for 5 days prior to blast exposure and were tested at 1, 2, 3, 5 and 7 days post-injury. One way ANOVA and a Student-Newman-Keuls were used for data analysis.

Histopathological Analysis: Rats were fully anesthetized and perfused with saline followed by 4% paraformaldehyde. Frozen brain tissues were cut in coronal sections (30 µm). The sections were processed using Neurosilver kit (FD Neurotechnologies). Following 0.2% Triton X-100 solution permeabilization and blacking with 10% Goat serum blocking, brain sections were incubation with primary antibodies (GFAP or CCR2) overnight at 4°C. After incubated with Alexa Fluor-conjugated secondary antibody, sections were mounted in SlowFade gold antifade reagent with DAP1 (Invitrogen). Decalcification in 0.12 M EDTA in 0.1 M PB (pH 7.0) for 5 days, ear tissues were embedded into paraffin and cut in longitude sections (10 µm) of the cochlea. Serial sections were stained with hematoxylin and eosin (H&E). All images were examined under AX-80 Olympus microscope.

***RNA extraction and qRT-PCR*:** Tissue samples were homogenized in ice cold TRIzol (Life Technologies), and RNA was isolated following the TRIzol protocol. RNA purity was determined using NanoDrop ND-1000 (Thermo Fisher). According to the manufacturer's instructions, 800 ng of high-quality RNA for each sample was converted into cDNA and applied to PCR array plates using the RT2 PCR array kit (QIAGEN). All reactions were processed in the 7500 Fast Real-Time PCR System (Life Technologies). Data were interpreted by using QIAGEN's web-based PCR array data analysis tool.

RESULTS

1 *Functional deficit after blast exposure*

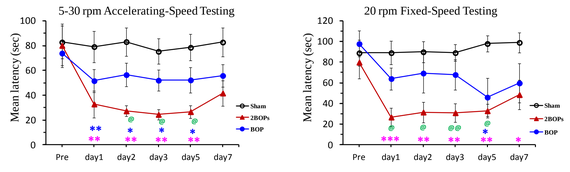

- Rat's performance on the rotarod before and post-injury
- Experimental groups: Sham (without blast), BOP (single 19 psi), 2BOPS (double 19 psi), 7 rats each group
- 2 BOPs vs. sham: *p < 0.05, **p< 0.01, *** p< 0.005; 2 BOPs vs. BOP, @p < 0.05, @@p< 0.01; BOP vs. sham, *p < 0.05, **p< 0.01

2 *Effect of blast exposure(s) on middle and inner ears*

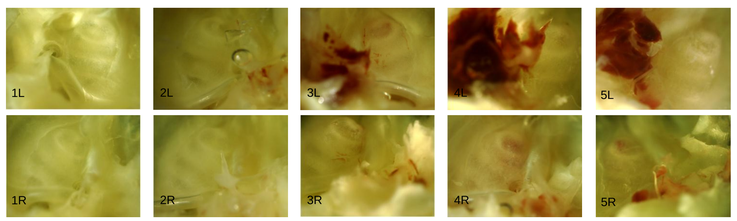

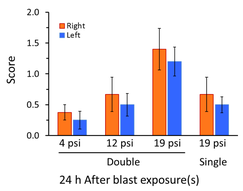

- 24 h after blast exposure, temporal bones were removed and tympanic bullae were opened
- Images were taken under microscope with a 20x magnification
- Sham (1L, 1R), 2BOPs_5 psi (2L, 2R), 2BOPs_12 psi (3L, 3R), 2BOPs_19 psi (4L, 4R), BOP_19 psi (5L, 5R)

3 *Inner ear hemorrhage after blast exposures*

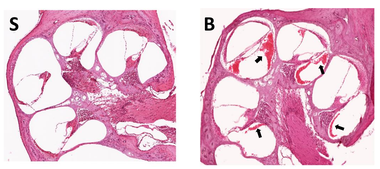

- 14 d after blast exposures
- Sham (S), 2BOPs_19psi (B)
- Cross sections with H & E staining
- Original magnification: x 200
- Hemorrhage (arrow)

4 *Effect of blast exposure on cerebellum and brainstem*

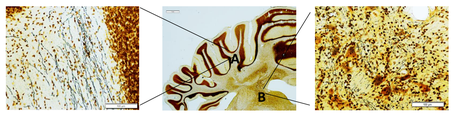

- Silver staining
- High dense precipitation in vestibular center (B) at 7 d after double blast exposures

5 *Effect of blast exposure on auditory cortex*

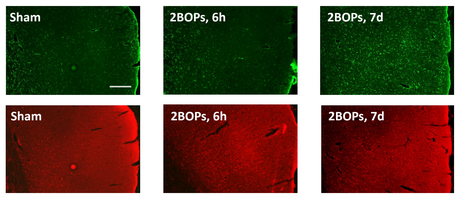

- Immunohistochemistry on brain sections
- at 6 h and 7 d after TBI
- Expression of GFAP (green) and CCR2 (red)
- Scale bar = 200 µm

6 *Blast-induced inflammation related gene expression*

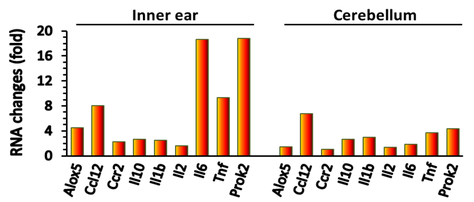

- Tissues were collected at 6 h after double blast exposures
- Groups: sham and 2BOPs , 3 rats for each group

CONCLUSIONS

- Peripheral and central auditory and vestibular systems are vulnerable to a blast-related injury
- Compared to sham controls and single blast exposure, repeated blasts caused significant motor coordination deficits and damage to middle and inner ear
- Severities of middle and inner ear injuries were blast intensity-dependent
- Inner ear hemorrhage was not observed at 6 h post exposure (data not showed), but was presented significantly at 24 h and up to 14 days that indicated an occurring of the secondary injury
- Repeated blast exposures elicit inner ear and CNS inflammation

JOURNAL OF NEUROTRAUMA 30:1645–1651 (October 1, 2013)

DOI: 10.1089/neu.2012.2834

Acute Mitochondrial Dysfunction after Blast Exposure: Potential Role of Mitochondrial Glutamate Oxaloacetate Transaminase

Peethambaran Arun, Rania Abu-Taleb, Samuel Oguntayo, Ying Wang, Manojkumar Valiyaveettil, Joseph B. Long, and Madhusoodana P. Nambiar

Abstract

Use of improvised explosive devices has significantly increased the incidence of traumatic brain injury (TBI) and associated neuropsychiatric deficits in the recent wars in Iraq and Afghanistan. Acute deleterious effects of single and repeated blast exposure can lead to long-term neurobiological effects and neuropsychiatric deficits. Using *in vitro* and *in vivo* shock tube models of blast-induced TBI, we studied changes in mitochondrial energy metabolism after blast exposure. Single and repeated blast exposures *in vitro* resulted in significant decreases in neuronal adenosine triphosphate (ATP) levels at 6 h post-blast that returned towards normal levels by 24 h. Similar changes in ATP also were observed in the cerebral cortices of mice subjected to single and repeated blast exposures. In neurons, mitochondrial glutamate oxaloacetate transaminase (GOT_2) plays a critical role in metabolism and energy production. Proteomic analysis of brain cortices showed a significant decrease in GOT_2 levels 6 h after repeated blast exposures, which was further confirmed by Western blotting. Western blot analysis of GOT_2 and pyruvate dehydrogenase in the cortex showed direct correlation only between GOT_2 and ATP levels. Activity of GOT_2 in the isolated cortical mitochondria also showed significant decrease at 6 h supporting the results of proteomic and Western blot analyses. Knowing the significant role of GOT_2 in the neuronal mitochondrial energy metabolism, it is quite likely that the down regulation of GOT_2 after blast exposure is playing a significant role in mitochondrial dysfunction after blast exposure.

Key words: adenosine triphosphate; blast exposure; glutamate oxaloacetate transaminase; mini citric acid cycle; mitochondrial dysfunction; pyruvate dehydrogenase; traumatic brain injury

Introduction

Exposure to blast has been reported as the major cause of traumatic brain injury (TBI) and associated disabilities in the recent wars in Iraq and Afghanistan.[1] Significant advances in personnel protection devices and medical care have decreased the mortality of blast victims, but increased the number of surviving casualties with mild, moderate and severe TBI.[2,3] Service members are commonly exposed to single or multiple blasts with different intervals. Preclinical studies in experimental animal models indicate that severity of brain injury increases with number of blast exposures.[3]

Due to the complexity and unique physical forces responsible for blast-induced TBI, it is now widely believed that the TBI resulting from blast exposure is relatively distinct from other closed head or penetrating brain injuries.[4] The primary, secondary, tertiary, and quaternary injury phases of blast exposure are believed to contribute to the multifaceted mechanisms involved in blast TBI. Although several clinical and animal studies have explored the biochemical/histopathological changes and behavioral deficits resulting from blast exposure,[3,5–11] the complex biochemical and molecular mechanisms of blast TBI and how it triggers subsequent secondary pathological processes and long-term neurobehavioral abnormalities are still not well understood. The lack of understanding of the precise mechanisms involved in blast TBI has hampered the development of personal protective gear and specific diagnostic tools for early detection and effective therapies for prevention/treatment.

Acute effects of blast exposure are not well studied because most of the significant pathological changes in the brain manifest during the secondary injury processes, which occur typically by 24 h post-blast exposures. Using an *in vitro* model of

Blast-Induced Neurotrauma Branch, Center for Military Psychiatry and Neuroscience, Walter Reed Army Institute of Research, Silver Spring, Maryland.

blast-induced TBI, we have shown that single and repeated blast exposures lead to transient changes in neuronal cell membrane integrity, which may be a potential mechanism contributing to the secondary injury processes.[12] Transient changes in cell membrane integrity also have been reported in the liver and muscle tissue after single and repeated blast exposures.[13] Acute deleterious effects of any direct or indirect insult on the brain can trigger secondary pathological changes, which lead to chronic neurobehavioral abnormalities. Thus, minimizing or preventing acute changes after brain injury is important to avert chronic neurobehavioral deficits.

In most of the cell types in the body, adenosine triphosphate (ATP) synthesis takes place through utilization of glucose, and mitochondrial pyruvate dehydrogenase (PDH) plays an important role. In the case of brain, amino acids—especially glutamate—also are utilized for the immediate and significant demands for ATP for energy.[14–16] In one study, removal of glucose significantly increased the transamination of glutamate to aspartate in brain synaptosomes and suggested that brain cells utilize glutamate, the most abundant molecule in the brain, for energy production.[15] Mitochondrial glutamate oxaloacetate transaminase (GOT_2) is the enzyme responsible for the transamination of glutamate to aspartate and α-ketoglutarate. Since α-ketoglutarate can directly enter the citric acid cycle to generate ATP, GOT_2 is believed to play major role in ATP production in neurons.[14–16]

In the present study, using the *in vitro* and *in vivo* models of blast-induced TBI, we studied changes in mitochondrial energy metabolism after blast exposure. We first analyzed ATP levels in the neuronal cells in culture and brain cortex after blast exposure to demonstrate mitochondrial energy dysfunction. Decreases in ATP levels were further compared between single and multiple blast exposures to determine its dependency upon the severity of injury. Since GOT_2 plays a central role in neuronal mitochondrial energy metabolism, we investigated its expression in the brain by proteomic analysis. Modulation of GOT_2 was further analyzed by Western-blotting of the brain cortex and enzyme activity analysis in the isolated mitochondria from the cerebral cortex to demonstrate a potential role of GOT_2 in the acute mitochondrial dysfunction after blast exposure.

Methods

Cell culture and blast exposure

SH-SY5Y human neuroblastoma cells, Dulbecco's modified Eagle's medium (DMEM) and fetal bovine serum (FBS) were obtained from American Type Culture Collection (Manassas, VA). One of the major advantageous of SH-SY5Y cells over primary cells and brain slices (derived from animals) is that the effect of blast exposure can be studied in cells of human origin. Cells were grown in DMEM with 10% heat inactivated FBS containing penicillin and streptomycin. The cells incubated at 37°C in a carbon dioxide (CO_2) incubator kept at 5% CO_2 and 95% air in a humidified atmosphere. Cells (4×104 cells/well) were grown on 96 well tissue culture plates 24 h before blast exposure. On the day of blast exposure, the medium was removed from the wells and fresh medium (360 μL) was added to fill the wells. Before blast exposure, the plates were sealed with gas permeable Mylar plate sealers as described previously.[12,17] The plates containing cells were subjected to single and triple blast exposures (21 psi) using shock tube as described earlier.[12,17] Intracellular adenosine triphosphate (ATP) content in the cells was determined at 6 and 24 h post-blast using ATPlite kits (Perkin Elmer, Waltham, MA) as previously described.[17] The ATPlite assay system is based on the production of luminescence caused by the reaction of ATP with added luciferase enzyme and D-luciferin substrate.

Animals and blast exposure

All animal experiments were conducted in accordance with the Animal Welfare Act and other federal statutes and regulations relating to animals and experiments involving animals and adhered to principles stated in the Guide for the Care and Use of Laboratory Animals (National Research Council Publication, 1996 edition). The animal protocol used was approved by Institutional Animal Care and Use Committee, Walter Reed Army Institute of Research. C57BL/6J male mice (8–10 weeks old) that weighed between 21–26 g (Jackson Laboratory, Bar Harbor, ME) were used in this study. Mice were exposed to single and triple blasts using a shock tube as described earlier.[3] Briefly, mice were anesthetized with 4% isofluorane gas (oxygen [O_2] flow rate 1.5 L/min) for 8 min and restrained in the prone position with a net to minimize the movements during blast exposure. Animals were subjected to single or triple blast exposures (21 psi) and brain cortex was dissected after euthanasia at 1, 6, or 24 h post-blast.

ATP determination in the brain cortex

Homogenate (20% w/v) of brain cortex was made in tissue protein extraction buffer (Pierce Chemical Co, Rockford, IL) containing protease and phosphatase inhibitor cocktails (Sigma-Aldrich, St. Louis, MO). The homogenate was centrifuged at 5000 g for 5 min and the ATP content in the supernatant was measured using ATPlite kit as described earlier.[18]

Proteomic analysis

Proteomic analysis of brain cortex was carried out as described by us earlier.[19] Briefly, proteins were isolated from the brain cortex of sham control and repeated blast exposed mice (3 animals/group) at 6 h post-blast using the ToPI-DIGE™ total protein isolation kit (ITSI-Biosciences, Johnstown, PA) and subjected to two-dimensional differential in-gel electrophoresis (2D-DIGE). After 2D-DIGE, the differentially-expressed (> 2-fold change in abundance) protein spots were identified, selectively picked, and subjected to protein digestion followed by LC/MS/MS to identify the peptides. The obtained MS/MS spectra were searched against the National Center for Biotechnology Information non-redundant protein sequence database using the SEQUEST computer algorithm to establish the protein identity.

Western blotting analysis

Polyclonal rabbit antibodies against GOT_2 and pyruvate dehydrogenase (PDH) were obtained from Sigma-Aldrich (St. Louis, MO) and Abcam (Cambridge, MA). Secondary antibody labeled with horse-radish peroxidase (HRP) was purchased from Santa Cruz Biotechnology (Santa Cruz, CA). Mouse monoclonal antibody to β-actin conjugated with HRP (Sigma-Aldrich, St. Louis, MO) was used as a control. Polyacrylamide gel electrophoresis and Western blotting analysis of brain cortex was carried out as described by us previously.[19] Both GOT_2 and PDH antibodies were used at a final dilution of 1:1000. After Western blotting analysis, the protein bands were detected using ECL-Plus Western blot detecting reagent (GE Healthcare, Piscataway, NJ) and the chemiluminescence was measured in an AlphaImage reader (Cell Biosciences, Santa Clara, CA).

Assay of GOT_2 activity in the mitochondrial fraction of brain cortex

Mitochondrial fraction was isolated from the cerebral cortex using Mitochondria Isolation Kit obtained from Thermo Scientific (Rockford, IL) according to the manufacturer's instructions. The

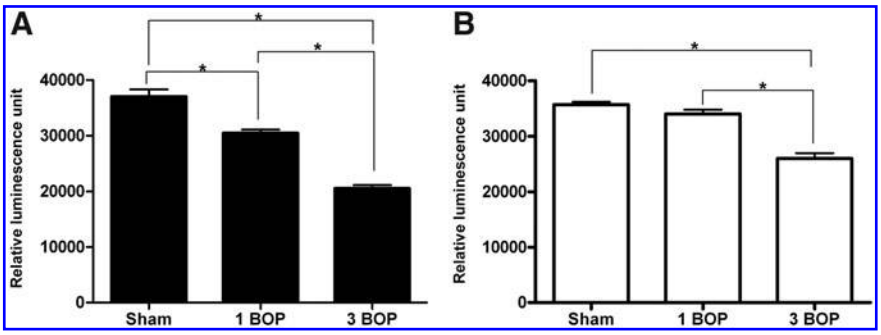

FIG. 1. Changes in adenosine triphosphate levels in SH-SY5Y cells at 6 h **(A)** and 24 h **(B)** after single and repeated blast exposures. Relative luminescence unit represents the total luminescence liberated by the cells in a single well of 96 well plate. Values are expressed as mean ± standard deviation. $*p < 0.05$ ($n = 12$). BOP, blast overpressure exposure.

mitochondrial pellet was suspended in the enzyme assay buffer and disrupted using a sonifier for the enzyme assay. The activity of GOT_2 was measured using the diagnostic kit for measuring GOT, obtained from Randox Laboratories (Kearneysville, WV) according to the manufacturer's instructions. The assay system utilizes the decrease in optical density at 340 nm due to the consumption of NADH during the formation of oxaloacetate and glutamate from aspartic acid and α-ketoglutaric acid catalyzed by GOT.

Statistical analysis

Statistical analysis was carried out by analysis of variance (ANOVA) using SAS software version 9.3 (SAS Institute, Inc., Cary, NC). For single variance, one-way ANOVA followed by *t* test was carried out. For multiple variance, two-way ANOVA followed by Tukey's post-hoc test using HSD multiple comparisons were used. A *p* value of less than 0.05 was considered significant.

Results

Blast exposure leads to acute decrease in neuronal ATP levels

Blast exposure causes a significant decrease in endogenous ATP levels in SH-SY5Y human neuroblastoma cells in a time-dependent manner with the highest decrease at 6 h post-blast, compared with 24 h post-blast (Fig. 1). Neuronal ATP levels were further decreased with multiple blast exposures. After single blast exposure, the ATP level decreased by 17.7% at 6 h, whereas no significant decrease was observed at 24 h post-blast. In the case of triple blast exposures, the ATP levels decreased by 44.6% and 27.7% by 6 h and 24 h, respectively.

ATP levels decreased in the cerebral cortex after blast exposures

Figure 2 shows the changes in ATP levels in the mouse brain cortex at different intervals after single and repeated blast exposures. Similar to the *in vitro* results, blast exposure of mice also resulted in a decrease in brain ATP levels, which varied relative to the time and number of blast exposures. Single blast exposure resulted in a 19.5% decrease in ATP levels at 6 h, whereas triple blasts resulted in a 23.4% decrease as early as 1 h. ATP levels were decreased by 39.7% at 6 h after repeated blast exposures, whereas the decrease was only 11.8% at 24 h post-blast. Thus, compared with by 6 h post-blast, the ATP levels were higher in the brain by 24 h post-blast but still lower than the sham controls which were not exposed to blast.

Proteomic analysis of the cerebral cortex to identify modulation of GOT_2 expression

Proteomic analysis data showed few proteins with >2 fold change in the cerebral cortex at 6 h after triple blast exposures. The proteins which showed >2 fold increase in expression after blast exposure include 14-3-3 protein gamma, calretinin, parvalbumin alpha, 14-3-3 protein zeta/delta, and calpastatin. One of the down-regulated proteins was identified by LC/MS/MS analysis as GOT_2 by matching five peptides. Figure 3 shows the image of the 2D-gel portion showing the expression of GOT_2 in the cortex after repeated blast exposures. GOT_2 expression showed a statistically significant abundance ratio (3.13 ± 0.76) between sham control and blast exposed mice suggesting that blast exposure alters the expression of GOT_2.

Western blotting of GOT_2 and PDH in the cerebral cortex after blast exposure

Western blotting using antibodies specific to GOT_2 showed a significant decrease (47.9%) in the expression of GOT_2 in the

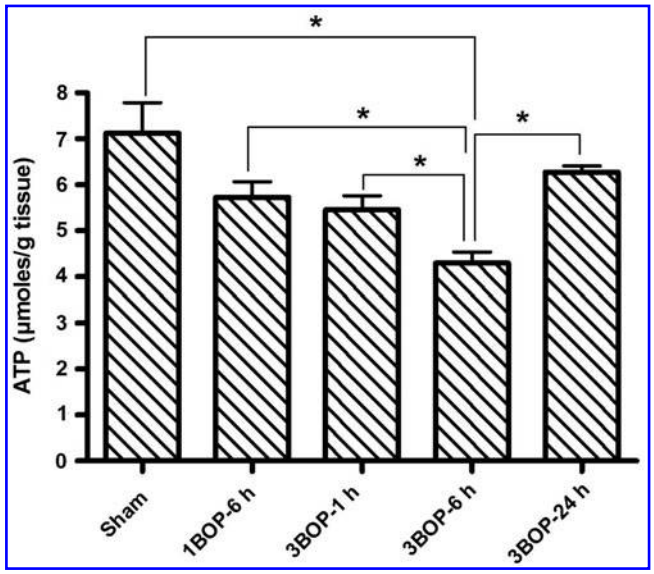

FIG. 2. Changes in adenosine triphosphate levels in cerebral cortex at different intervals after single and repeated blast exposures. Values are expressed as mean ± standard deviation. $*p < 0.05$ ($n = 6$). BOP, blast overpressure exposure.

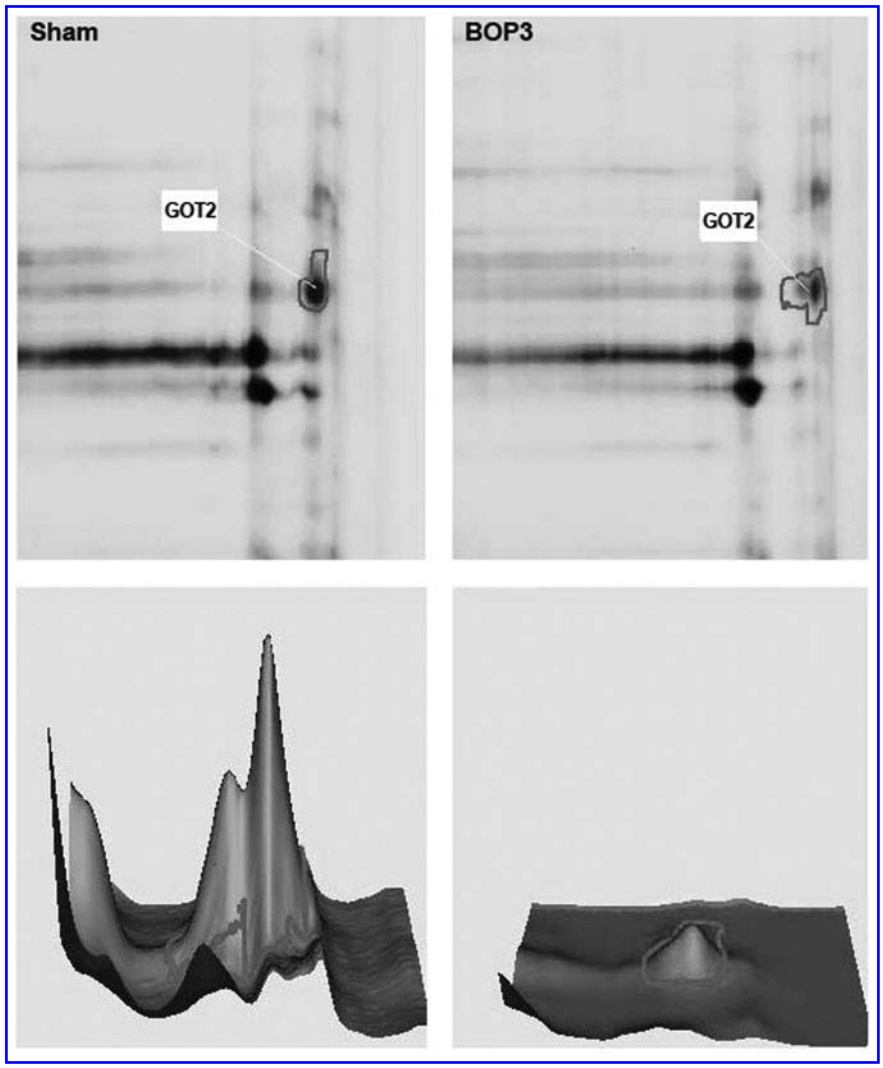

FIG. 3. Representative two-dimensional differential in-gel electrophoresis figure from three different animals in the sham control and blast exposed groups focusing the spot of glutamate oxaloacetate transaminase. Procedures used are detailed in the methods section. The bottom two panels show the sum of pixel intensities within the boundary of each spot in the fluorescent image to demonstrate the level of the protein.

cerebral cortex at 6 h after triple blast exposures, compared with sham controls (Fig. 4A). The ratio of GOT_2 to actin was 0.161 ± 0.025 for sham controls, whereas the ratios were 0.084 ± 0.028 for 6 h ($p = 0.021$) and 0.142 ± 0.036 for 24 h ($p = 0.44$; Fig. 4B). Compared with sham controls, single blast exposure at 6 h and triple blast exposure at 1 h, respectively, showed 20% (ratio of GOT_2 to actin was 0.124 ± 0.016, $p = 0.032$) and 29.9% (ratio of GOT_2 to actin was 0.113 ± 0.032, $p = 0.036$) decreases in the expression of GOT_2 in the cortex. Thus, similar to the reduction in ATP levels, the expression of GOT_2 decreased in the cerebral cortex after blast exposure. The decrease in GOT_2 expression depended upon the number of blast exposures, as well as the time after blast exposure; lowest expression was recorded at 6 h and returned toward normal levels by 24 h post-blast.

Western blotting of PDH with specific antibodies (Fig. 4A, C) showed significant decreases in the cerebral cortex at 6 h post-blast exposure. The decrease in the PDH level does not seem to correlate with ATP levels at 24 h after blast exposure.

Cerebral cortex mitochondrial GOT_2 activity after blast exposure

To determine further that the cerebral cortex mitochondrial GOT_2 activity was indeed decreased after blast exposure, the mitochondrial fraction was isolated from the cerebral cortex to avoid interference from the cytosolic isoform, GOT_1. Disrupted mitochondrial sample was used for measuring GOT_2 activity as described in the methods. The activity of GOT_2 in the mitochondrial fraction showed a 28.8 % decrease at 1 h and a 41.4 % decrease at 6 h after triple blast exposures. No significant changes in mitochondrial GOT_2 activity were observed at 24 h post-blast (Fig. 5).

Discussion

Our results show for the first time in an animal model that blast exposure leads to an acute mitochondrial dysfunction and an associated significant decrease in ATP levels in the brain. After a rapid decrease, the brain ATP levels return toward normal levels at 24 h post-blast exposures. Using the *in vitro* model of blast-induced

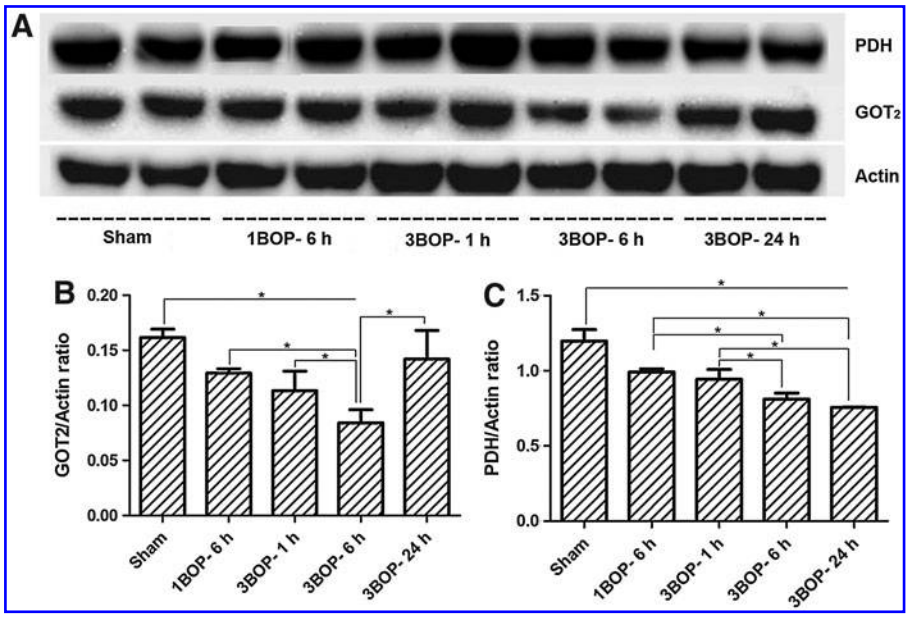

FIG. 4. Western blotting analysis of mice cerebral cortex at different intervals after single and repeated blast exposures. **(A)** Representative figure of the blot obtained from two animals each out of four animals in different groups studied. **(B)** Ratio of the band intensities corresponding to glutamate oxaloacetate transaminase and actin. Values are mean ± standard deviation (*$p < 0.05$, $n = 4$). **(C)** Ratio of the band intensities corresponding to PDH and actin. Values are mean ± standard deviation (*$p < 0.05$, n = 4).

TBI with NG108–15 cells (combination of neuroblastoma and glioblastoma cells), we have shown in a previous study that ATP levels decrease at 24 h after blast exposure.[17] Time points earlier than 24 h were not evaluated in that study. In the current study, we observed that a decrease in ATP levels after blast exposure occurs immediately and was most pronounced at 6 h, compared with at 24 h, indicating severe neuronal mitochondrial dysfunction acutely after blast exposure. The changes in ATP levels after blast exposure were similar *in vitro* and *in vivo*.

Acute mitochondrial dysfunction in the brain has been reported in different animal models of TBI.[18,20–22] Unlike blast-induced TBI, the mitochondrial dysfunction and associated decrease in ATP levels persisted for longer durations in the other forms of TBI. In a controlled cortical impact model of TBI, the ATP levels ipsilateral to the injury were only about 22 % of sham control even after six days post-injury.[18] In that study, the ATP levels measured ipsilaterally may have been associated with significant cell/tissue loss and the cells adjacent to the site of injury might have been undergoing necrosis/apoptosis. In the present study, we have shown that mitochondrial dysfunction and impaired energy production in the brain after blast exposure takes place acutely and the energy levels return toward normal levels by 24 h post-blast. This could be due to the lack of significant tissue loss in the brain after blast exposure. [3] Since delayed neuronal degeneration occurs after blast exposure,[1] it is possible that there could be a secondary phase of mitochondrial dysfunction after blast exposure, which would become evident several days post-exposure.

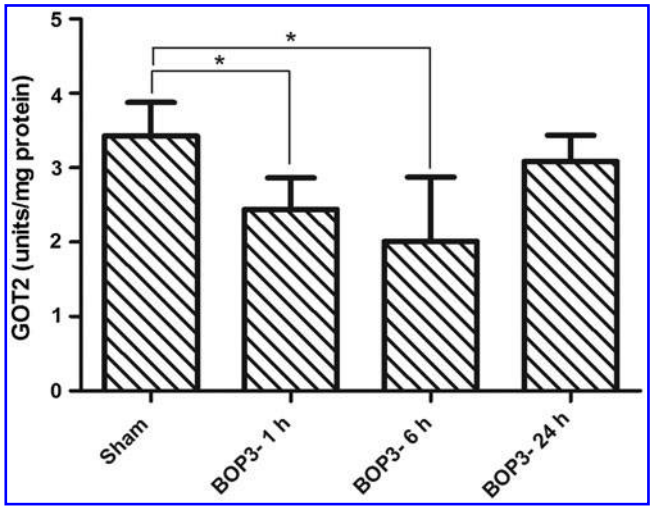

FIG. 5. Activity of glutamate oxaloacetate transaminase in the mitochondrial fraction of mice cerebral cortex at different intervals after repeated blast exposures. Values are mean ± standard deviation (*p < 0.05, $n = 6$).

In the present study, we found a correlation between the decrease in brain ATP levels and the reduced expression/activity of mitochondrial GOT_2. The protein expression and activity of GOT_2 were lowest in the brain at 6 h post-blast and were associated with the maximum decrease in ATP levels. The GOT_2 levels returned to almost normal by 24 h and the ATP level also was significantly restored. These data suggest a potential role of GOT_2 in the acute brain mitochondrial dysfunction associated with blast exposure. Detailed study is required to find out whether the synthesis or degradation of GOT_2 in the brain is affected after blast exposure. Using the same model system, it has been reported that modest levels of neuronal cell death occur immediately after repeated blast exposures, which also could contribute to the decreased tissue levels of ATP and GOT_2 measured after blast exposure.[3] The documented proliferation of astrocytes and microglia in the brain at 24 h after repeated blast exposure[11] can similarly contribute to the apparent recovery of ATP and GOT_2 by 24 h after repeated blast exposures.

A significant role for PDH in mitochondrial dysfunction after TBI has been reported in different brain injury models other than

SCIENTIFIC REPORTS

OPEN

SUBJECT AREAS:
WHITE MATTER INJURY
NEURODEGENERATION

Received
29 January 2014

Accepted
27 March 2014

Published
2 May 2014

Correspondence and requests for materials should be addressed to D.V.A. (denes.agoston@usuhs.edu.)

* Current address: Department of Neurosurgery, VA Medical Center-Research 151, Medical College of Wisconsin, 5000 West National Ave., Milwaukee, WI 53295.

Diffusion Tensor Imaging Reveals Acute Subcortical Changes after Mild Blast-Induced Traumatic Brain Injury

Alaa Kamnaksh[1,2], Matthew D. Budde[3]*, Erzsebet Kovesdi[4], Joseph B. Long[5], Joseph A. Frank[3] & Denes V. Agoston[1]

[1]Department of Anatomy, Physiology and Genetics, The Uniformed Services University, 4301 Jones Bridge Road, Bethesda, MD 20814, [2]Center for Neuroscience and Regenerative Medicine, The Uniformed Services University, 4301 Jones Bridge Road, Bethesda, MD 20814, [3]Radiology and Imaging Sciences, National Institute of Biomedical Imaging and Bioengineering, National Institutes of Health, Room B1N256 MSC 1074, 10 Center Drive, Bethesda, MD 20892, [4]US Department of Veterans Affairs, Veterans Affairs Central Office, 810 Vermont Avenue NW, Washington, DC 20420, [5]Blast-Induced Neurotrauma Branch, Center for Military Psychiatry and Neuroscience, Walter Reed Army Institute of Research, 503 Robert Grant Avenue, Silver Spring, MD 20910.

Mild blast-induced traumatic brain injury (mbTBI) poses special diagnostic challenges due to its overlapping symptomatology with other neuropsychiatric conditions and the lack of objective outcome measures. Diffusion tensor imaging (DTI) can potentially provide clinically relevant information toward a differential diagnosis. In this study, we aimed to determine if single and repeated (5 total; administered on consecutive days) mild blast overpressure exposure results in detectable structural changes in the brain, especially in the hippocampus. Fixed rat brains were analyzed by ex vivo DTI at 2 h and 42 days after blast (or sham) exposure(s). An anatomy-based region of interest analysis revealed significant interactions in axial and radial diffusivity in a number of subcortical structures at 2 h only. Differences between single- and multiple-injured rats were largely in the thalamus but not the hippocampus. Our findings demonstrate the value and the limitations of DTI in providing a better understanding of mbTBI pathobiology.

Mild traumatic brain injury (mTBI) continues to be the least understood form of traumatic brain injury (TBI) despite its high incidence and substantial toll on patients and health care systems[1]. In the military, mTBIs are mostly caused by the exposure to low levels of blast from improvised explosive devices resulting in mild blast-induced TBI (mbTBI)[2–4]. The diagnosis of mbTBI currently relies on subjective assessments and self-reports of symptoms such as disorientation, altered states of consciousness, headaches, and emotional and cognitive dysfunction—all of which are involved in post-traumatic stress disorder (PTSD)[5]. Because of the mild and transient nature of symptoms that follow mbTBI, soldiers typically return to duty and are frequently re-exposed to additional mild blasts. Studies have suggested that repeated mbTBI is a risk factor for developing late onset neurodegenerative conditions such as chronic traumatic encephalopathy (CTE)[6].

Objective outcome measures can provide especially valuable, clinically relevant information in a non-/minimally invasive and repeatable manner. Various modalities of magnetic resonance imaging (MRI), including diffusion tensor imaging (DTI), have been utilized in clinical settings following TBI[7–10]. However, only a limited number of clinical studies included readouts at several post-injury time points in Veterans[11–17]. DTI's sensitivity relative to conventional imaging tools has prompted its recent use in experimental mTBI[18–20] with a few rodent blast-induced TBI (bTBI) studies[21–24]. These studies identified a number of brain regions, including the hippocampus and the cerebellum, as being affected in mbTBI[25]. Injury-induced changes in serum, cerebrospinal fluid, and tissue protein biomarker levels have also been extensively investigated in both clinical and experimental TBI[26–28]. Together, imaging and molecular biomarkers would enable the monitoring of pathological processes over time and allow for more direct comparisons between experimental findings and clinical TBI cases.

The full potential and limitations of using imaging and molecular biomarkers in the diagnosis and monitoring of TBIs, especially mTBIs, are currently unknown due to a substantial gap between clinical and experimental findings and their translatability[29]. Furthermore, our understanding of how structural changes relate to cellular, molecular, and functional changes in TBI is very limited. Our previous works using the rodent model of single and repeated mbTBI recapitulated some of the behavioral changes that are observed in human bTBI[30]. Using histo-

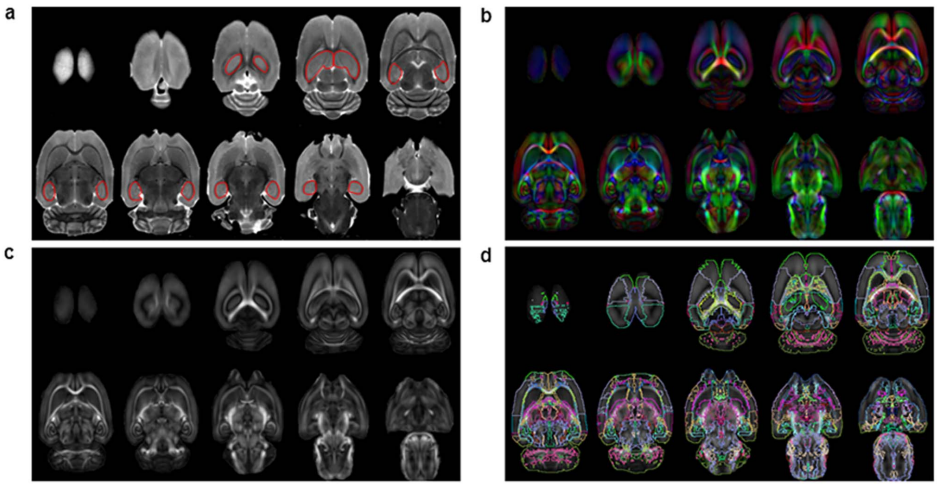

Figure 1 | MRI data analysis. (a) A T2-weighted image from a single subject with the hippocampus manually outlined in red. (b) A mean directionally encoded color image. (c) Map of FA derived from DTI of all spatially registered brains (every second slice is shown). (d) The registered anatomical ROIs derived from the atlas overlaid on the FA map for visualization.

logic and proteomic analyses of functionally relevant brain regions and peripheral blood, we identified several pathologies at different post-injury time points. These include neuronal and glial damage and/or death, axonal damage, metabolic and vascular changes, and inflammation. Additionally, we identified several pathologies that include neuronal and glial damage and/or death, axonal damage, metabolic and vascular changes, and inflammation at different post-injury time points using histologic and proteomic analyses of functionally relevant brain regions and peripheral blood[31–33]. In this preliminary imaging study, we aimed to determine if the same exposure to single and repeated mild blast overpressure that resulted in the abovementioned changes also induced structural changes that are detectable by DTI.

Results

We selected two of our previously tested post-injury termination time points, 2 h and 42 days, for the DTI analyses to mimic early and delayed clinical interventions. A manual region of interest (ROI) analysis was first used to assess hippocampal volume and fractional anisotropy (FA) in the hippocampus as shown in Fig. 1a. No significant differences were identified in hippocampal volume or FA values at either time point (Fig. 2). An anatomically defined ROI analysis was then performed as shown in Fig. 1b–d. In rats terminated ~2 h after blast (or sham) exposure(s), no brain regions had a significant interaction for FA. However, axial diffusivity (AD) and radial diffusivity (RD) had significant interactions in regions of the stria terminalis, thalamic subregions, and the cerebellum. Post hoc analysis revealed that the single-injured (SI) and multiple-injured (MI) groups were significantly different from one another largely in the thalamus and thalamic nuclei. Regions exhibiting significant blast event-related differences (i.e., single vs. repeated blast) are shown in Fig. 3 and Table 1; mean DTI values for these regions are provided in Fig. 4. No brain regions exhibited significant ROI changes in rats terminated 42 days after blast (or sham) exposure(s).

Discussion

Elucidating the role of repeated mbTBI in the development of neurodegenerative conditions is a pressing issue for the military health care system. To that end, a better understanding of mbTBI pathobiology, the period of cerebral vulnerability between insults, and the synergistic effect of repeated injury is critical. In conducting a series of studies comparing single and repeated mild blast injury (5 overpressure exposures administered on consecutive days), we aimed to assess the extent of the damage accumulation in mbTBI (i.e., the

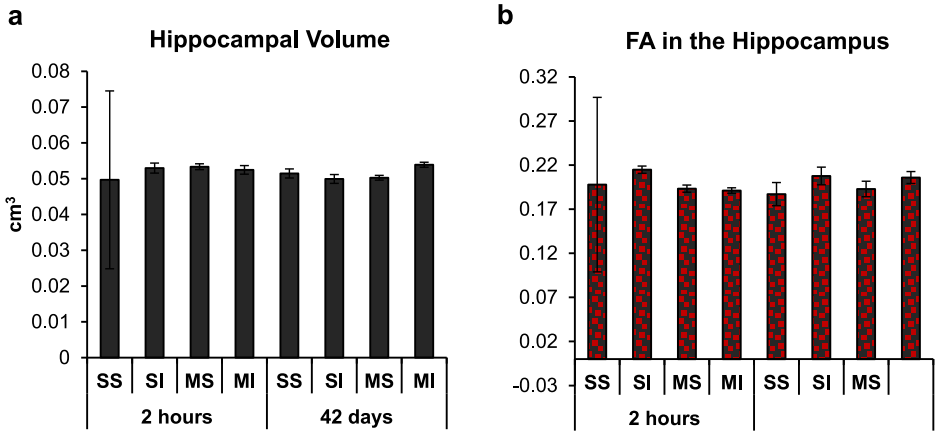

Figure 2 | Volumetric and DTI measures in the hippocampus. (a) Hippocampal volume (cm^3) of sham (SS, single sham; MS, multiple sham) and injured (SI, single-injured; MI, multiple-injured) rats terminated at 2 h and 45 days after blast (or sham) exposure(s). (b) Fractional anisotropy (FA) in the hippocampi of rats at the same time points. Data are presented as the mean ± SEM.

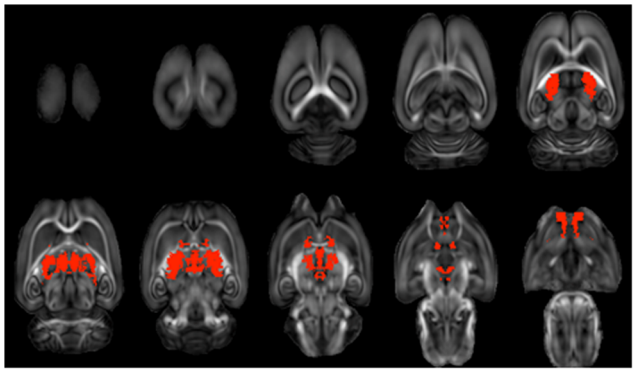

Figure 3 | Brain regions exhibiting significant ROI changes. Regions with a significant Blast x No. of Events interaction were first identified; those with significant differences between single-injured and multiple-injured rats (corrected for multiple comparisons) are shown in red.

cumulative effect of the injury) at different post-injury time points. Of particular interest to us is correlating cellular and molecular level changes with structural and neurocognitive changes toward a definitive diagnosis for mbTBI. The objective of this study was to determine if the exposure to single and repeated mild blast overpressure, which resulted in significant functional, cellular, and molecular changes, also induced structural changes that are detectable by ex vivo DTI.

Based on a number of bTBI studies that implicate the hippocampus in the development of neurobehavioral symptoms, we expected to detect injury-induced structural and/or volumetric changes in this region due to its involvement in TBI[34,35]. We previously found significantly increased numbers of apoptotic, TUNEL-positive cells in the hilus and granular cell layer of the hippocampus as early as 2 h post-injury in both single- and multiple-injured rats[36]. However, we found no significant changes in hippocampal volume or FA in the hippocampus in our current study. This discrepancy may be related to the current spatial resolution of DTI. Another plausible explanation is that even though we found significantly increased rates of cell death in the hippocampus, we also found a substantive gliotic response[30,31,33,37]. Such astroglial hypertrophy can potentially compensate for the loss in volume caused by cell death.

A recent ex vivo DTI rodent study has shown that the microstructure of the hippocampus can be significantly affected in mbTBI[23]. Consistent with impaired cognitive performance, FA values were significantly decreased in select brain regions of blast-exposed rats relative to their sham controls at 4 and 30 days post-injury. The affected brain regions included the hippocampus, thalamus, and brainstem. It is important to note, however, that the blast model and experimental design of our and the Budde et al. study are very different. Nonetheless, hippocampal abnormalities have been found in a number of clinical mbTBI studies using various imaging modalities[12,15,17,38–40].

Since no significant hippocampal changes were detected in our work, an automated, anatomical ROI analysis without a priori assumptions of affected regions was used to examine the brains[23]. Compared to a voxel by voxel approach that includes thousands of independent statistical tests, the whole brain anatomical ROI approach reduces the number of statistical comparisons but avoids tedious manual definition of brain regions[41]. The results of this analysis demonstrated significant changes that are largely confined to midline thalamic structures and the cerebellum. Post hoc analysis revealed that SI and MI rats were significantly different from one another in the thalamus and thalamic nuclei. Previous bTBI studies also found changes in the thalamus using DTI[23] and histological methods[42]. Thalamus-mediated functions account for a significant number of the most frequently reported neurobehavioral symptoms in clinical mbTBI. Among the leading complaints are sleep and emotional disturbances as well as altered sensory sensitivities, both auditory and visual[14].

Cerebellar abnormalities have been found in most human bTBI imaging studies[12,15,16,43] and in a recent rodent bTBI study[24]. These findings illustrate the region-specific vulnerability of the brain to different types of physical insults—an important albeit poorly understood issue in TBI. The cerebellum's susceptibility to injury maybe due to its anatomy; it is located in a relatively small sub-compartment of the skull and the ratio between cerebellar white and grey matters is different from that in the cerebrum. Primary blast injury mainly exerts damage at the interface of biological materials with differing physiochemical properties (e.g., grey and white matter). Indeed, white matter damage—including cerebellar white matter—has been found in virtually all human bTBI imaging studies. Functionally, the cerebellum is involved in certain cognitive and learning functions,

Table 1 | Brain regions exhibiting significant blast event-related effects at 2 h post-injury

	Fractional Anisotropy		Axial Diffusivity				Radial Diffusivity			
	Blast x No. of Events Interaction		Blast x No. of Events Interaction		SI vs. MI *t*-Test		Blast x No. of Events Interaction		SI vs. MI *t*-Test	
Brain Region	*F* value	*p* value[a]	*F* value	*p* value[b]	*t* value	*p* value[b]	*F* value	*p* value[b]	*t* value	*p* value[b]
Stria Terminalis	4.55	0.065	19.28	0.017	6.34	**0.023**	11.91	0.068	4.80	0.099
Posterior Hypothalamic Nucleus	1.25	0.296	13.56	0.043	3.78	0.145	13.57	0.048	4.06	0.189
Islands of Calleja	1.95	0.200	26.50	0.006	−9.89	**0.004**	34.55	0.003	−6.23	**0.042**
Olfactory Tubercle	1.02	0.341	35.79	0.002	−5.28	**0.048**	70.63	0.000	−7.95	**0.010**
Ventral Nucleus of Thalamus	0.98	0.352	29.78	0.004	9.02	**0.007**	20.89	0.014	6.81	**0.026**
Lateral Dorsal Nucleus of Thalamus	3.60	0.094	15.33	0.032	7.01	**0.017**	18.44	0.021	7.28	**0.021**
Lateral Posterior Nucleus of Thalamus	2.06	0.189	15.96	0.026	5.55	**0.040**	18.47	0.018	5.65	0.059
Central Lateral Nucleus of Thalamus	3.09	0.117	20.11	0.014	7.18	**0.014**	24.46	0.009	8.05	**0.005**
Medial Dorsal Thalamus	1.93	0.203	15.71	0.029	7.74	**0.011**	17.07	0.026	7.31	**0.016**
Midline Thalamic Nuclei	7.55	0.025	21.27	0.011	10.00	**0.002**	15.91	0.031	6.72	**0.031**
Thalamus	0.35	0.568	13.29	0.047	4.85	0.065	13.89	0.044	4.77	0.108
Cerebellum	4.24	0.073	17.26	0.022	−3.41	0.212	21.95	0.011	−5.05	0.089

[a]uncorrected.
[b]false discovery rate corrected.
SI, single-injured ($n = 3$); MI, multiple-injured ($n = 3$).
Statistically significant differences between SI and MI rats are indicated in boldface.

hence the detected changes are consistent with clinically observed abnormalities[44,45].

Among the other affected brain structures is the stria terminalis, which serves as a major relay site within the hypothalamic-pituitary-adrenal axis[46]. Similar changes were also found in the olfactory tubercule, including the islands of Calleja. The olfactory tubercule has been shown to play a role in behavioral response as it is interconnected with several brain regions with sensory and arousal/reward functions[47]. In fact, injury to the islands as a result of restricted blood flow has been linked to a number of behavioral and emotional responses such as amnesia and changes in personality—behavioral changes that are not possible to assess in animal models.

A critical limitation toward better understanding human mbTBI is inherent variability as well as the unknown biophysical forces that are experienced during injury. Additionally, most existing DTI studies of veterans have been performed years after the injury. Animal models of mbTBI allow for direct testing of the many effects of blast wave characteristics under carefully controlled conditions[48]. However, we currently have no clear understanding of how human years (physiologically and pathologically speaking) translate into rat months (or weeks). Furthermore, the lack of a consensus regarding a high fidelity experimental bTBI model—as demonstrated by the imaging findings obtained using various blast models—is a major impediment to studying the physical and biological effects of primary blast injury.

Another pressing issue is how DTI findings in mbTBI (or any other neurological disorder) relate to changes detectable by proteomics or histology. We emphasize this point because although rats terminated at 42 days did not exhibit significant ROI changes as measured by DTI, proteomic analyses of plasma at the same time point showed significant and persistent molecular pathologies in SI as well as MI rats[36,49]. These include inflammation, metabolic and vascular changes, neuronal and glial cell damage and/or death, and axonal damage.

A technical limitation of our study is the use of fixed tissues in ex vivo DTI, mainly due to altered diffusivity of water molecules. Nonetheless, previous studies have demonstrated that ex vivo DTI provides valuable structural information that correlates with in vivo changes albeit to a varying extent. This may partially account for the poor correlation between cellular changes obtained by conventional histology and volumetric/DTI measures in the hippocampus. It should be noted that animal in vivo imaging has its own issues with scanning times (and corresponding anesthesia times), image acquisition protocols, and motion artifacts being the major ones.

Despite the increased attention in recent years on blast as a mechanism of mTBI, the subject of how blast waves affect the brain along with diagnosing mbTBI are still a matter of considerable debate. The abovementioned caveats underline the importance of combining objective and clinically relevant outcome measures in experimental TBI to validate and correlate findings, to enable more direct comparisons of pathologies observed in animal and in clinical TBI research, and to enable the development of sensitive and specific diagnostics for mbTBI[29].

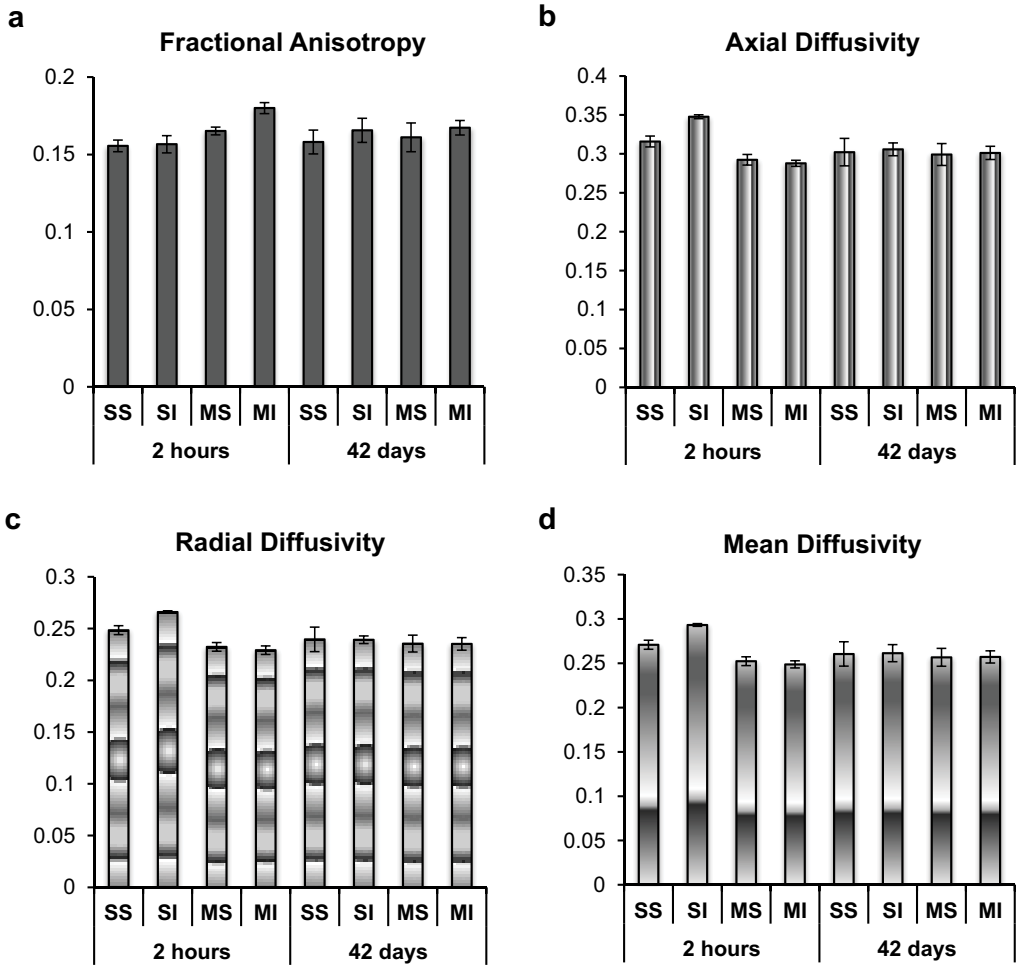

Figure 4 | Mean DTI values at the two time points. Data were extracted from each subject as a single value from the ROIs showing significance in the anatomical ROI analysis. Data are presented as the mean ± SEM for each experimental group (SS, single sham; SI, single-injured; MS, multiple sham; MI, multiple-injured).

Methods

Animals and housing conditions. A total of 60 male Sprague Dawley rats (weight at arrival: 245–265 g) (Charles River Laboratories, Wilmington, MA) were used in the original experiments[36,49]. All animals were housed in standard rat cages with a built-in filter in a reverse 12-h light 12-h dark cycle with food and water ad lib. Animals were handled according to protocol approved by the Institutional Animal Care and Use Committee at the Uniformed Services University (USU; Bethesda, MD).

Experimental groups and manipulations. All animals underwent a 5 day acclimation and handling period and were later assigned to the following groups: naïve, single sham (SS), single-injured (SI), multiple sham (MS), and multiple-injured (MI) as described earlier[36,49]. Rat numbers in the early and late termination groups were: ($N = 30$; naïve = 3, SS = 6, SI = 7, MS = 6, MI = 8) and ($N = 30$; naïve = 3, SS = 6, SI = 7, MS = 6, MI = 8), respectively. Naïve rats were kept in the animal facility at USU without any manipulation for the duration of the studies. SS rats were transported once from USU to Walter Reed Army Institute of Research (Silver Spring, MD) and anesthetized in an induction chamber with a 4% isoflurane (Forane; Baxter Healthcare Corporation, Deerfield, IL) in air mixture delivered at 2 L/min for 6 min. MS rats were similarly transported and anesthetized once per day for 5 consecutive days. SI and MI rats underwent the same procedures as their respective sham controls in addition to receiving a single or multiple (5 total) mild blast exposure(s)[36,49].

Injury conditions. Anesthetized rats in chest protection (weight at injury: 300–330 g) were placed in the shock tube holder in a transverse prone position with the right side facing the direction of the membrane and the incidence of the blast waves. Blast overpressure was generated using a compressed air-driven shock tube yielding a single blast overpressure wave (average peak total pressure: ~137 kPa at the animal level) to produce a mild injury as described in detail[31,37,50]. Following blast (or equivalent time spent anesthetized as a sham), animals were moved to an adjacent bench top for observation and then transported back to the USU animal facility at the conclusion of each injury day.

Preparation of specimens for imaging. A subset of animals from each experiment [(2 h termination: $n = 11$; SS = 2, SI = 3, MS = 3, MI = 3) and (42 day termination: $n = 16$; SS = 4, SI = 4, MS = 4, MI = 4)] was used for MRI/DTI analyses; all other animals were used for proteomics as described earlier[36,49]. Rats were deeply anesthetized with isoflurane inhalant until a tail pinch produced no reflex movement, then transcardially perfused with cold phosphate-buffered saline (PBS) followed by a 4% paraformaldehyde in 1x PBS solution. The brains were removed and post-fixed in the same solution overnight at 4°C and then transferred to a 1x PBS solution containing 0.1% sodium azide until scanning. No hemorrhage or any other signs of macroscopic damage were detected in any of the animals.

Image acquisition. Fixed brains underwent ex vivo DTI within 2 days of perfusion fixation on a Bruker 7 T vertical bore system. Brains were immersed in susceptibility-matching fluid (Fomblin; Solvay Solexis, Inc., West Deptford, NJ) and inserted into a radiofrequency coil 3 cm in diameter. A three-echo diffusion-weighted spin echo sequence was employed (TR = 4 s; TE = 20 ms (first echo; 7.5 ms echo spacing) to acquire diffusion-weighted images (b = 1200 s/mm^2) along 30 directions[51] with diffusion gradient duration (δ) and separation (Δ) of 4 and 10 ms, respectively, along with 5 non diffusion-weighted images[52]. The slice thickness was 0.5 mm with an in-plane resolution of 0.234 mm^2 and a 30 mm^2 field of view (128^2 matrix). The full experiment required 6 h of continuous imaging. DTI data was reconstructed using a linear least squares fit to derive parameter maps of FA, AD, and RD using custom Matlab routines[53].

Data analysis. The analysis of MRI data included volumetric and DTI measures in the hippocampus and an anatomical ROI analysis of DTI data without a priori assumptions of affected regions. Hippocampal volume and FA in the hippocampus were derived from manual segmentation of the hippocampus on T2-weighted and FA maps, respectively, by an operator blinded to animal conditions. For unbiased quantification of DTI measures using anatomically based ROIs, DTI volumes from all subjects were first registered to a common space using an iterative, tensor-based registration routine implemented in DTI-TK[54]. Rigid-body, affine, and diffeomorphic (piecewise affine) methods were used in succession to progressively improve registration accuracy, as this approach has been shown to be superior to other routines[55]. The final image resolution was 120 × 120 × 500 μm^3. Anatomical ROIs were derived from a digital rat brain atlas included as part of the Medical Image Visualization and Analysis Software (MIVA) software package[56]. The regions consisted of 87 subregions of the brain initially derived from the Paxinos Rat brain atlas[57]. A mask of white matter regions derived from the atlas was registered to a mask of white matter regions derived from DTI by thresholding the FA maps at 0.2. An FA value of 0.2 was chosen empirically since it effectively masked the white matter tracts. It should be noted that this threshold value was used for the registration of the ROIs, not for quantification. Registration employed a point-set based registration metric incorporated into Advanced Normalization Tools (ANTS) software package, including elastic warping[58]. The resulting overlap demonstrated high correspondence between the DTI and atlas-based white matter structures (Fig. 1C). The mean FA, AD, and RD within each ROI were derived from each of the registered DTI volumes from each subject for subsequent statistical analysis (Fig. 4).

Statistical analysis. Twenty-seven animals were used for the analyses (2 h termination, $N = 11$; 42 day termination, $N = 16$). A mixed-effect ANOVA was first performed to identify any significant effects of left/right (L/R) asymmetry. Since none of the brain regions exhibited a significant Blast x No. of Events x Side (L/R) interaction, the effect of side was collapsed for all subsequent analyses. For hippocampal volume and FA in the hippocampus, ANOVAs followed by Tukey's HSD test were performed separately at each time point. Subsequently, a one-way ANOVA was performed for each condition across the two time points.

For DTI, a two-way ANOVA was performed to compare the main effects of Blast x No. of Events interaction. Regions that exhibited a significant interaction were subjected to post-hoc analysis using a Student's t-test to compare the SI and MI groups. All statistical tests were corrected for multiple comparisons (87 individual ROIs) by controlling for the false discovery rate[59]. A Spearman correlation analysis was used to identify brain regions significantly correlated to either the number of blast events or the number of sham events. A corrected p value of 0.05 was considered significant for all tests.

1. Laker, S. R. Epidemiology of concussion and mild traumatic brain injury. *PM R* **3**, S354–358; DOI:10.1016/j.pmrj.2011.07.017 (2011).
2. Hendricks, A. M. *et al.* Screening for mild traumatic brain injury in OEF-OIF deployed US military: an empirical assessment of VHA's experience. *Brain. Inj.* **27**, 125–134; DOI:10.3109/02699052.2012.729284 (2013).
3. Vanderploeg, R. D. *et al.* Health outcomes associated with military deployment: mild traumatic brain injury, blast, trauma, and combat associations in the Florida National Guard. *Arch. Phys. Med. Rehabil.* **93**, 1887–1895; DOI:10.1016/j.apmr.2012.05.024 (2012).
4. Xydakis, M. S., Ling, G. S., Mulligan, L. P., Olsen, C. H. & Dorlac, W. C. Epidemiologic aspects of traumatic brain injury in acute combat casualties at a major military medical center: a cohort study. *Ann. Neurol.* **72**, 673–681; DOI:10.1002/ana.23757 (2012).
5. Brenner, L. A., Vanderploeg, R. D. & Terrio, H. Assessment and diagnosis of mild traumatic brain injury, posttraumatic stress disorder, and other polytrauma conditions: burden of adversity hypothesis. *Rehabil. Psychol.* **54**, 239–246; DOI:10.1037/a0016908 (2009).
6. Stern, R. A. *et al.* Long-term consequences of repetitive brain trauma: chronic traumatic encephalopathy. *PM R* **3**, S460–467; DOI:10.1016/j.pmrj.2011.08.008 (2011).
7. Aoki, Y., Inokuchi, R., Gunshin, M., Yahagi, N. & Suwa, H. Diffusion tensor imaging studies of mild traumatic brain injury: a meta-analysis. *J. Neurol. Neurosurg. Psychiatry* **83**, 870–876; DOI:10.1136/jnnp-2012-302742 (2012).
8. Shenton, M. E. *et al.* A review of magnetic resonance imaging and diffusion tensor imaging findings in mild traumatic brain injury. *Brain Imaging Behav.* **6**, 137–192; DOI:10.1007/s11682-012-9156-5 (2012).
9. Voelbel, G. T., Genova, H. M., Chiaravalotti, N. D. & Hoptman, M. J. Diffusion tensor imaging of traumatic brain injury review: implications for neurorehabilitation. *NeuroRehabilitation* **31**, 281–293; DOI:10.3233/nre-2012-0796 (2012).
10. Xiong, K. L., Zhu, Y. S. & Zhang, W. G. Diffusion tensor imaging and magnetic resonance spectroscopy in traumatic brain injury: a review of recent literature. *Brain Imaging Behav.* DOI:10.1007/s11682-013-9288-2 (2014).
11. Benzinger, T. L. *et al.* Blast-related brain injury: imaging for clinical and research applications: report of the 2008 st. Louis workshop. *J. Neurotrauma* **26**, 2127–2144; DOI:10.1089/neu.2009-0885 (2009).
12. Levin, H. S. *et al.* Diffusion tensor imaging of mild to moderate blast-related traumatic brain injury and its sequelae. *J. Neurotrauma* **27**, 683–694; DOI:10.1089/neu.2009.1073 (2010).
13. Mendez, M. F. *et al.* Mild traumatic brain injury from primary blast vs. blunt forces: post-concussion consequences and functional neuroimaging. *NeuroRehabilitation* **32**, 397–407; DOI:10.3233/nre-130861 (2013).
14. Petrie, E. C. *et al.* Neuroimaging, behavioral, and psychological sequelae of repetitive combined blast/impact mild traumatic brain injury in Iraq and Afghanistan war veterans. *J. Neurotrauma* **31**, 425–436; DOI:10.1089/neu.2013.2952 (2014).
15. Matthews, S. C. *et al.* A multimodal imaging study in U.S. veterans of Operations Iraqi and Enduring Freedom with and without major depression after blast-related concussion. *Neuroimage* **54**, S69–75; DOI:10.1016/j.neuroimage.2010.04.269 (2011).
16. Mac Donald, C. *et al.* Cerebellar white matter abnormalities following primary blast injury in US military personnel. *PLoS ONE* **8**, e55823; DOI:10.1371/journal.pone.0055823 (2013).
17. Matthews, S. C., Spadoni, A. D., Lohr, J. B., Strigo, I. A. & Simmons, A. N. Diffusion tensor imaging evidence of white matter disruption associated with loss versus alteration of consciousness in warfighters exposed to combat in Operations Enduring and Iraqi Freedom. *Psychiatry Res.* **204**, 149–154; DOI:10.1016/j.pscychresns.2012.04.018 (2012).
18. Bennett, R. E., Mac Donald, C. L. & Brody, D. L. Diffusion tensor imaging detects axonal injury in a mouse model of repetitive closed-skull traumatic brain injury. *Neurosci. Lett.* **513**, 160–165; DOI:10.1016/j.neulet.2012.02.024 (2012).
19. Albensi, B. C. *et al.* Diffusion and high resolution MRI of traumatic brain injury in rats: time course and correlation with histology. *Exp. Neurol.* **162**, 61–72; DOI:10.1006/exnr.2000.7256 (2000).

20. Cernak, I. *et al.* The pathobiology of moderate diffuse traumatic brain injury as identified using a new experimental model of injury in rats. *Neurobiol. Dis.* **17**, 29–43; DOI:10.1016/j.nbd.2004.05.011 (2004).
21. Henninger, N. *et al.* Differential recovery of behavioral status and brain function assessed with functional magnetic resonance imaging after mild traumatic brain injury in the rat. *Crit. Care Med.* **35**, 2607–2614; DOI:10.1097/01.ccm.0000286395.79654.8d (2007).
22. van de Looij, Y. *et al.* Diffusion tensor imaging of diffuse axonal injury in a rat brain trauma model. *NMR Biomed.* **25**, 93–103; DOI:10.1002/nbm.1721 (2012).
23. Budde, M. D. *et al.* Primary blast traumatic brain injury in the rat: relating diffusion tensor imaging and behavior. *Front. Neurol.* **4**, 154; DOI:10.3389/fneur.2013.00154 (2013).
24. Calabrese, E. *et al.* Diffusion tensor imaging reveals white matter injury in a rat model of repetitive blast-induced traumatic brain injury. *J. Neurotrauma.* DOI:10.1089/neu.2013.3144 (2014).
25. Morey, R. A. *et al.* Effects of chronic mild traumatic brain injury on white matter integrity in Iraq and Afghanistan war veterans. *Hum. Brain Mapp.* **34**, 2986–2999; DOI:10.1002/hbm.22117 (2013).
26. Di Battista, A. P., Rhind, S. G. & Baker, A. J. Application of blood-based biomarkers in human mild traumatic brain injury. *Front. Neurol.* **4**, 44; DOI:10.3389/fneur.2013.00044 (2013).
27. Kobeissy, F. H. *et al.* Neuroproteomics and systems biology-based discovery of protein biomarkers for traumatic brain injury and clinical validation. *Proteomics Clin. Appl.* **2**, 1467–1483; DOI:10.1002/prca.200800011 (2008).
28. Wang, K. K. *et al.* Proteomic identification of biomarkers of traumatic brain injury. *Expert Rev. Proteomics* **2**, 603–614; DOI:10.1586/14789450.2.4.603 (2005).
29. Agoston, D. V., Risling, M. & Bellander, B. M. Bench-to-bedside and bedside back to the bench; coordinating clinical and experimental traumatic brain injury studies. *Front. Neurol.* **3**, 3; DOI:10.3389/fneur.2012.00003 (2012).
30. Kwon, S. K. *et al.* Stress and traumatic brain injury: a behavioral, proteomics, and histological study. *Front. Neurol.* **2**, 12; DOI:10.3389/fneur.2011.00012 (2011).
31. Kamnaksh, A. *et al.* Factors affecting blast traumatic brain injury. *J. Neurotrauma* **28**, 2145–2153; DOI:10.1089/neu.2011.1983 (2011).
32. Kovesdi, E. *et al.* The effect of enriched environment on the outcome of traumatic brain injury; a behavioral, proteomics, and histological study. *Front. Neurosci.* **5**, 42; DOI:10.3389/fnins.2011.00042 (2011).
33. Kovesdi, E. *et al.* Acute minocycline treatment mitigates the symptoms of mild blast-induced traumatic brain injury. *Front. Neurol.* **3**, 111; DOI:10.3389/fneur.2012.00111 (2012).
34. Orrison, W. W. *et al.* Traumatic brain injury: a review and high-field MRI findings in 100 unarmed combatants using a literature-based checklist approach. *J. Neurotrauma* ***26***, 689–701; DOI:10.1089/neu.2008.0636 (2009).
35. Bigler, E. D. Quantitative magnetic resonance imaging in traumatic brain injury. *J. Head Trauma Rehabil.* **16**, 117–134 (2001).
36. Kamnaksh, A. *et al.* Neurobehavioral, cellular, and molecular consequences of single and multiple mild blast exposure. *Electrophoresis* **33**, 3680–3692; DOI:10.1002/elps.201200319 (2012).
37. Ahmed, F. *et al.* Time-dependent changes of protein biomarker levels in the cerebrospinal fluid after blast traumatic brain injury. *Electrophoresis* **33**, 3705–3711; DOI:10.1002/elps.201200299 (2012).
38. Hetherington, H. P. *et al.* MRSI of the medial temporal lobe at 7 T in explosive blast mild traumatic brain injury. *Magn. Reson. Med.* **71**, 1358–1367; DOI:10.1002/mrm.24814 (2014).
39. Masel, B. E. *et al.* Galveston Brain Injury Conference 2010: clinical and experimental aspects of blast injury. *J. Neurotrauma* **29**, 2143–2171; DOI:10.1089/neu.2011.2258 (2012).
40. Scheibel, R. S. *et al.* Altered brain activation in military personnel with one or more traumatic brain injuries following blast. *J. Int. Neuropsychol. Soc.* **18**, 89–100; DOI:10.1017/s1355617711001433 (2012).
41. Lu, H. *et al.* Registering and analyzing rat fMRI data in the stereotaxic framework by exploiting intrinsic anatomical features. *Magn. Reson. Imaging* **28**, 146–152; DOI:10.1016/j.mri.2009.05.019 (2010).
42. Goldstein, L. E. *et al.* Chronic traumatic encephalopathy in blast-exposed military veterans and a blast neurotrauma mouse model. *Sci. Transl. Med.* **4**, 134ra60; DOI:10.1126/scitranslmed.3003716 (2012).
43. Jorge, R. E. *et al.* White matter abnormalities in veterans with mild traumatic brain injury. *Am. J. Psychiatry* **169**, 1284–1291; DOI:10.1176/appi.ajp.2012.12050600 (2012).
44. Stoodley, C. J. The cerebellum and cognition: evidence from functional imaging studies. *Cerebellum* **11**, 352–365; DOI:10.1007/s12311-011-0260-7 (2012).
45. Van Overwalle, F., Baetens, K., Marien, P. & Vandekerckhove, M. Social cognition and the cerebellum: A meta-analysis of over 350 fMRI studies. *Neuroimage* **86**, 554–572; DOI:10.1016/j.neuroimage.2013.09.033 (2014).
46. Crestani, C. C. *et al.* Mechanisms in the bed nucleus of the stria terminalis involved in control of autonomic and neuroendocrine functions: a review. *Curr. Neuropharmacol.* **11**, 141–159; DOI:10.2174/1570159x11311020002 (2013).
47. Rodrigo, J. *et al.* Physiology and pathophysiology of nitric oxide in the nervous system, with special mention of the islands of Calleja and the circunventricular organs. *Histol. Histopathol.* **17**, 973–1003 (2002).
48. Bass, C. R. *et al.* Brain injuries from blast. *Ann. Biomed. Eng.* **40**, 185–202; DOI:10.1007/s10439-011-0424-0 (2012).
49. Ahmed, F. A., Kamnaksh, A., Kovesdi, E., Long, J. B. & Agoston, D. V. Long-term consequences of single and multiple mild blast exposure on select physiological parameters and blood-based biomarkers. *Electrophoresis* **34**, 2229–2233; DOI:10.1002/elps.201300077 (2013).
50. Long, J. B. *et al.* Blast overpressure in rats: recreating a battlefield injury in the laboratory. *J. Neurotrauma* ***26***, 827–840; DOI:10.1089/neu.2008.0748 (2009).
51. Hasan, K. M., Parker, D. L. & Alexander, A. L. Comparison of gradient encoding schemes for diffusion-tensor MRI. *J. Magn. Reson. Imaging* **13**, 769–780 (2001).
52. Budde, M. D. & Frank, J. A. Examining brain microstructure using structure tensor analysis of histological sections. *Neuroimage* **63**, 1–10, DOI:10.1016/j.neuroimage.2012.06.042 (2012).
53. Budde, M. D., Janes, L., Gold, E., Turtzo, L. C. & Frank, J. A. The contribution of gliosis to diffusion tensor anisotropy and tractography following traumatic brain injury: validation in the rat using Fourier analysis of stained tissue sections. *Brain* **134**, 2248–2260; DOI:10.1093/brain/awr161 (2011).
54. Zhang, H., Yushkevich, P. A., Alexander, D. C. & Gee, J. C. Deformable registration of diffusion tensor MR images with explicit orientation optimization. *Med. Image Anal.* **10**, 764–785; DOI:10.1016/j.media.2006.06.004 (2006).
55. Adluru, N. *et al.* A diffusion tensor brain template for rhesus macaques. *Neuroimage* **59**, 306–318; DOI:10.1016/j.neuroimage.2011.07.029 (2012).
56. Ferris, C. F. *et al.* Functional magnetic resonance imaging in awake animals. *Rev. Neurosci.* **22**, 665–674; DOI:10.1515/rns.2011.050 (2011).
57. Paxinos, G. & Watson, C. *The Rat Brain in Stereotactic Coordinates.* (Academic Press, 2007).
58. Avants, B. B. *et al.* A reproducible evaluation of ANTs similarity metric performance in brain image registration. *Neuroimage*, **54**, 2033–2044; DOI:10.1016/j.neuroimage.2010.09.025 (2011).
59. Benjamini, Y., Drai, D., Elmer, G., Kafkafi, N. & Golani, I. Controlling the false discovery rate in behavior genetics research. *Behav. Brain Res.* **125**, 279–284 (2001).

Acknowledgments

We thank the Neurotrauma Team at the Walter Reed Army Institute of Research for their technical help during the exposures, along with Eric Gold and Lindsay Janes for assistance with the MRI experiments. This work was supported by the Center for Neuroscience and Regenerative Medicine grant number G1703F.

Author contributions

A.K. and E.K. carried out animal studies, including the preparation of specimens for imaging. J.L. designed and supervised blast overpressure exposures at Walter Reed. M.B. performed and analyzed MRI/DTI measures under J.F.'s supervision at the NIH. A.K., M.B., and D.A. wrote the main manuscript text; A.K. and M.B. generated and formatted figures 1–4 and table 1. A.K. and D.A. reviewed the manuscript prior to submission.

Additional information

Competing financial interests: The authors declare no competing financial interests.

How to cite this article: Kamnaksh, A. *et al.* Diffusion Tensor Imaging Reveals Acute Subcortical Changes after Mild Blast-Induced Traumatic Brain Injury. *Sci. Rep.* **4**, 4809; DOI:10.1038/srep04809 (2014).

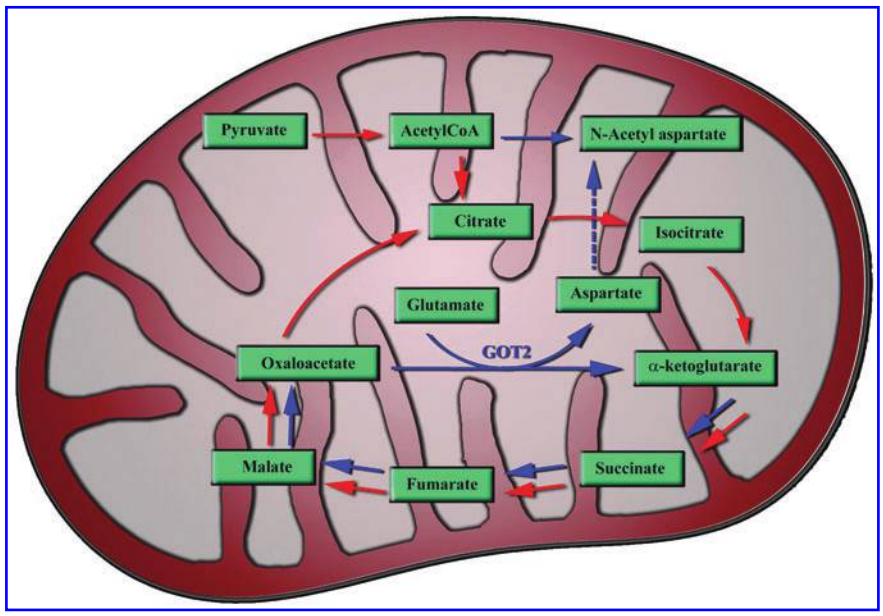

FIG. 6. Schematic representation of the neuronal mitochondria showing the proposed ''mini citric acid cycle'' involving glutamate oxaloacetate transaminase. Red arrow shows the regular citric acid cycle pathway and the blue arrow shows the ''mini citric acid cycle.'' Most of the energy producing steps is in the ''mini citric acid cycle.''

blast TBI.[23,24] Following controlled cortical impact (CCI) in rats, Opii and colleagues showed that PDH activity decreases in the cortex due to oxidative modification of the enzyme.[24] In another CCI study, the level of PDH decreased in the ipsilateral and contralateral sides of the brain at 4 h and decreased further by 24 h post-injury, similar to our present results following blast exposure.[25] Phosphorylation of PDH (p-PDH) has been implicated in the decrease of its activity in the CCI model.[25] After CCI injury, the ratio of p-PDH/PDH decreased at 4 h, increased at 24 h and decreased again at seven days indicating that the activity of PDH will be less at 24 h, compared with at 4 h and at seven days.[25] An imbalance in the activities of PDH kinase and PDH phosphatase in the brain has been implicated in the decreased activity of PDH after CCI.[26] A significant decrease in PDH also was observed in the brain at 72 h following fluid percussion injury, which was the single time point studied.[27] Our results in the blast TBI model also showed decreased expression of PDH, but did not show a direct correlation with the changes in ATP levels.

The potential role of GOT_2 in mitochondrial energy metabolism in the brain has been described earlier.[14,28–30] Figure 6 shows the schematic representation of the role of GOT_2 in brain energy metabolism involving the ''mini citric acid cycle,'' which was proposed by Yudkoff and colleagues in 1994.[16] Using radiolabeled aspartate and glutamine in brain synaptosomal preparations, Yudkoff and colleagues showed that amino acids could provide an alternate source of energy to help maintain ATP levels in the brain through ''mini citric acid cycle''.[16] They also found that in the brain synaptosomes, the fastest reaction that provides metabolite input to the citric acid cycle is that of GOT_2.[16] The ''mini citric acid cycle'' in the brain utilizes glutamine/glutamate for energy production instead of pyruvate, and bypasses a few initial steps in the regular citric acid cycle for faster energy production as required for neuronal activity.[14–16] As shown in the Figure 6, GOT_2 plays a major role in the truncated citric acid cycle. The excess aspartate formed through the ''mini citric acid cycle'' is used for N-acetyl aspartate (NAA) synthesis in the mitochondria,[14] which also explains the high concentrations of glutamate and NAA in the brain, where they are the most abundant molecules. By using GOT_2 to convert glutamate to α-ketogutarate, neurons avoid the formation of toxic ammonia, which is critical in the absence of a urea cycle in the brain.[14,28] Thus, GOT_2 plays a significant role in neuronal energy metabolism and its down regulation after blast exposure might contribute to the decreased ATP levels in the brain. Since low levels of ATP can significantly affect neuronal function, pharmaceutical interventions, which can rapidly restore or provide ATP rapidly to neurons, would potentially be beneficial after blast TBI. In this connection, supplementation to the brain of acetate, which can generate ATP, significantly increased brain ATP levels and improved motor performances in rats subjected TBI using CCI.[18]

Disclaimer

The contents, opinions and assertions contained herein are private views of the authors and are not to be construed as official or reflecting the views of the Department of the Army or the Department of Defense.

Acknowledgments

Support from Mrs. Irene Gist, Blast-induced Neurotrauma Branch, COL, Paul Bliese, Director, Center for Military Psychiatry and Neurosciences at the Walter Reed Army Institute of Research, and Mrs. Patricia Stroy is gratefully acknowledged.

Author Disclosure Statement

No competing financial interests exist

References

1. Magnuson, J., Leonessa, F., and Ling, G.S. (2012). Neuropathology of explosive blast traumatic brain injury. Curr. Neurol. Neurosci. Rep. 12, 570–579.

2. Warden, D. (2006). Military TBI during the Iraq and Afghanistan wars. J. Head Trauma Rehabil. 21, 398–402.
3. Wang, Y., Wei, Y., Oguntayo, S., Wilkins, W., Arun, P., Valiyaveettil, M., Song, J., Long, J., and Nambiar, M.P. (2011). Tightly coupled repetitive blast-induced traumatic brain injury: Development and Characterization in Mice. J. Neurotrauma 28, 2171–2183.
4. Duckworth, J.L., Grimes, J., and Ling G.S. (2013). Pathophysiology of battlefield associated traumatic brain injury. Pathophysiology 20, 23–30.
5. Kocsis, J.D., and Tessler, A. (2009). Pathology of blast-related brain injury. J. Rehabil. Res. Dev. 46, 667–672.
6. Saljo, A., Bao, F., Shi, J., Hamberger, A., Hansson, H.A., and Haglid, K.G. (2002). Expression of c-Fos and c-Myc and deposition of beta-APP in neurons in the adult rat brain as a result of exposure to short-lasting impulse noise. J. Neurotrauma 19,379–385.
7. Cernak, I., Wang, Z., Jiang, J., Bian, X., and Savic, J. (2001). Ultrastructural and functional characteristics of blast injury-induced neurotrauma. J. Trauma 50, 695–706.
8. Cernak, I., Wang, Z., Jiang, J., Bian, X., and Savic, J. (2001). Cognitive deficits following blast injury-induced neurotrauma: possible involvement of nitric oxide. Brain Inj. 15, 593–612.
9. Svetlov, S.I., Prima, V., Kirk, D.R., Gutierrez, H., Curley, K.C., Hayes, R.L., and Wang,. K.K. (2010). Morphologic and biochemical characterization of brain injury in a model of controlled blast overpressure exposure. J. Trauma 69, 795–804
10. Long, J.B., Bentley, T.L., Wessner, K.A., Cerone, C., Sweeney, S., and Bauman, R.A. (2009). Blast overpressure in rats: recreating a battlefield injury in the laboratory. J. Neurotrauma 26, 827–840.
11. Cernak, I., Merkle, A.C., Koliatsos, V.E., Bilik, J.M., Luong, Q.T., Mahota, T.M., Xu, L., Slack, N., Windle, D., and Ahmed, F.A. (2011). The pathobiology of blast injuries and blast-induced neurotrauma as identified using a new experimental model of injury in mice. Neurobiol. Dis. 41:538–551.
12. Arun, P., Abu-Taleb, R., Valiyaveettil, M., Wang, Y., Long, J.B., and Nambiar, M.P. (2012). Transient changes in neuronal cell membrane permeability after blast exposure. Neuroreport 23, 342–346.
13. Arun, P., Oguntayo, S., Alamneh, Y., Honnold, C., Wang, Y., Valiyaveettil, M., Long, J.B., and Nambiar, M.P. (2012). Rapid release of tissue enzymes into blood after blast exposure: potential use as biological dosimeters. PLoS One 7, e33798.
14. Moffett, J.R., Ross, B., Arun, P., Madhavarao, C.N., and Namboodiri, A.M. (2007). N-Acetylaspartate in the CNS: from neurodiagnostics to neurobiology. Prog. Neurobiol. 81, 89–131.
15. Erecinska, M., Zaleska, M.M., Nissim, I., Nelson, D., Dagani, F., and Yudkoff, M. (1988). Glucose and synaptosomal glutamate metabolism: studies with [15N]glutamate. J. Neurochem. 51, 892–902.
16. Yudkoff, M., Nelson, D., Daikhin, Y., and Erecinska, M. (1994). Tricarboxylic acid cycle in rat brain synaptosomes. Fluxes and interactions with aspartate aminotransferase and malate/aspartate shuttle. J. Biol. Chem. 269, 27414–27420.
17. Arun, P., Spadaro, J., John, J., Gharavi, R.B., Bentley, T.B., and Nambiar, M.P. (2011). Studies on blast traumatic brain injury using in-vitro model with shock tube. Neuroreport 22, 379–384.
18. Arun, P., Ariyannur, P.S., Moffett, J.R., Xing, G., Hamilton, K., Grunberg, N.E., Ives, J.A., and Namboodiri, A.M. (2010). Metabolic acetate therapy for the treatment of traumatic brain injury. J. Neurotrauma 27, 293–298.
19. Arun, P., Valiyaveettil., M., Biggemann., L., Alamneh., Y., Wei., Y., Oguntayo., S., Wang., Y., Long., J.B., and Nambiar, M.P. (2012). Modulation of hearing related proteins in the brain and inner ear following repeated blast exposures. Intervent. Med. Appl. Sci. 4, 125–131.
20. Signoretti, S., Marmarou, A., Tavazzi, B., Lazzarino, G., Beaumont, A., and Vagnozzi, R. (2001). N-Acetylaspartate reduction as a measure of injury severity and mitochondrial dysfunction following diffuse traumatic brain injury. J. Neurotrauma 18, 977–991.
21. Lee, S.M., Wong, M.D., Samii, A., and Hovda, D.A. (1999). Evidence for energy failure following irreversible traumatic brain injury. Ann. N. Y. Acad. Sci. 893, 337–340.
22. Tavazzi, B., Signoretti, S., Lazzarino, G., Amorini, A.M., Delfini, R., Cimatti, M., Marmarou, A., and Vagnozzi, R. (2005). Cerebral oxidative stress and depression of energy metabolism correlate with severity of diffuse brain injury in rats. Neurosurgery 56, 582–589.
23. Robertson, C.L., Saraswati, M., and Fiskum, G. (2007). Mitochondrial dysfunction early after traumatic brain injury in immature rats. J. Neurochem. 101, 1248–1257.
24. Opii, W.O., Nukala, V.N., Sultana, R., Pandya, J.D., Day, K.M., Merchant, M.L., Klein, J.B., Sullivan, P.G., and Butterfield, D.A. (2007). Proteomic identification of oxidized mitochondrial proteins following experimental traumatic brain injury. J. Neurotrauma 24, 772–789.
25. Xing, G., Ren, M., Watson, W.D,, O'Neill, J.T., and Verma, A. (2009). Traumatic brain injury-induced expression and phosphorylation of pyruvate dehydrogenase: a mechanism of dysregulated glucose metabolism. Neurosci. Lett. 454, 38–42.
26. Xing, G., Ren, M., O'Neill, J.T., Verma, A., and Watson, W.D. (2012). Controlled cortical impact injury and craniotomy result in divergent alterations of pyruvate metabolizing enzymes in rat brain. Exp. Neurol. 234, 31–38.
27. Sharma, P., Benford, B., Li, ZZ., and Ling, G.S. (2009). Role of pyruvate dehydrogenase complex in traumatic brain injury and Measurement of pyruvate dehydrogenase enzyme by dipstick test. J. Emerg. Trauma Shock 2, 67–72.
28. Madhavarao, C.N., Namboodiri, A.M. (2006). NAA synthesis and functional roles. Adv. Exp. Med. Biol. 576, 49–66.
29. Madhavarao, C.N., Arun, P., Moffett, J.R., Szucs, S., Surendran, S., Matalon, R., Garbern, J., Hristova, D., Johnson, A., Jiang, W., and Namboodiri, M.A. (2005). Defective N-acetylaspartate catabolism reduces brain acetate levels and myelin lipid synthesis in Canavan's disease. Proc. Natl. Acad. Sci. U S A 102, 5221–5226.
30. Madhavarao, C.N., Chinopoulos, C., Chandrasekaran, K., Namboodiri, M.A. (2003). Characterization of the N-acetylaspartate biosynthetic enzyme from rat brain. J. Neurochem. 86, 824–835.

Address correspondence to:
Peethambaran Arun, PhD
Blast-Induced Neurotrauma Branch
Center for Military Psychiatry and Neurosciences
Walter Reed Army Institute of Research
Silver Spring, MD 20910

E-mail: peethambaran.arun.ctr@mail.mil

This article has been cited by:

1. G. Mahmood, Z. Mei, H. Hojjat, E. Pace, S. Kallakuri, J.S. Zhang. 2014. Therapeutic effect of sildenafil on blast-induced tinnitus and auditory impairment. *Neuroscience* **269**, 367-382. [CrossRef]
2. Matthew Boyko, Shaun E. Gruenbaum, Benjamin F. Gruenbaum, Yoram Shapira, Alexander Zlotnik. 2014. Brain to blood glutamate scavenging as a novel therapeutic modality: a review. *Journal of Neural Transmission* . [CrossRef]
3. Ana Paula Oliveira Ferreira, Fernanda Silva Rodrigues, Iuri Domingues Della-Pace, Bibiana Castagna Mota, Sara Marchesan Oliveira, Camila de Campos Velho Gewehr, Franciane Bobinski, Clarissa Vasconcelos de Oliveira, Juliana Sperotto Brum, Mauro Schneider Oliveira, Ana Flavia Furian, Claudio Severo Lombardo de Barros, Juliano Ferreira, Adair Roberto Soares dos Santos, Michele Rechia Fighera, Luiz Fernando Freire Royes. 2013. The effect of NADPH-oxidase inhibitor apocynin on cognitive impairment induced by moderate lateral fluid percussion injury: Role of inflammatory and oxidative brain damage. *Neurochemistry International* . [CrossRef]

JOURNAL OF NEUROTRAUMA 31:1–13 (XXXX 00, 2014)

DOI: 10.1089/neu.2013.3144

Diffusion Tensor Imaging Reveals White Matter Injury in a Rat Model of Repetitive Blast-Induced Traumatic Brain Injury

Evan Calabrese,[1] Fu Du,[2] Robert H. Garman,[3] G. Allan Johnson,[1] Cory Riccio,[4] Lawrence C. Tong,[4] and Joseph B. Long[4]

Abstract

Blast-induced traumatic brain injury (bTBI) is one of the most common combat-related injuries seen in U.S. military personnel, yet relatively little is known about the underlying mechanisms of injury. In particular, the effects of the primary blast pressure wave are poorly understood. Animal models have proven invaluable for the study of primary bTBI, because it rarely occurs in isolation in human subjects. Even less is known about the effects of repeated primary blast wave exposure, but existing data suggest cumulative increases in brain damage with a second blast. MRI and, in particular, diffusion tensor imaging (DTI), have become important tools for assessing bTBI in both clinical and preclinical settings. Computational statistical methods such as voxelwise analysis have shown promise in localizing and quantifying bTBI throughout the brain. In this study, we use voxelwise analysis of DTI to quantify white matter injury in a rat model of repetitive primary blast exposure. Our results show a significant increase in microstructural damage with a second blast exposure, suggesting that primary bTBI may sensitize the brain to subsequent injury.

Key words: blast neurotrauma; diffusion tensor imaging; MRI; traumatic brain injury; voxelwise analysis

Introduction

Blast-induced traumatic brain injury (bTBI) is one of the most common injuries seen in U.S. military personnel returning from Iraq and Afghanistan. Although exact numbers are difficult to calculate, the prevalence of bTBI has been estimated to be as high as 18% among U.S. combat veterans.[1] The nature of current military conflicts, as well as improvements in body armor and battlefield trauma care, have resulted in an increasing number of veterans with bTBI as their sole, persisting, combat-related morbidity.[2,3] These patients experience a wide range of subtle neurological symptoms including persistent headache, insomnia, vertigo, tinnitus, psychomotor agitation, and difficulty concentrating.[1] These symptoms are often extremely debilitating and can prevent veterans from returning to civilian employment after leaving active duty.[4] Unfortunately, relatively little is known about the exact mechanism of injury underlying bTBI, and there is currently no universally accepted standard for diagnosis, prognosis, or treatment of bTBI. Further, the long-term sequelae of bTBI are largely unknown, although it has been theorized that bTBI may contribute to a number of psychological diseases including post-traumatic stress disorder and other anxiety disorders.[4] These uncertainties surrounding bTBI highlight the need for a more rigorous understanding of the underlying mechanisms of injury.

There is considerable clinical overlap between bTBI and civilian TBI caused by acute blunt head trauma (e.g., from accidents) and/or repetitive low-impact blows to the head (e.g., from participation in full contact sports).[1,2,5–7] This has led many to assume that the underlying mechanisms of injury are the same; however, this simplistic view may overlook some of the fundamental physical differences between bTBI and civilian TBI. Blast-induced brain injury is often divided into several different mechanisms of injury, each of which likely contributes to the overall clinical syndrome associated with bTBI. The most commonly cited model divides bTBI into primary (the direct result of the propagating blast pressure wave), secondary (caused by shrapnel and debris accelerated by the explosion), and tertiary injury (a coup-countercoup injury caused by rapid acceleration and deceleration of the brain inside the neurocranium).[8] Of these mechanisms of injury, only primary bTBI differs significantly from the types of injury commonly seen in

[1]Center for In Vivo Microscopy, Department of Radiology, Duke University Medical Center, Durham, North Carolina.
[2]FD NeuroTechnologies, Inc., Ellicott City, Maryland.
[3]Safar Center for Resuscitation Research, University of Pittsburgh School of Medicine, Pittsburgh, Pennsylvania.
[4]Blast-Induced Neurotrauma Branch, Center for Military Psychiatry and Neuroscience, Walter Reed Army Institute of Research, Silver Spring, Maryland.

civilian TBI. There is considerable debate on what, if any, effect primary bTBI has on the injury as a whole. This debate stems from the fact that primary bTBI is rarely seen in isolation in clinical populations; however, the limited number of case reports that do exist suggest that primary bTBI may be a key difference between bTBI and civilian TBI.[9–11]

A number of recent animal studies have provided evidence indicating that primary bTBI may play an important role in both direct brain injury and in sensitization to further brain injury.[12–16] Animal models allow primary bTBI to be studied in isolation and, perhaps more importantly, allow a more comprehensive assessment of brain pathology than is possible in human subjects. In particular, compression driven shock tubes can provide a robust and reproducible simulation of primary blast overpressure in rats and mice.[12,15] The shock tube model can be used to study numerous aspects of primary bTBI including the scope, location, and time course of the associated brain injury. Interestingly, a small number of shock tube studies have shown that repeated exposure to blast overpressure causes significantly increased neuronal damage, suggesting a synergistic effect.[17–20] This has lead some to theorize that primary bTBI may be a key sensitization to subsequent brain injury.[6] Animal studies may be the single most important tool for understanding the fundamental differences between bTBI and civilian TBI, which will be essential for guiding treatments designed to prevent, mitigate, and treat the associated brain injury.

Light-microscopy–based histology is the current ''gold standard'' for assessing neuropathology in animal models of bTBI. Conventional histology has several important limitations in this application; first, it is destructive, and therefore pathology can only be assessed in a single plane; second, it is time-consuming and labor intensive, making whole-brain assessment impractical; third, light microscopy images are difficult to quantify because tissue volume is often altered during sectioning, and stain density is highly variable between specimens; finally, conventional histology is only possible in fixed, *ex vivo* tissue, and therefore is not translatable to clinical populations.

MRI-based microimaging techniques are emerging as a valuable alternative to conventional histology for assessing neuropathology in animal models.[21–23] Like conventional histology, MRI can be used to assess neuropathology on the microscopic scale; however, MRI has several key advantages[24]; it is non-destructive and can be performed with the brain *in situ* in the neurocranium; it can survey the entire brain in three dimensions with isotropic spatial resolution, allowing assessment in any arbitrary plane as well as in three dimensions; it is inherently digital, and many MRI contrasts are quantitative in nature; finally, small animal MRI data can be processed and analyzed using the same tools and methodology used in clinical MRI data, making results directly translatable to humans.[25]

Diffusion tensor imaging (DTI) is an MRI acquisition strategy that provides quantitative, brain-wide maps of water diffusion characteristics that reveal underlying tissue microstructure.[26] Several of these tissue microstructural parameters are useful for detecting neuropathology. For example, fractional anisotropy (FA) is sensitive to white matter integrity, and mean diffusivity (MD) is altered in necrosis, edema, and gliosis.[27] Importantly, there is a growing body of clinical data demonstrating the use of diffusion tensor parameters to quantify bTBI.[6,28] These studies show a range of bTBI-associated injuries that can be detected with DTI, particularly in major white matter tracts. For example, Sponheim and associates[28] and Mac Donald and colleagues[29] showed statistically significant decreases in anisotropy in several major white matter pathways of U.S. military personnel with bTBI, including the corpus callosum, and cerebellar peduncles. DTI has also been used to detect TBI in a number of small animal studies[12,30,31]; however, none of these studies have assessed the effects of repeated primary bTBI.

In this study, we use voxelwise analysis of diffusion tensor parameters to quantify brain microstructural changes in a rat model of repetitive bTBI. These data reveal dramatic differences in the microstructural brain damage caused by a single blast exposure and a tightly temporally coupled double blast exposure. We further validate our findings using conventional histology and show that changes in DTI microstructural metrics correlate with histological changes. The methods presented here allow quantitative assessment of primary bTBI in an animal model with clinically translatable image processing techniques. These data add to a growing body of data suggesting that blast overpressure contributes to bTBI associated brain injury and may be a key sensitization to subsequent brain injury.

Methods

Animals and experimental design

All experiments and procedures were performed with the approval of both the Walter Reid Army Institute of Research and the Duke University Institutional Animal Care and Use Committee. Adult, male Sprague-Dawley rats (250–300 g) were housed on a 12-h/12-h light/dark cycle and were provided access to standard rat chow *ad libitum*. Rats were randomized into three experimental groups of nine animals each: a sham control group, a single blast exposed group, and double blast exposed group. All three groups were deeply anesthetized in an induction box by breathing a 4% isoflurane mixture in air delivered at 2 L/min for 6 min. The sham control group was handled in an identical manner but was not exposed to blast overpressure. The single blast group was exposed to a single shockwave (18.3 PSI static pressure, 8.8 msec positive phase duration). The double blast group was exposed to two identical shockwaves separated temporally by 1 min. All three groups were given 72 h to recover from anesthesia and blast exposure before euthanasia and imaging experiments.

Air-blast exposure

Air-blast exposure was generated using a 1-ft-diameter shock tube consisting of a 2.5-ft-long air compression chamber and a 15-ft-long expansion chamber separated by a Mylar membrane manufactured to rupture at a specific pressure. A high-volume air compressor was used to pressurize the compression chamber with room air until the Mylar membrane rupture pressure was reached. Flow conditions were recorded using piezoresistive pressure transducers (Meggit Inc., San Juan Capistrano, CA) mounted in the rat holder and provided measurements of total and side-on pressure waveforms. All rats were tautly secured in a transverse prone position in coarse mesh netting 2.5 ft within the mouth of the expansion chamber with the right side of the head facing the pressure chamber. Blast overpressure exposure was generally well tolerated; however, one rat in the double-blast group died shortly after blast exposure and was excluded from the analysis.

Specimen preparation for imaging experiments

Animals were perfusion-fixed using the active staining technique described more completely by Johnson et al.[32] Perfusion fixation was achieved using a 10% solution of neutral buffered formalin (NBF) containing 10% (50 mM) gadoteridol (ProHance, Bracco Diagnostics, Milan, Italy). After perfusion fixation, rat heads were removed and immersed in 10% NBF for 24 h. Finally, fixed rat heads were transferred to a 0.1 M solution of phosphate

buffered saline containing 1% (5 mM) gadoteridol at 4°C for 5–7 days. Before imaging, specimens were placed in custom-made, MRI-compatible tubes and immersed in Fomblin® low viscosity perfluoropolyether (Ausimont USA, Thorofare, NJ) for susceptibility matching and to prevent specimen dehydration. All imaging experiments were performed with the brain in the neurocranium to preserve tissue integrity and native spatial relationships.

Image acquisition

Imaging was performed on a 7 Tesla small animal MRI system (Magnex Scientific, Yarnton, Oxford, UK) equipped with 650 mT/m Resonance Research gradient coils (Resonance Research, Inc., Billerica, MA), and controlled with a General Electric Signa console (GE Medical Systems, Milwaukee, WI). RF transmission and reception was achieved using a custom 30 mm diameter × 50 mm long solenoid coil. T2*-weighted gradient recalled echo (GRE) anatomical images were acquired using a three-dimensional (3D) sequence (TR = 50 ms, TE = 8.3 ms, NEX = 2, $\alpha = 60$ degrees). The acquisition matrix was $1024 \times 512 \times 512$ over a $40 \times 20 \times 20$ mm field of view (FOV). The Nyquist isotropic spatial resolution was 39 μm.

Diffusion tensor data sets were acquired using a spin-echo pulse sequence (TR = 100 ms, TE = 16.2 ms, NEX = 1). Diffusion preparation was accomplished using a modified Stejskal-Tanner diffusion-encoding scheme[33] with a pair of unipolar, half-sine diffusion gradient waveforms (width $\delta = 4$ ms, separation $\Delta = 8.5$ ms, gradient amplitude = 450 mT/m). One b0 image and six high b-value images (b = 1500 s/mm^2) were acquired with diffusion sensitization along each of six non-colinear diffusion gradient vectors: (1, 1, 0), (0, 1, 1), (1, 0, 1), (1, −1, 0), (0, 1, −1), and (−1, 0, 1). The acquisition matrix was $512 \times 256 \times 256$ over a $40 \times 20 \times 20$ mm FOV. The Nyquist isotropic spatial resolution was 78 μm. All images were derived from fully sampled k-space data with no zero-filling. All images had a signal-to-noise-ratio (SNR) of 30 or greater.

DTI processing

Diffusion data were processed with a custom image-processing pipeline that comprised freely available software packages including Perl (http://www.perl.org), ANTs (http://www.picsl.upenn.edu/ANTS/), and Diffusion Toolkit (http://www.trackvis.org). This automated pipeline was created to ensure that all data were processed in the same way and to reduce the potential for user error. First, diffusion-weighted image volumes were rigidly aligned to the b0 volume using ANTs to correct for the linear component of eddy current distortions. Next, diffusion tensor estimation and calculation of tensor-derived data sets were performed using Diffusion Toolkit (http://trackvis.org/dtk/). Finally, data were organized into a consistent file architecture and archived in NIfTI format (http://nifti.nimh.nih.gov) in an on-site Oracle database.[34]

Image registration and averaging

Interspecimen registration of MR data was accomplished with the ANTs software package.[35,36] T2*-weighted anatomical images were used to drive all registration steps. Before registration, anatomical images were skull-stripped using an automated algorithm based on intensity thresholding and morphologic operations. Skull-stripped images were registered via affine transformation followed by a multiresolution, iterative, greedy symmetric normalization (SyN) non-linear registration. An average template was constructed from the sham control group using a minimum deformation template (MDT) strategy, which uses pairwise, non-linear image registrations to construct an unbiased template needing the minimum amount of deformation from each of the starting points.[37] The MDT algorithm was implemented in Linux shell script using ANTs as the registration program. This initial template construction step yields bidirectional transforms between each sham control individual and the template space. The two treatment groups were then spatially normalized to the average sham control template using a similar registration algorithm. In all cases, the similarity metric used for registration was cross-correlation computed for a kernel radius of 4 voxels. The algorithm converged at each step of the registration. The resultant transformations were applied directly to DTI-derived scalar images (described in the next section) to create population averages and were applied to tensor volumes using log-Euclidean math operations to create average tensors for tractography.[38]

Voxelwise analysis of diffusion tensor parameters

After image registration, voxelwise comparisons of diffusion tensor parameters were carried out in MATLAB using the SurfStat voxelwise analysis toolkit (http://www.math.mcgill.ca/keith/surfstat/). We analyzed differences in four parameters between the sham control and treatment groups: MD, axial diffusivity (AD), radial diffusivity (RD), and FA. All image data were spatially smoothed before voxelwise analysis using a $3 \times 3 \times 3$ voxel smoothing kernel to correct for minor misregistrations. We tested for statistically significant voxels across a whole-brain mask that had undergone morphologic erosion to avoid false positives on the surface of the brain resulting from imperfect skull-stripping. Multiple comparison correction was achieved with using the false discovery rate (FDR) algorithm with a significance threshold of $q < 0.05$ (referred to as the ''adjusted p value'' hereafter). Significant clusters smaller than 100 voxels were excluded from the analysis.

Tractography-based analysis

To further focus our results, we tested for voxelwise statistical significance across a white matter region of interest (ROI) defined by diffusion tractography. We performed whole-brain tractography on the sham control group average tensor using an FA threshold of 0.25, a turning angle threshold of 45 degrees, and a length threshold of 1 mm. These tracking parameters were chosen based on previous experience with similar data and are consistent with those used in a recently published DTI atlas of the adult rat brain.[39] Tractography-based voxelwise analysis was performed on all voxels containing three or more tractography streamlines. Once again, we chose a significance threshold of adjusted $p < 0.05$ after FDR correction for multiple comparisons.

Histotechnical procedures

After imaging, fixed brains were removed from the heads and postfixed in the same fixative solution for 6 h at 4°C. After cryoprotection in 0.1 M phosphate buffer (pH 7.4) containing 20% sucrose for 72 h at 4°C, brains were rapidly frozen and stored at −80°C. Serial sections of 40 μm thickness were cut on a cryostat coronally through the cerebrum, the brainstem, and the cerebellum, approximately from bregma 0.00 mm to −12.48 mm.[40] Every tenth section (interval: 400 μm) was collected separately in FD section storage solution™ (FD NeuroTechnologies) and stored at −20°C before further processing. Sections were processed for the detection of neurodegeneration with de Olmos amino-cupric-silver technique, which is described in detail elsewhere.[13,41] After silver staining, sections were washed thoroughly in distilled water, mounted on gelatin-coated slides, and counterstained with FD Neutral red solution™ (FD NeuroTechnologies). After dehydration in ethanol and clearing in xylene, sections were coverslipped with Permount® (Fisher Scientific, Fair Lawn, NJ).

Histopathologic evaluations

There were 30 coronal sections of the brain for each of the 26 animals included in this component of the study (i.e., 10 slides with three sections/slide for each rat). The most rostral section was at the

level of the optic chiasm and/or anterior commissure, and the most caudal at the level of the deep cerebellar nuclei. All sections were examined in non-blinded fashion by a neuropathologist. Note that a non-blinded approach is most appropriate for microscopic evaluations in this type of study, because this allows for periodic comparisons of the patterns of silver staining in both control and experimental animals. Microscopic findings were subjectively graded on a five-tiered scale (minimal to marked) and recorded for 44 representative neuroanatomic regions using a PC-based histopathology program (GLPath™).

Results

Experimental design and air blast exposure

Three experimental groups were used to study the effects of repetitive primary blast overpressure exposure: a sham control group, a single blast exposed group, and a double blast exposed group (Fig. 1). All three experimental groups consisted of nine animals each. The sham control group was only exposed to inhalation anesthesia and handling without blast overpressure exposure.

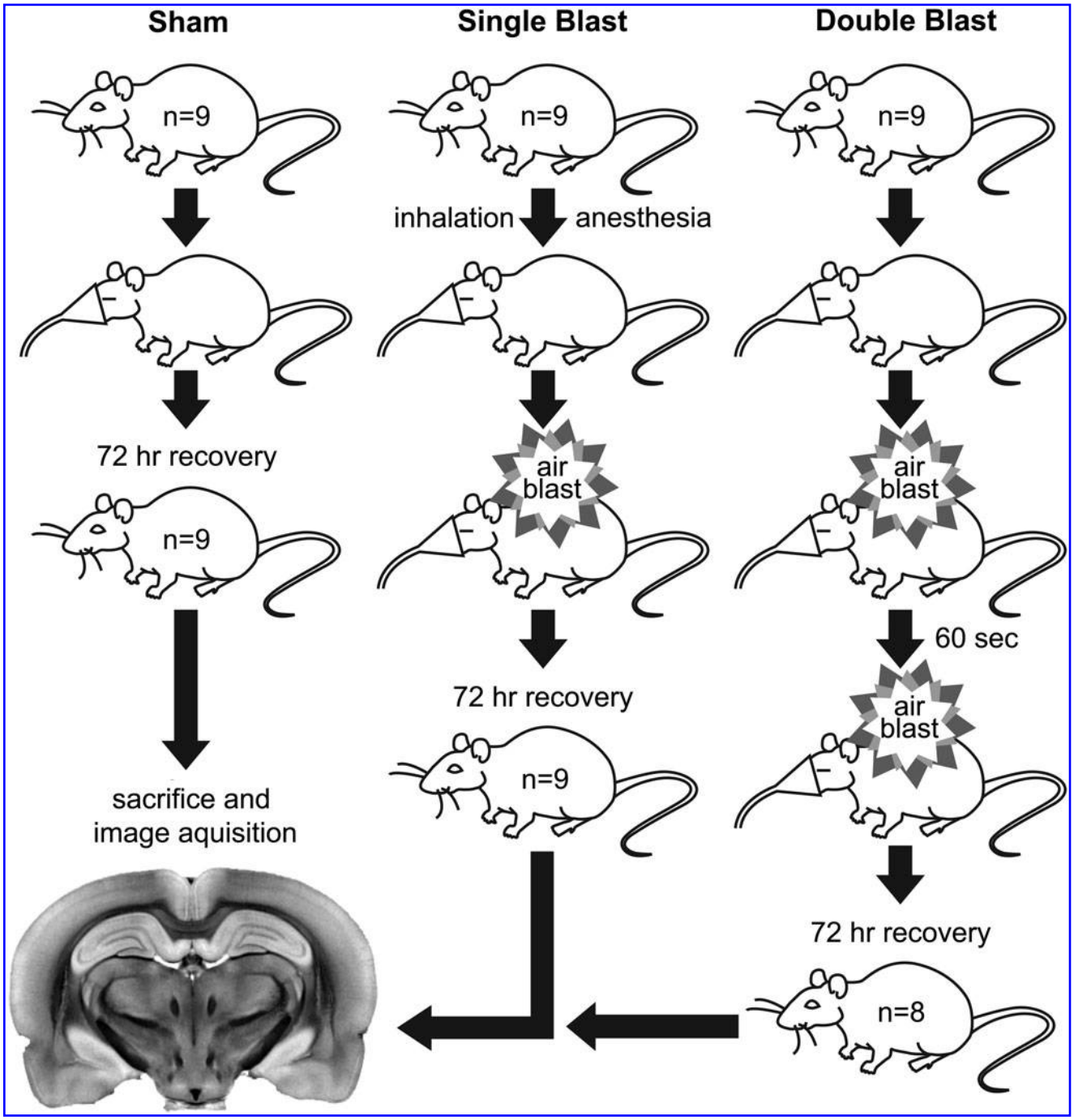

FIG. 1. Experimental design. There were three experimental groups: sham control, single blast, and double blast, each with $n = 9$. All animals were deeply anesthetized with inhalation anesthesia. Animals in the single blast group were exposed to a single air blast. Animals in the double blast group were exposed to two air blasts 60 sec apart. After a 72-h recovery period, animals were euthanized and imaged. A single animal in the double blast group died after exposure and was not imaged.

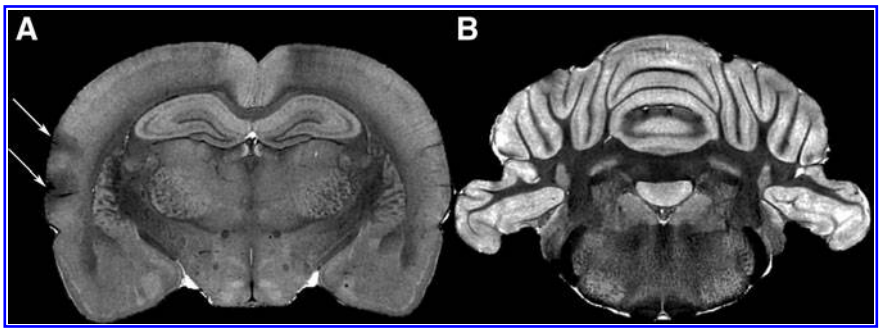

FIG. 2. Representative anatomical image data from a double blast exposed animal. Coronal slices through the dorsal hippocampus (**A**) and the deep cerebellar nuclei (**B**) are shown. Five of eight double blast exposed animals had cortical contusions of varying sizes, with and without associated subdural hemorrhage (arrows). No gross pathology was visible in the cerebellar white matter.

The single blast group was exposed to a single air blast. The double blast group was exposed to two air blasts temporally separated by 60 sec. All three groups received anesthesia for approximately the same period. No external injuries were observed in any of the experimental animals; however, one animal in the double blast group died shortly after exposure and was not imaged. After a 72-h recovery and observation period, rats were euthanized and prepared for imaging.

Anatomic image data

High resolution T2*-weighted anatomical images from all three groups were examined for gross pathological changes (Fig. 2). No gross pathology was visible in anatomical images from either the sham control or single blast group; however, several specimens in the double blast group had prominent cortical contusions (indicated in Fig. 2 with white arrows) with and without subdural hemorrhage. Contusions were observed in five of the eight brains from the double blast group, principally located in the auditory and secondary somatosensory cortical areas. The remaining three double blast exposed brains had no visible cortical pathology. No gross pathology was observed in the cerebellar white matter or other major white matter structure in any of the three experimental groups. Complete anatomic image data from all three groups are available from the Duke University Center for In Vivo Microscopy.

DTI data

FA images were also examined for gross pathology (Fig. 3). DTI-derived images like FA, although lower resolution, can be more sensitive for detecting neuropathology than anatomical images. FA images from all three groups were qualitatively very similar; however, subtle FA differences between groups were noted in the cerebellar white matter (indicated in Fig. 3 with white arrows). Both blast exposed groups appeared to have lower FA values in the cerebellar white matter than sham control animals, and this effect was more pronounced in the double blast group. Qualitative differences in other DTI-derived images were difficult to appreciate. Complete tensor volumes from all three groups are available from the Duke University Center for In Vivo Microscopy at http://www.civm.duhs.duke.edu/rat_btbi/.

Whole-brain voxelwise analysis

Voxelwise analysis was used to test for statistically significant differences in DTI-derived images between the three experimental groups. No statistically significant differences were found in MD or AD, and these results are not included here. The results of the FA and RD comparisons are shown in Figures 4 and 5. Voxelwise analysis results were visualized both in 3D (Fig. 4) and as two-dimensional color overlays on anatomical images (Fig. 5). Videos of statistically significant voxel clusters rotating in 3D to allow

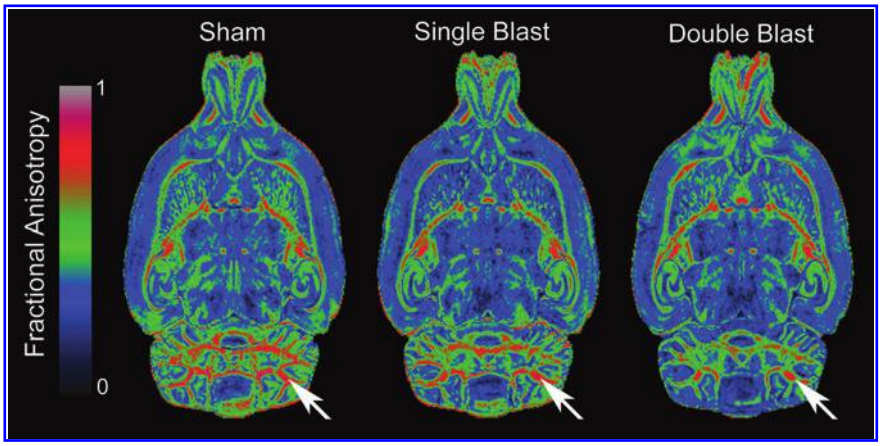

FIG. 3. Representative fractional anisotropy (FA) maps from all three experimental groups. Horizontal FA images through the dorsoventral center of the cerebellar white matter are displayed with a heat-map lookup table (see legend) to highlight differences. FA differences between groups are apparent in the cerebellar white matter (arrows). Color image is available online at www.liebertpub.com/neu

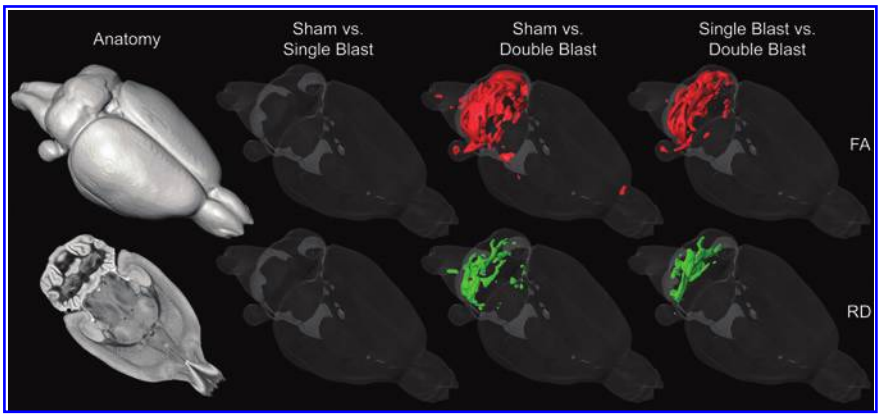

FIG. 4. Three-dimensional (3D) maps of statistically significant differences in diffusion tensor imaging parameters between all three experimental groups. Voxel clusters with an adjusted *p* value less than 0.05 are displayed as 3D, colored surfaces within a transparent surface rendering of the entire brain. Statistically significant differences in fractional anisotropy (red) and radial diffusivity (green) are shown for each pair of experimental groups. The left-most column contains anatomical references including an opaque surface rendering of the entire brain (top) and a single horizontal slice of the average anatomical image volume (bottom). Color image is available online at www.liebertpub.com/neu

visualization of the full 3D extent of the detected injury are available from the Duke University Center for In Vivo Microscopy at http://www.civm.duhs.duke.edu/rat_btbi/.

There were no statistically significant differences between sham control and single blast groups; however, there were small decreases in FA and increases in RD in the cerebellar white matter and axial hindbrain (Fig. 5, left).

The sham versus double blast comparison (Fig. 5, middle) revealed extensive and highly significant decreases in FA throughout the cerebellar white matter tree and cerebellar peduncles. The

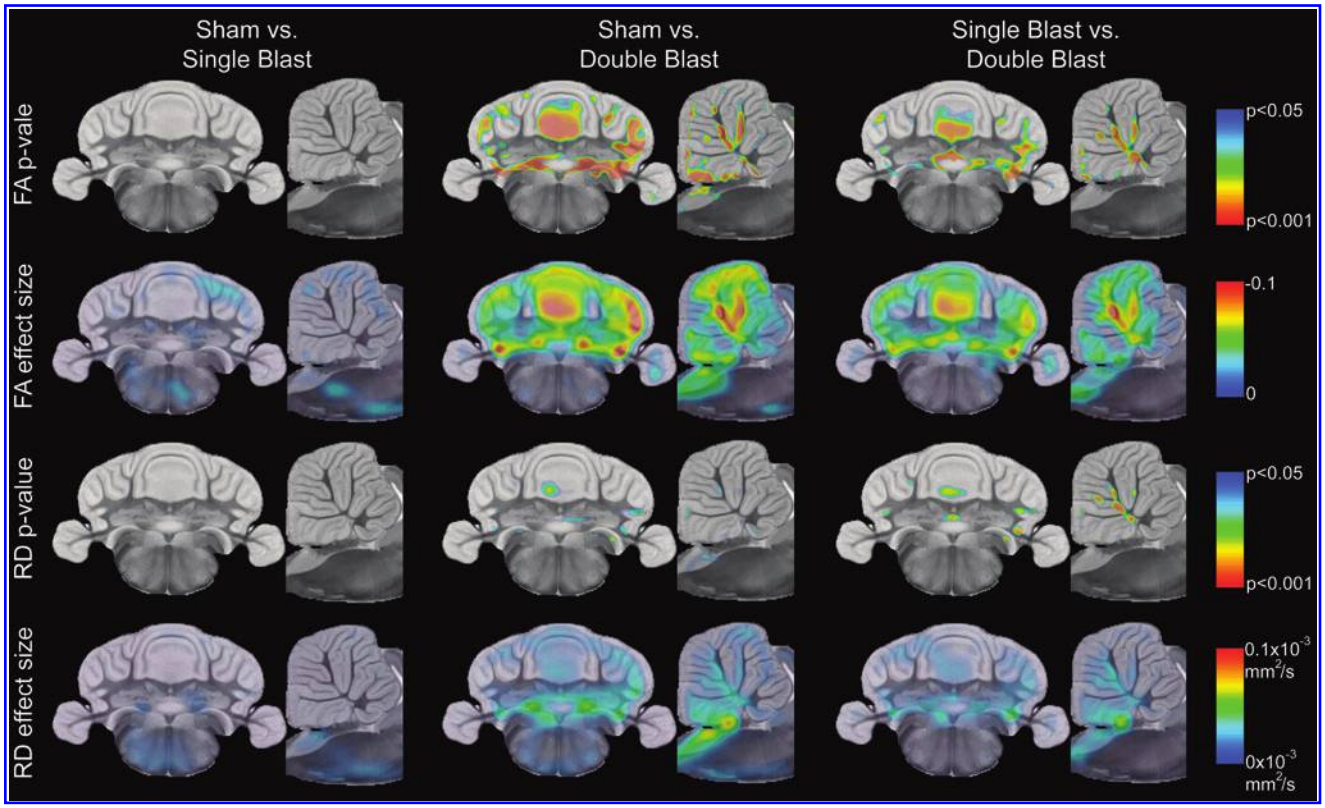

FIG. 5. Statistical significance and effect size maps of diffusion tensor imaging parameter differences between all three experimental groups. Adjusted *p* value maps (rows one and three) indicate statistically significant differences (adjusted *p* value less than 0.05) with color; hotter colors indicate increased confidence. Effect size maps (rows two and four) are shown across the entire brain irrespective of significance with hotter colors indicating increased effect size. FA, fractional anisotropy; RD, radial diffusivity. Color image is available online at www.liebertpub.com/neu

measured effect size in statistically significant areas was generally close to -0.1 arbitrary units. There were also several small regions of statistically significant increase in RD in cerebellar white matter in the sham versus double blast comparison, with effect size ranging from 5×10^{-5} mm^2/sec to 1×10^{-4} mm^2/sec. There was a particularly large RD increase ($\approx 1\times10^{-4}$ mm^2/sec) in the dorsal hindbrain, a small portion of which reached statistical significance.

The results of the single blast versus double blast (Fig. 5, right) were quite similar to those of the sham versus double blast comparison. Statistically significant decreases in FA were detected in the same regions, although to a lesser spatial extent and magnitude. Statistically significant increases in RD were actually slightly more extensive in the single blast versus double blast comparison, although the effect size was smaller.

There are a few areas in which statistical significance maps appear to extend from white matter tracts to adjacent gray matter areas (e.g., Fig. 5, center). These areas of apparent gray matter significance could be: (1) false positives from residual misregistrations between groups, (2) true positive differences in gray matter structures, or (3) blurring of true positive results in white matter caused by the spatial smoothing kernel used during voxelwise analysis preprocessing.

Tractography-based analysis

Tractography-based analysis was used to focus statistical comparisons with white matter, thereby excluding a large number of gray matter voxels where blast injury is not expected. This

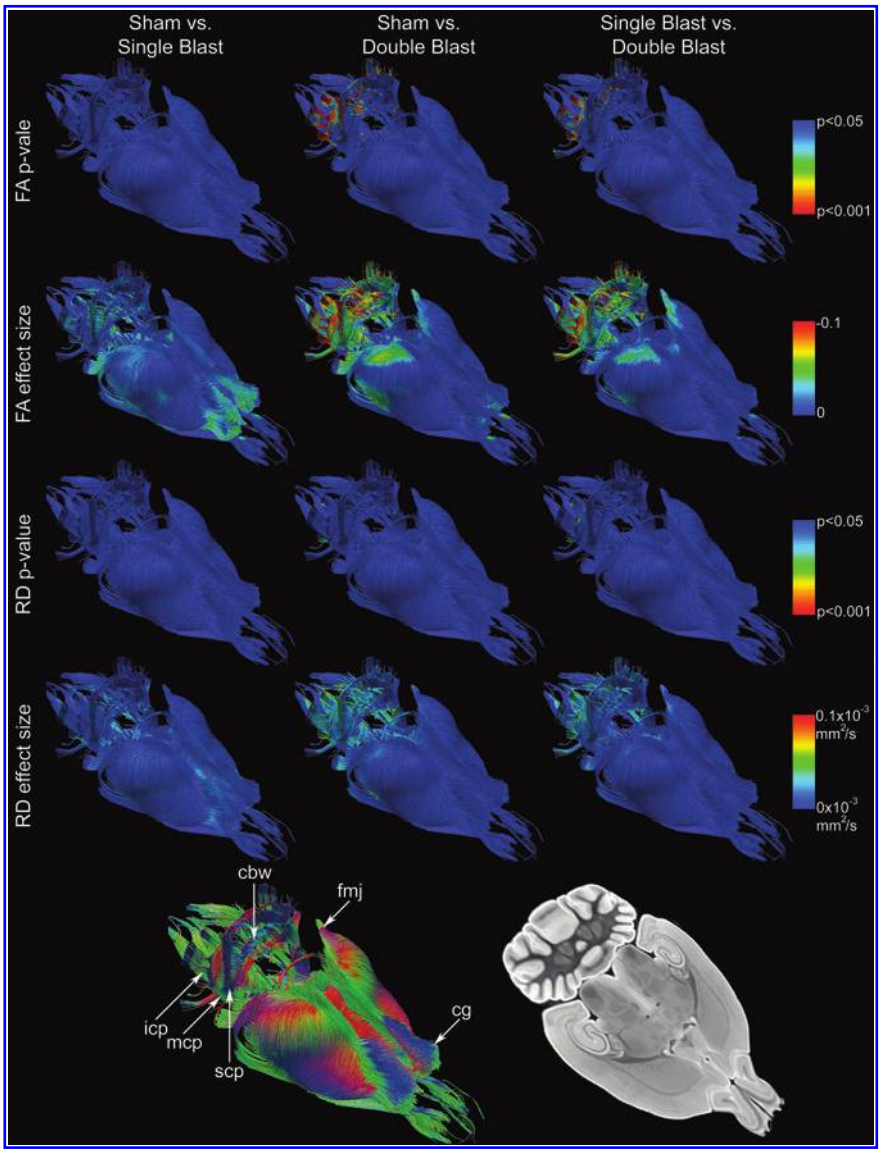

FIG. 6. Tractography-based analysis of diffusion tensor parameter differences between all three experimental groups. Statistical significance and effect size for each comparison (columns) are shown as colored tractography streamlines with hotter colors indicating increased statistical certainty (adjusted *p* value maps) or increased effect size (effect size maps). Anatomical references are included at the bottom of the figure including directionally colored tractography streamlines (left) and a horizontal slice of the anatomical image volume (right). Labeled structures are: cerebellar white matter (cbw); forceps major of the corpus callosum (fmj); cingulum bundle (cg); inferior, middle and superior cerebellar peduncles (icp, mcp, and scp respectively). FA, fractional anisotropy; RD, radial diffusivity. Color image is available online at www.liebertpub.com/neu

technique also allows 3D visualization of affected white matter tracts (Fig. 6). Once again, we were unable to detect statistically significant differences between sham and single blast groups; however, we did observe small decreases in FA (≈ 0.04 arbitrary units) in the rostral cingulum bundle and the cerebellar white matter (Fig. 6, left). Modest increases in RD ($\approx 3\times10^{-5}$ mm^2/sec) were observed in the same regions.

The sham versus double blast comparison (Fig. 6, center) yielded the most robust differences; FA was reduced throughout the cerebellum and hindbrain, and small decreases extended anteriorly as far as the caudal forceps major of the corpus callosum. FA decreases achieved statistical significance throughout the deep cerebellar white matter and in the inferior, middle, and superior cerebellar peduncles. RD increases were present in the cerebellar white matter and in all three cerebellar peduncles; however, only a limited number of tracts in the cerebellar white matter and middle cerebellar peduncle survived FDR multiple comparison correction.

The single blast versus double blast comparison (Fig. 6, right) once again revealed similar, although less extensive and lower magnitude differences than the sham versus double blast comparison. Statistically significant decreases in FA were most prominent in the cerebellar white matter and the inferior cerebellar peduncle and statistically significant increases in RD were limited to the cerebellar white matter. High-definition videos of tractography-based analysis results rotating in 3D are available from the Duke University Center for In Vivo Microscopy.

Silver stained histology

Silver stained histology was used to validate voxelwise analysis findings because FA and RD, although sensitive, are not specific for white matter injury. Representative histology results are shown in Figure 7. In histology sections stained with amino cupric silver, damaged neurons and neuronal processes stain black and often take on a fragmented appearance. The sham control group in this study did not show significant silver staining anywhere in the brain. Silver staining in blast exposed animals was divided into patterns suggestive of neuronal degeneration and/or diffuse axonal injury. No degenerating neurons were present in the single blast group; however, 3/8 animals in the double blast group showed evidence of mild to moderate neuron degeneration in various regions of the cortex (*viz* frontal, parietal, temporal, and occipital).

Axonal staining in a pattern suggestive of diffuse axonal injury was more prominent than neuron degeneration. In both the single and double blast groups, the cerebellar white matter, optic tracts, and cerebellar peduncles were most commonly affected (Fig. 7). Specifically, the cerebellar white matter was affected in 8/9 rats in the single blast group (average severity = mild) versus 8/8 rats in the double blast group (average severity = moderate). The optic tracts were affected in 6/9 rats in the single blast group (average severity = mild) versus 8/8 rats in the double blast group (average severity = moderate). The cerebellar peduncles were affected in 6/9 rats in the single blast group (average severity = minimal) versus 8/8 rats in the double blast group (average severity = mild). No other neuroanatomical regions showed significant degrees of axonal damage in the single blast group. Some brains in the double blast group, however, also had evidence of axonal injury within the spinal trigeminal tract (7/8), midbrain (3/8), cochlear nucleus/nerve (3/8), and within the third and/or fourth cranial nerves (4/8).

Overall perfusion fixation was very effective at flushing the cerebral vasculature of blood; however, clotted blood was observed in the subdural space of several specimens with prominent cortical contusions. This iron-laden clotted blood could affect MRI results through susceptibility artifacts, but these effects would likely be limited to the cortical surface.

Discussion

Air-blast exposure

The blast overpressure exposure used in this study and more thoroughly characterized elsewhere[42,43] reproducibly recreates

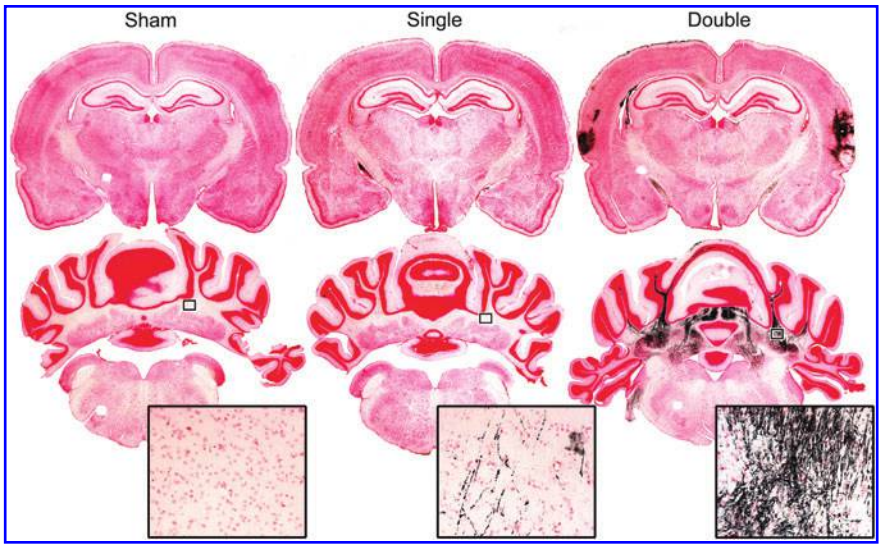

FIG. 7. Representative silver degeneration-stained coronal brain sections from all three experimental groups: sham control (left) single blast exposed (center) and double blast exposed (right). Two coronal sections are shown for each group—one at the level of the dorsal hippocampus at approximately Bregma −3.3 mm (top), and one through the cerebellum at approximately Bregma −11.4 mm (bottom). Magnified insets are medium-high power micrographs (20× objective) of the cerebellar white matter showing silver staining of axons and the formation of axon retraction balls typical of those seen in traumatic axonal injury. Color image is available online at www.liebertpub.com/neu

with some fidelity the primary blast pressure wave created by explosive detonations. Unfortunately, comparing experimental blast conditions with combat-related blast exposure is difficult because of the intrinsic limitations of the shock tube model, as well as significant anatomical and physiological differences between humans and rodents. Nonetheless, similar experimental conditions are widely used to study the effects of blast overpressure in small animal models. This exposure technique provides the opportunity to study the effects of a realistic primary blast pressure wave in the absence of concomitant secondary or tertiary blast injury. Blast wind-induced head acceleration has recently received attention as a primary injury mechanism contributing to experimental blast-related TBI[44]; however, in the present study, these contributions have been minimized by secure immobilization of each subject in the holder during blast overpressure exposure. Previous histological assessment of this model has shown extensive axonal damage in several major white matter tracts, most notably the cerebellar white matter.[17] These histological findings, coupled with impaired performance in motor tasks, correlate well with some injuries and symptoms seen in clinical populations.[10,18,29]

We chose to study the effects of repeated blast exposure based on previous experimental and clinical observations that repeated head injuries can cause cumulative or even synergistic neurological damage.[45,46] The rationale for administering blast exposures 1 min apart was based on previous observations in mice, in which greatly exacerbated mortality, neuropathological changes, and neurobehavioral disruptions were noted with blast exposures separated by 1 and 30 min.[17] In future studies, this model will allow characterization of the window of vulnerability to a second blast exposure.

Anatomic image data

The anatomical image data presented in Figure 2 highlights the difficulty in traditional image-based assessment of bTBI. Anatomical imaging yielded inconsistent results that did not correlate well with DTI findings. The only grossly visible lesions were cortical contusions of varying severity with or without subdural hemorrhage in five of the eight double-blasted specimens. These imaging findings are quite similar to those seen in clinical populations where cortical contusions and subdural hemorrhages are among the most commonly observed lesions.[47] Interestingly, our results suggest that these lesions, which are often associated with cortical impact and/or acceleration/deceleration injury, can result from primary blast pressure wave exposure alone. There were no grossly evident lesions in the cerebellum or hindbrain despite these being the primary sites of axonal injury as detected by voxelwise analysis of DTI parameters. These results highlight the need for advanced imaging and computational approaches to assess occult microstructural injury in bTBI. It is possible that grossly visible lesions resulting from bTBI are merely the ''tip of the iceberg'' indicating more extensive and possibly more clinically relevant occult white matter injury.

DTI parameter data

Diffusion tensor parameters, such as FA and RD, have garnered attention as highly sensitive, yet non-specific, markers of white matter microstructural integrity. These quantitative parameters, which are based on the microscopic diffusion properties of water, have the potential to reveal microstructural damage at a scale that is much smaller than the voxel size of the image itself.[26] For example, axonal injury causes decreases in FA, often accompanied by increases in RD, although many other microstructural changes, such as edema and gliosis, can produce similar findings.[27] We observed subtle, although grossly visible decreases in FA in the cerebellum that were more severe in the double blast group than the single blast group (Fig. 3). Unfortunately, these differences are small, and it is difficult to appreciate their full spatial extent from simple, ROI-based image comparisons.

Pitfalls of voxelwise analysis

Voxelwise analysis of DTI parameters is a powerful investigational technique that allows researchers to test for significant differences across the entire brain without predefined anatomical hypotheses. Unfortunately, voxelwise analysis is vulnerable to a number of pitfalls that can lead to false positive results. Two of the most common causes of false positive results are minor misregistrations between treated and control groups, and failure to correct for multiple comparisons.[48,49] In this study, we have taken a number of steps to ensure accurate registration including the use of: (1) high-resolution, high-SNR diffusion-weighted images, (2) an unbiased MDT registration strategy, and (3) registration software specifically optimized for small animal image data. To correct for any residual misregistrations, images were spatially smoothed with a three-voxel 3D Gaussian kernel consistent with general guidelines for voxelwise analysis.[49,50] Multiple comparison correction was achieved using the FDR method, which is less stringent than family wise error rate methods, but more robust than arbitrarily defined *p*-thresholds. We have used this cautious methodology to identify only the most robust and reproducible injuries resulting from primary blast exposure, because these are likely to be the most meaningful targets for intervention.

Voxelwise analysis of repeated primary blast exposure

The results of our voxelwise analysis show a consistent pattern of injury to the major cerebellar white matter tracts in double blast exposed animals. These areas show FA loss concomitant with RD increase—a pattern that is frequently observed in traumatic axonal injury.[51,52] Interestingly, we observed no statistically significant differences in AD, suggesting that RD increases are the primary cause of anisotropy loss in affected areas. AD decrease is also a common finding in acute axonal injury, although it often normalizes in the sub-acute and chronic setting.[51,53] It is possible that AD decreases are not a major feature of primary bTBI or that the changes are too small and/or variable to detect using our methods. In addition, the DTI parameter changes that we observed are likely only present in the acute to sub-acute (i.e., < 72 h) post-injury period. Assessment of later post-injury time points may reveal completely different DTI parameter changes driven by edema, necrosis, and/or gliosis.

We were unable to detect any statistically significant differences between single blast and sham control groups; however, there were large and highly significant differences between the single blast and double blast groups. By all imaging metrics, the single blast group more closely resembled the sham control group than the double blast group. This result suggests a synergistic effect with repeated blast exposure. One possible explanation is that initial blast exposure sensitizes the brain, either physiologically or mechanically, to damage from a subsequent blast. Several physiological changes are known to occur immediately after closed head injury in animal models, including increases in heart rate, arterial blood pressure, and intracranial pressure.[54,55] Each of these parameters could potentially magnify subsequent blast injury by altering the

intracranial fluid pressure dynamics that are thought to underlie primary blast wave associated injury.[7,56] Mechanical sensitization could occur by weakening or degradation of the neuronal cytoskeleton, which has also been observed in rodent models of primary bTBI.[57,58] Further studies are needed to determine what, if any, are the mechanisms of sensitization to further injury. For example, real-time monitoring of intracranial and intravascular pressures during repeated blast exposure could elucidate the role of pressure dynamics, and immunofluorescence or electron microscopy studies could be used to assess cytoskeletal injury. Because DTI is non-destructive, it can easily be combined and correlated with higher resolution imaging techniques such as electron microscopy.[22]

Tractography-based analysis

Tractography-based analysis is a special case of voxelwise analysis that is well suited for detection and visualization of white matter injury.[59] Applying tractography-based analysis to this study is justified based on a number of previous studies suggesting that primary bTBI is predominantly a white matter injury.[6,9,10,29] Tractography-based analysis has two main advantages over whole-brain voxelwise analysis. First, it provides more focused and potentially less biased results by limiting the analysis to a white matter skeleton defined by the control group average tractography streamlines.[60,61] Second, it permits 3D visualization of significance and effect size maps through the use of color-coded tractography streamlines.

The tractography-based analysis presented here allowed precise localization of blast-induced white matter injury to the cerebellar white matter and cerebellar peduncles. Tractography-based results also highlight the dramatic differences between single blast and double blast-associated injury. The second blast dramatically increased both the spatial extent and the magnitude of the associated white matter injury. Together, these results suggest that specific subtentorial white matter tracts, like the cerebellar white matter, may be uniquely susceptible to repeated primary bTBI. Interestingly, similar injury patterns have been reported in both clinical populations[6,10,29] and in previous animal studies.[13,16,17] Further, hindbrain white matter injury is consistent with several common symptoms of bTBI including tinnitus, vertigo, and balance/motor-coordination problems. Previously published behavioral assessments of the blast injury model used in this study have demonstrated impaired performance on standardized motor coordination tests such as beam walking and the Morris water maze.[15] Future studies are needed to explore the correlation between motor task performance and cerebellar white matter injury as detected by DTI.

Histological validation of voxelwise analysis results

The results of our histological examination of neuronal injury correlate well with voxelwise analysis results, both in spatial extent and in magnitude. Silver staining revealed modest and inconsistent axonal injury in the cerebellar white matter of single blasted brains. This low magnitude and highly variable injury explains why DTI parameter changes did not reach statistical significance for the single blast versus sham control comparison. In contrast, histological examination of double blasted brains revealed severe and consistent axonal injury within the cerebellar white matter tree. These results closely match the statistically significant regions of RD decrease and FA increase detected with voxelwise analysis of the double blast group.

Comparison of histology results with DTI voxelwise analysis results demonstrates the benefits and drawbacks of each technique. Silver stained histology is far more sensitive and can detect injury as small as a single damaged neuron. DTI has neither the spatial resolution nor the sensitivity to detect such small-scale damage; however, DTI has several major advantages over histology. First, DTI is 3D and non-destructive, so pathology can be detected throughout the entire brain without distortion or sectioning artifact. Second, DTI parameters allow straightforward quantitative comparisons, and voxelwise analysis techniques can be used to test for statistically significant differences throughout the entire brain without an *a priori* anatomical hypothesis. Although quantitative analysis of histology is possible, it is often technically difficult, time consuming, limited to predefined anatomical regions, and/or non-parametric. Nonetheless, quantitative histology is the *de facto* gold standard for assessing neuropathological alterations resulting from blast injury, as is evident from a large body of previously published work. Although the current study is focused on quantitative assessment of DTI rather than histology, a comparison of both quantitative techniques will undoubtedly be an important area of future work. Finally, although the present study uses fixed *ex vivo* specimens, voxelwise analysis of DTI parameters is possible *in vivo* and may even be more sensitive for detecting differences in living subjects.[62]

Limitations of this study

This study has several important limitations. First, the rat may not be the ideal model system for studying human brain injury.[63] Non-human primate models may more closely recapitulate human bTBI; however, ethical and technical considerations make rodent models much more desirable. Further, a large body of previous research supports the use of rodents for studying human bTBI. Second, both death and tissue fixation are known to affect diffusion tensor parameter measurements, which is an important consideration for *ex vivo* studies. Formalin fixation is known to reduce tissue diffusivity; however, it appears to do so both proportionally and uniformly throughout the brain, thus preserving anisotropy.[64] As a result, the relative RD differences that we report likely reflect *in vivo* changes, but the absolute magnitudes do not. Importantly, fixation also seems to reduce the sensitivity of DTI in detecting axonal damage, suggesting a comparable *in vivo* study may be able to detect even more subtle injury.[62] Nevertheless, *ex vivo* imaging has several important benefits including higher SNR and higher spatial resolution.[65] Finally, there is considerable debate over the proper acquisition protocol for measuring diffusion tensor parameters, with some studies recommending as many as 30 gradient directions[66,67]; however, these studies are based on clinical data where patient movement, low SNR, and susceptibility artifacts are major sources of error. Any error resulting from a six-direction strategy is, to some extent, compensated for by the increased image quality, SNR, and spatial accuracy that *ex vivo* DTI can provide.[68,69]

Conclusions

This work contributes to the growing body of data suggesting that primary blast injury is an important component of bTBI. Further, we provide preclinical evidence that brain injury increases synergistically with repeated exposure to blast overpressure. Our results suggest that the primary blast wave sensitizes the brain to more severe injury from subsequent blast exposure, even in the absence of radiologically detectable gross pathology. This

conclusion, if supported by further studies, has widespread significance for the treatment of soldiers subjected to blasts in the battlefield, many of whom remain on active duty after exposure. A critical area of future research will be to determine the time-course of primary bTBI associated sensitization to further brain injury. For example, if the observed sensitization effect is related to intravascular and/or intracranial pressure dynamics, then it may only persist for minutes to hours until equilibrium is restored. Conversely, if sensitization is caused by cytoskeletal damage, then it would be expected to persist for hours to days until repair completes. A follow-up study with varying time intervals between blasts will be important in understanding both the underlying mechanism of sensitization and the implications for human bTBI patients.

The methods and model system described here have exciting potential to further our understanding of the effects of the primary blast wave on the brain. Voxelwise analysis of DTI parameters has proven to be a useful and sensitive tool for detecting primary bTBI in rodent models and is readily translatable to human studies. We look forward to using similar techniques to study not only the time-course of primary bTBI, but also its interaction with other forms of blast injury. Unfortunately, combat-related bTBI usually involves acceleration/deceleration and/or cranial impact injuries, which may have complex interactions with primary blast injury. These interactions could be explored using a combination of shock tube blast overpressure and other rodent TBI models such as weight-drop contusion or controlled cortical impact. Although such studies present a significant logistical challenge, they may ultimately prove to be more clinically relevant than the repetitive injury model presented here. Finally, we would like to reiterate that all image data, including full tensor volumes, are available from the Duke University Center for In Vivo Microscopy. We welcome and encourage further analysis, because we are confident there is still more valuable information to be extracted from this dataset.

Acknowledgments

The views, opinions, and/or findings contained herein are those of the authors and should not be construed as an official position, policy, or decision of the Department of the Army or the Department of Defense.

Animal handling and treatments were conducted in compliance with the Animal Welfare Act and other Federal statutes and regulations related to animals and experiments involving animals, and adhered to principles stated in the Guide to the Care and Use of Laboratory Animals, National Research Council. The facilities are fully accredited by the Association for Assessment and Accreditation of Laboratory Animal Care International.

Blast exposure was performed at the Walter Reed Army Institute of Research under the support of the CDMRP Psychological Health and Traumatic Brain Injury Research Program (W81XWH-11-2-0127). Imaging work was performed at the Duke University Center for In Vivo Microscopy, an NIH/NIBIB Biomedical Technology Resource Center (P41 EB015897). We are grateful to Sally Gewalt and James Cook for assistance with the imaging pipelines. We thank Andrea Edwards, Joseph Andrist, and Donna Wilder for assistance with blast exposures, and Dr. Yi Qi, and Gary Cofer for assistance in specimen preparation and scanning.

Author Disclosure Statement

No competing financial interests exist.

References

1. Hoge, C.W., McGurk, D., Thomas, J.L., Cox, A.L., Engel, C.C., and Castro, C.A. (2008). Mild traumatic brain injury in U.S. Soldiers returning from Iraq. N. Engl. J. Med. 358, 453–463.
2. Warden, D. (2006). Military TBI during the Iraq and Afghanistan wars. J. Head Trauma Rehabil. 21, 398–402.
3. Okie, S. (2005). Traumatic brain injury in the war zone. N. Engl. J. Med. 352, 2043–2047.
4. Schneiderman, A I., Braver, E.R., and Kang, H.K. (2008). Understanding sequelae of injury mechanisms and mild traumatic brain injury incurred during the conflicts in Iraq and Afghanistan: persistent postconcussive symptoms and posttraumatic stress disorder. Am. J. Epidemiol. 167, 1446–1452.
5. DeKosky, S.T., Ikonomovic, M.D., and Gandy, S. (2010). Traumatic brain injury—football, warfare, and long-term effects. N. Engl. J. Med. 363, 1293–1296.
6. Mac Donald, C.L., Johnson, A.M., Cooper, D., Nelson, E.C., Werner, N.J., Shimony, J.S., Snyder, A.Z., Raichle, M.E., Witherow, J.R., Fang, R., Flaherty, S.F., and Brody, D.L. (2011). Detection of blast-related traumatic brain injury in U.S. military personnel. N. Engl. J. Med. 364, 2091–2100.
7. Taylor, P.A., and Ford, C.C. (2009). Simulation of blast-induced early-time intracranial wave physics leading to traumatic brain injury. J. Biomech. Eng. 131, 061007.
8. Cernak, I., and Noble-Haeusslein, L J. (2010). Traumatic brain injury: an overview of pathobiology with emphasis on military populations. J. Cereb. Blood Flow Metab. 30, 255–266.
9. Hayes, J.P., Morey, R.A., and Tupler, L.A. (2012). A case of frontal neuropsychological and neuroimaging signs following multiple primary-blast exposure. Neurocase 18, 258–269.
10. Warden, D.L., French, L.M., Shupenko, L., Fargus, J., Riedy, G., Erickson, M.E., Jaffee, M.S., and Moore, D.F. (2009). Case report of a soldier with primary blast brain injury. Neuroimage 47, Suppl 2, T152–T153.
11. Sylvia, F.R., Drake, A.I., and Wester, D.C. (2001). Transient vestibular balance dysfunction after primary blast injury. Mil. Med. 166, 918–920.
12. Rubovitch, V., Ten-Bosch, M., Zohar, O., Harrison, C.R., Tempel-Brami, C., Stein, E., Hoffer, B.J., Balaban, C.D., Schreiber, S., Chiu, W.T., and Pick, C.G. (2011). A mouse model of blast-induced mild traumatic brain injury. Exp. Neurol. 232, 280–289.
13. Garman, R.H., Jenkins, L.W., Switzer, R.C. III, Bauman, R.A., Tong, L.C., Swauger, P.V., Parks, S., Ritzel, D.V., Dixon, C.E., Clark, R., Bayir, H., Kagan, V., Jackson, E., and Kochanek, P.M. (2011). Blast exposure in rats with body shielding is characterized primarily by diffuse axonal injury. J. Neurotrauma 28, 947–959.
14. Mao, J.C., Pace, E., Pierozynski, P., Kou, Z., Shen, Y., Vandevord, P., Haacke, E.M., Zhang, X., and Zhang, J. (2012). Blast-induced tinnitus and hearing loss in rats: behavioral and imaging assays. J. Neurotrauma 29, 430–444.
15. Long, J.B., Bentley, T.L., Wessner, K.A., Cerone, C., Sweeney, S., and Bauman, R.A. (2009). Blast overpressure in rats: recreating a battlefield injury in the laboratory. J. Neurotrauma 26, 827–840.
16. Bauman, R.A., Ling, G., Tong, L., Januszkiewicz, A., Agoston, D., Delanerolle, N., Kim, Y., Ritzel, D., Bell, R., Ecklund, J., Armonda, R., Bandak, F., and Parks, S. (2009). An introductory characterization of a combat-casualty-care relevant swine model of closed head injury resulting from exposure to explosive blast. J. Neurotrauma 26, 841–860.
17. Wang, Y., Wei, Y., Oguntayo, S., Wilkins, W., Arun, P., Valiyaveettil, M., Song, J., Long, J.B., and Nambiar, M P. (2011). Tightly coupled repetitive blast-induced traumatic brain injury: development and characterization in mice. J. Neurotrauma 28, 2171–2183.
18. Peskind, E.R., Petrie, E.C., Cross, D.J., Pagulayan, K., McCraw, K., Hoff, D., Hart, K., Yu, C.E., Raskind, M.A., Cook, D.G., and Minoshima, S. (2011). Cerebrocerebellar hypometabolism associated with repetitive blast exposure mild traumatic brain injury in 12 Iraq war Veterans with persistent post-concussive symptoms. Neuroimage 54, Suppl 1, S76–S82.
19. Säljö, A., Svensson, B., Mayorga, M., Hamberger, A., and Bolouri, H. (2009). Low-level blasts raise intracranial pressure and impair cognitive function in rats. J. Neurotrauma 26, 1345–1352.
20. Mazurkiewicz-Kwilecki, I.M. (1980). Single and repeated air blast stress and brain histamine. Pharmacol. Biochem. Behav. 12, 35–39.

21. Johnson, G.A., Badea, A., and Jiang, Y. (2011). Quantitative neuromorphometry using magnetic resonance histology. Toxicol. Pathol. 39, 85–91.
22. Calabrese, E., and Johnson, G.A. (2013). Diffusion tensor magnetic resonance histology reveals microstructural changes in the developing rat brain. Neuroimage 79, 329–339.
23. Liu, C., Li, W., Johnson, G.A., and Wu, B. (2011). High-field (9.4T) MRI of brain dysmyelination by quantitative mapping of magnetic susceptibility. Neuroimage 56, 930–938.
24. Johnson, G.A., Benveniste, H., Black, R.D., Hedlund, L.W., Maronpot, R.R., and Smith, B.R. (1993). Histology by magnetic resonance microscopy. Magn. Reson. Q. 9, 1–30.
25. Johnson, G.A., Cofer, G.P., Fubara, B., Gewalt, S.L., Hedlund, L.W., and Maronpot, R.R. (2002). Magnetic resonance histology for morphologic phenotyping. J. Magn. Reson. Imaging 16, 423–429.
26. Basser, P.J. (1995). Inferring microstructural features and the physiological state of tissues from diffusion-weighted images. NMR Biomed. 8, 333–344.
27. Mukherjee, P., Berman, J.I., Chung, S.W., Hess, C.P., and Henry, R.G. (2008). Diffusion tensor MR imaging and fiber tractography: theoretic underpinnings. AJNR Am. J. Neuroradiol. 29, 632–641.
28. Sponheim, S.R., McGuire, K.A., Kang, S.S., Davenport, N.D., Aviyente, S., Bernat, E.M., and Lim, K.O. (2011). Evidence of disrupted functional connectivity in the brain after combat-related blast injury. Neuroimage 54, Suppl 1, S21–S29.
29. Mac Donald, C., Johnson, A., Cooper, D., Malone, T., Sorrell, J., Shimony, J., Parsons, M., Snyder, A., Raichle, M., Fang, R., Flaherty, S., Russell, M., and Brody, D.L. (2013). Cerebellar white matter abnormalities following primary blast injury in US military personnel. PLoS ONE 8, e55823.
30. Mac Donald, C.L., Dikranian, K., Song, S.K., Bayly, P.V., Holtzman, D.M., and Brody, D.L. (2007). Detection of traumatic axonal injury with diffusion tensor imaging in a mouse model of traumatic brain injury. Exp. Neurol. 205, 116–131.
31. Bennett, R.E., Mac Donald, C.L., and Brody, D.L. (2012). Diffusion tensor imaging detects axonal injury in a mouse model of repetitive closed-skull traumatic brain injury. Neurosci. Lett. 513, 160–165.
32. Johnson, G.A., Cofer, G.P., Gewalt, S.L., and Hedlund, L.W. (2002). Morphologic phenotyping with MR microscopy: the visible mouse. Radiology 222, 789–793.
33. Stejskal, E.O., and Tanner, J.E. (1965). Spin diffusion measurements: spin echoes in the presence of a time-dependent field gradient. J. Chem. Phys. 42, 288–292.
34. Johnson, G.A., Ali-Sharief, A., Badea, A., Brandenburg, J., Cofer, G., Fubara, B., Gewalt, S., Hedlund, L.W., and Upchurch, L. (2007). High-throughput morphologic phenotyping of the mouse brain with magnetic resonance histology. Neuroimage 37, 82–89.
35. Avants, B.B., Epstein, C.L., Grossman, M., and Gee, J.C. (2008). Symmetric diffeomorphic image registration with cross-correlation: evaluating automated labeling of elderly and neurodegenerative brain. Med. Image Anal. 12, 26–41.
36. Avants, B.B., Tustison, N.J., Song, G., Cook, P.A., Klein, A., and Gee, J.C. (2011). A reproducible evaluation of ANTs similarity metric performance in brain image registration. Neuroimage 54, 2033–2044.
37. Kochunov, P., Lancaster, J.L., Thompson, P., Woods, R., Mazziotta, J., Hardies, J., and Fox, P. (2001). Regional spatial normalization: toward an optimal target. J. Comput. Assist. Tomogr. 25, 805–816.
38. Arsigny, V., Fillard, P., Pennec, X., and Ayache, N. (2006). Log-Euclidean metrics for fast and simple calculus on diffusion tensors. Magn. Reson. Med. 56, 411–421.
39. Johnson, G.A., Calabrese, E., Badea, A., Paxinos, G., and Watson, C. (2012). A multidimensional magnetic resonance histology atlas of the Wistar rat brain. Neuroimage 62, 1848–1856.
40. Paxinos, G., and Watson, C. (2007). *The Rat Brain in Stereotaxic Coordinates.* 6th ed. Elsevier Academic Press: San Diego.
41. de Olmos, J.S., Beltramino, C.A., and de Olmos de Lorenzo, S. (1994). Use of an amino-cupric-silver technique for the detection of early and semiacute neuronal degeneration caused by neurotoxicants, hypoxia, and physical trauma. Neurotoxicol. Teratol. 16, 545–561.
42. Long, J.B., Tong, L., Bauman, R.A., Atkins, J.L., Januszkiewicz, A.J., Riccio, C., Gharavi, R., Shoge, R., Parks, S., Ritzel, D.V., and Bentley, T.B. (2010). Blast-induced traumatic brain injury: using a shock tube to recreate a battlefield injury in the laboratory. IFMBE Proc, 32, pp. 26–30.
43. Kamnaksh, A., Kovesdi, E., Kwon, S.K., Wingo, D., Ahmed, F., Grunberg, N.E., Long, J., and Agoston, D.V. (2011). Factors affecting blast traumatic brain injury. J. Neurotrauma 28, 2145–2153.
44. Goldstein, L.E., Fisher, A.M., Tagge, C.A., Zhang, X.L., Velisek, L., Sullivan, J.A., Upreti, C., Kracht, J.M., Ericsson, M., Wojnarowicz, M.W., Goletiani, C.J., Maglakelidze, G.M., Casey, N., Moncaster, J.A., Minaeva, O., Moir, R.D., Nowinski, C.J., Stern, R.A., Cantu, R.C., Geiling, J., Blusztajn, J.K., Wolozin, B.L., Ikezu, T., Stein, T.D., Budson, A.E., Kowall, N.W., Chargin, D., Sharon, A., Saman, S., Hall, G.F., Moss, W.C., Cleveland, R. O., Tanzi, R.E., Stanton, P.K., and McKee, A.C. (2012). Chronic traumatic encephalopathy in blast-exposed military veterans and a blast neurotrauma mouse model. Sci. Transl. Med. 4, 134ra60.
45. Laurer, H.L., Bareyre, F.M., Lee, V.M., Trojanowski, J.Q., Longhi, L., Hoover, R., Saatman, K.E., Raghupathi, R., Hoshino, S., Grady, M.S., and McIntosh, T.K. (2001). Mild head injury increasing the brain's vulnerability to a second concussive impact. J. Neurosurg. 95, 859–870.
46. Longhi, L., Saatman, K.E., Fujimoto, S., Raghupathi, R., Meaney, D.F., Davis, J., McMillan B. S., Conte, V., Laurer, H.L., Stein, S., Stocchetti, N., and McIntosh, T.K. (2005). Temporal window of vulnerability to repetitive experimental concussive brain injury. Neurosurgery 56, 364–374.
47. Taber, K.H., Warden, D.L., and Hurley, R.A. (2006). Blast-related traumatic brain injury: what is known? J. Neuropsychiatry Clin. Neurosci. 18, 141–145.
48. Jones, D.K., and Cercignani, M. (2010). Twenty-five pitfalls in the analysis of diffusion MRI data. NMR Biomed. 23, 803–820.
49. Abe, O., Takao, H., Gonoi, W., Sasaki, H., Murakami, M., Kabasawa, H., Kawaguchi, H., Goto, M., Yamada, H., Yamasue, H., Kasai, K., Aoki, S., and Ohtomo, K. (2010). Voxel-based analysis of the diffusion tensor. Neuroradiology 52, 699–710.
50. Jones, D.K., Symms, M.R., Cercignani, M., and Howard, R.J. (2005). The effect of filter size on VBM analyses of DT-MRI data. Neuroimage 26, 546–554.
51. Song, S.K., Sun, S.W., Ju, W.K., Lin, S.J., Cross, A.H., and Neufeld, A.H. (2003). Diffusion tensor imaging detects and differentiates axon and myelin degeneration in mouse optic nerve after retinal ischemia. Neuroimage 20, 1714–1722.
52. Newcombe, V. F., Williams, G.B., Nortje, J., Bradley, P.G., Harding, S.G., Smielewski, P., Coles, J.P., Maiya, B., Gillard, J.H., Hutchinson, P.J., Pickard, J.D., Carpenter, T.A., and Menon, D.K. (2007). Analysis of acute traumatic axonal injury using diffusion tensor imaging. Br. J. Neurosurg. 21, 340–348.
53. Sidaros, A., Engberg, A.W., Sidaros, K., Liptrot, M.G., Herning, M., Petersen, P., Paulson, O.B., Jernigan, T.L., and Rostrup, E. (2008). Diffusion tensor imaging during recovery from severe traumatic brain injury and relation to clinical outcome: a longitudinal study. Brain 131, 559–572.
54. Marmarou, A., Foda, M.A., van den Brink, W., Campbell, J., Kita, H., and Demetriadou, K. (1994). A new model of diffuse brain injury in rats. Part I: Pathophysiology and biomechanics. J. Neurosurg. 80, 291–300.
55. Rooker, S., Jorens, P.G., Van Reempts, J., Borgers, M., and Verlooy, J. (2003). Continuous measurement of intracranial pressure in awake rats after experimental closed head injury. J. Neurosci. Methods 131, 75–81.
56. Chafi, M.S., Karami, G., and Ziejewski, M. (2010). Biomechanical assessment of brain dynamic responses due to blast pressure waves. Ann. Biomed. Eng. 38, 490–504.
57. Säljö, A., Bao, F., Haglid, K. G., and Hansson, H. A. (2000). Blast exposure causes redistribution of phosphorylated neurofilament subunits in neurons of the adult rat brain. J. Neurotrauma 17, 719–726.
58. Park, E., Gottlieb, J.J., Cheung, B., Shek, P.N., and Baker, A.J. (2011). A model of low-level primary blast brain trauma results in cytoskeletal proteolysis and chronic functional impairment in the absence of lung barotrauma. J. Neurotrauma 28, 343–357.
59. Yushkevich, P.A., Zhang, H., Simon, T.J., and Gee, J.C. (2008). Structure-specific statistical mapping of white matter tracts. Neuroimage 41, 448–461.
60. Yendiki, A., Panneck, P., Srinivasan, P., Stevens, A., Zöllei, L., Augustinack, J., Wang, R., Salat, D., Ehrlich, S., Behrens, T., Jbabdi, S., Gollub, R., and Fischl, B. (2011). Automated probabilistic reconstruction of white-matter pathways in health and disease using an atlas of the underlying anatomy. Front. Neuroinform. 5, 23.

61. Goodlett, C., Davis, B., Jean, R., Gilmore, J., and Gerig, G. (2006). Improved correspondence for DTI population studies via unbiased atlas building. Med. Image Comput. Comput. Assist. Interv. 9, 260–267.
62. Sun, S.W., Liang, H.F., Xie, M., Oyoyo, U., and Lee, A. (2009). Fixation, not death, reduces sensitivity of DTI in detecting optic nerve damage. Neuroimage 44, 611–619.
63. Cenci, M.A., Whishaw, I. Q., and Schallert, T. (2002). Animal models of neurological deficits: how relevant is the rat? Nat. Rev. Neurosci. 3, 574–579.
64. Sun, S.W., Neil, J.J., Liang, H.F., He, Y.Y., Schmidt, R.E., Hsu, C.Y., and Song, S.K. (2005). Formalin fixation alters water diffusion coefficient magnitude but not anisotropy in infarcted brain. Magn. Reson. Med. 53, 1447–1451.
65. Lerch, J.P., Gazdzinski, L., Germann, J., Sled, J.G., Henkelman, R.M., and Nieman, B.J. (2012). Wanted dead or alive? The tradeoff between in-vivo versus ex-vivo MR brain imaging in the mouse. Front. Neuroinform. 6, 6.
66. Ni, H., Kavcic, V., Zhu, T., Ekholm, S., and Zhong, J. (2006). Effects of number of diffusion gradient directions on derived diffusion tensor imaging indices in human brain. AJNR Am. J. Neuroradiol. 27, 1776–1781.
67. Landman, B.A., Farrell, J.A., Jones, C.K., Smith, S.A., Prince, J.L., and Mori, S. (2007). Effects of diffusion weighting schemes on the reproducibility of DTI-derived fractional anisotropy, mean diffusivity, and principal eigenvector measurements at 1.5T. Neuroimage 36, 1123–1138.
68. Anderson, A.W. (2001). Theoretical analysis of the effects of noise on diffusion tensor imaging. Magn. Reson. Med. 46, 1174–1188.
69. Alexander, A.L., Hasan, K.M., Lazar, M., Tsuruda, J.S., and Parker, D.L. (2001). Analysis of partial volume effects in diffusion-tensor MRI. Magn. Reson. Med. 45, 770–780.

Address correspondence to:
Joseph B. Long, PhD
Blast-Induced Neurotrauma Branch
Center for Military Psychiatry and Neuroscience
Walter Reed Army Institute of Research
Robert Grant Avenue, Building 503
Silver Spring, MD 20910

E-mail: joseph.long@us.army.mil

This article has been cited by:

1. Peter R. Leeds, Fengshan Yu, Zhifei Wang, Chi-Tso Chiu, Yumin Zhang, Yan Leng, Gabriel R. Linares, De-Maw Chuang. 2014. A New Avenue for Lithium: Intervention in Traumatic Brain Injury. *ACS Chemical Neuroscience* 140411152540005. [CrossRef]

Neuroscience Letters 552 (2013) 87–91

Contents lists available at ScienceDirect

Neuroscience Letters

journal homepage: www.elsevier.com/locate/neulet

Distinct patterns of expression of traumatic brain injury biomarkers after blast exposure: Role of compromised cell membrane integrity

Peethambaran Arun[a,*], Rania Abu-Taleb[a], Samuel Oguntayo[a], Mikiei Tanaka[b], Ying Wang[a], Manojkumar Valiyaveettil[a], Joseph B. Long[a], Yumin Zhang[b], Madhusoodana P. Nambiar[a]

[a] Blast-Induced Neurotrauma Branch, Center for Military Psychiatry and Neurosciences, Walter Reed Army Institute of Research, 503 Robert Grant Avenue, Silver Spring, MD 20910, USA
[b] Department of Anatomy, Physiology and Genetics, Uniformed Services University of the Health Sciences, 4301 Jones Bridge Road, Bethesda, MD 20814, USA

HIGHLIGHTS

- Repeated blast exposures causes acute decrease in GFAP and *Tau* in brain and plasma.
- GFAP and *Tau* levels increases acutely in the liver and spleen after blast exposure.
- No acute changes in GFAP and *Tau* mRNA levels in the liver after blast exposure.
- The acute changes in GFAP and *Tau* suggest blast-induced cell membrane disruption.

ARTICLE INFO

Article history:
Received 29 May 2013
Received in revised form 17 July 2013
Accepted 27 July 2013

Keywords:
Blast exposure
Cell membrane integrity
GFAP
Tau
Polytrauma

ABSTRACT

Glial fibrillary acidic protein (GFAP), a protein enriched in astrocytes, and *Tau*, a protein abundant in neuronal microtubules, are being widely studied as biomarkers of brain injury, and persistent severity-dependent increases in brain and blood have been reported. Studies on the acute changes of these proteins after blast exposure are limited. Using a mouse model of closely-coupled repeated blast exposures, we have evaluated acute changes in the levels of GFAP and total *Tau* by Western blotting. Brain levels of GFAP and *Tau* proteins decreased significantly at 6 h and increased considerably at 24 h after repeated blast exposures. Plasma samples showed a similar initial decrease and later increase over this timeframe. This biphasic pattern points to possible absorption or sequestration of these proteins from plasma immediately after repeated blast exposures. Liver and spleen tissue showed significant increases in the levels of GFAP and *Tau* protein at 6 and 24 h post-blast exposures whereas semi-quantitative RT-PCR analysis of liver showed no significant changes in the levels of GFAP or *Tau* mRNAs. These results suggest that blast exposure causes transient changes in cell membrane integrity in multiple organs leading to abnormal migration of proteins from the tissues to the plasma and *vice versa.* This transient changes in cell membrane permeability and subsequent bidirectional movement of molecules may contribute to the pathophysiology of TBI and polytrauma after blast exposure.

1. Introduction

The incidence of traumatic brain injury (TBI) increased tremendously during the recent wars and exposure to blast from improvised explosive devices has been reported as the major cause of battlefield TBI and associated disabilities in service members [14]. One of the major differences between blast-induced TBI and other closed head or penetrating brain injuries is that blast exposure concomitantly injures other organs of the body, especially air filled organs, resulting in polytrauma. Military personnel are subject to both high intensity single or low intensity repeated blast exposures, and we have previously reported that the severity of brain injury increases with number of blast exposures [27].

Identification of sensitive and specific biomarkers of TBI is potentially useful for the diagnosis of injury and evaluation of the efficacy of therapies. Although no biomarkers unique to blast-induced TBI have been reported in clinical or pre-clinical blast exposure studies to date, several brain proteins that are being

Abbreviations: TBI, traumatic brain injury; GFAP, glial fibrillary acidic protein; BOP, blast overpressure; CSF, cerebrospinal fluid; mRNA, messenger ribonucleic acid; RT-PCR, reverse transcription-polymerase chain reaction.

* Corresponding author. Tel.: +1 301 319 2009; fax: +1 301 319 9839.
E-mail addresses: peethambaran.arun.ctr@mail.mil, peethambaran.arun@us.army.mil (P. Arun).

0304-3940/$ – see front matter © 2013 Elsevier Ireland Ltd. All rights reserved.
http://dx.doi.org/10.1016/j.neulet.2013.07.047

widely evaluated as biomarkers of other forms of brain injury have also been considered as biomarkers of blast TBI. Notably, glial fibrillary acidic protein (GFAP), a protein enriched in astrocytes, and *Tau*, a protein abundant in neuronal microtubules has been monitored after various forms of brain injury including blast-induced TBI [4,7,10,22,24,25].

Changes in blood and cerebrospinal fluid (CSF) levels of GFAP have been widely studied as sensitive biomarkers for the diagnosis TBI in humans [5,9,13,19,21,26,28] and significant up-regulation of GFAP levels in multiple regions of the brain has also been reported at different intervals after blast exposure in animal models of blast-induced TBI [4,7,10,24]. In all these pre-clinical studies, the changes in GFAP were evaluated after 24 h post-exposure. Changes in GFAP levels in the brain or body fluids immediately after single blast exposure have not been well documented. Besides, there are no studies addressing the effects on GFAP levels in the brain or blood after repeated blast exposures.

Apart from GFAP, up-regulation of total and phosphorylated *Tau* proteins have also been shown in the brain, CSF and blood of patients with different forms of TBI, and hence these proteins have been proposed as reliable biomarkers of outcome after TBI [11,15,20,23]. Total and phosphorylated *Tau* proteins in the brain were significantly increased in different animal models of TBI [7,11,22,25]. Limited studies have been carried out to assess the changes in total or phosphorylated *Tau* proteins in the brain or body fluids after blast exposure and there are no such studies after repeated blast exposures. Similar to studies evaluated GFAP levels, the differential expression of *Tau* protein was determined only at 24 h or later in single blast exposure and no studies so far investigated the acute changes in *Tau* proteins after repeated blast exposures.

In the present study, we assessed immediate changes in GFAP and total *Tau* protein in the brains and plasma of mice after closely coupled repeated blast overpressure exposures in a shock tube as described earlier [27]. Western blotting with specific antibodies was used to assess the levels of these potential blast injury biomarkers. Our results after repeated blast exposures showed an initial decrease and later increase in the levels of both GFAP and total *Tau* proteins in the brain and plasma. We further explored the potential mechanism of the contrasting changes in the two biomarkers of TBI after repeated blast exposures.

2. Materials and methods

2.1. Animals and blast exposures

All animal experiments were conducted in accordance with the Animal Welfare Act and other federal statutes and regulations relating to animals and experiments involving animals and adhered to principles stated in the Guide for the Care and Use of Laboratory Animals (NRC Publication 1996 edition). The animal protocol was approved by Institutional Animal Care and Use Committee, Walter Reed Army Institute of Research. C57BL/6J male mice (8–10 weeks old) that weighed between 21 and 26 g (Jackson Laboratory, Bar Harbor, ME) were used in this study. A compressed air-driven shock tube described earlier [12,27] was used for repeated blast exposures. Mice were anesthetized with 4% isoflurane gas (O_2 flow rate 1.5 L/min) for 8 min and restrained in the prone position with a tautly-drawn net to minimize the movements during blast exposure. Animals were subjected to three blast overpressure (BOP) exposures (21 psi) separated by 1 and 30 min as described earlier [28]. Blood plasma, brain, liver and spleen were collected after euthanasia at 6 or 24 h post-blast and frozen immediately. Cerebellum, which showed significant injury after blast exposure in previous studies [27] was dissected out immediately before freezing the brain.

2.2. Western blot analysis of tissue homogenates

Tissue homogenates (20%, w/v) were prepared in tissue protein extraction buffer (Pierce Chemical Co., Rockford, IL) containing protease and phosphatase inhibitor cocktails (Sigma–Aldrich, St. Louis, MO) using an ultrasonic homogenizer. The homogenates were centrifuged at $5000 \times g$ for 5 min at 4 °C and 2 μl each of supernatants were used for Western blotting. Rabbit polyclonal antibodies against GFAP and total *Tau* protein were obtained from Abcam (Cambridge, MA) and Santa Cruz Biotechnologies (Santa Cruz, CA), respectively. GFAP antibody was used at a dilution of 1:40,000 and an antibody to total *Tau* proteins was used at 1:1000 dilution. Secondary antibody labeled with horse-radish peroxidase (HRP) was also purchased from Santa Cruz Biotechnology and used at a dilution of 1:2500. A mouse monoclonal antibody to β-actin conjugated with HRP (Sigma–Aldrich, St. Louis, MO) was used as gel loading control at a dilution of 1:40,000. SDS–polyacrylamide gel electrophoresis and Western blotting analysis of protein extracts from cerebellum, liver and spleen was carried out as described earlier [3]. After Western blotting, the protein bands were detected using ECL-Plus Western blot detection reagent (GE Healthcare, Piscataway, NJ) and the chemiluminescence was imaged in an AlphaImage reader (Cell Biosciences, Santa Clara, CA). The band intensity was measured by densitometry using AlphaView software (Cell Biosciences, Santa Clara, CA).

2.3. Western blotting of GFAP and tau proteins in the plasma

Plasma was purified by removing albumins and globulins using ProteoExtract Albumin/IgG removal kit from EMD-Millipore Corporation (Chicago, IL) according to manufacturer's instructions. Briefly, 850 μl of binding buffer was allowed to pass through the column by gravity-flow. Plasma (35 μl) was diluted 10-fold with binding buffer, allowed to pass through the column and the flow-through was collected. The unbound proteins were also collected by passing 650 μl of binding buffer though the column twice. The collected flow-through fractions were pooled and concentrated using a 3000 MW cut off VIVASPIN 500 centrifugal filters (Sartorius Stedim, Bohemia, NY) according to manufacturer's instructions. Concentrated albumin and globulin free fractions corresponding to 5 μl of original plasma were used for Western blotting as described above.

2.4. Semi-quantitative RT-PCR analysis of liver tissue

Frozen mouse liver tissue was thawed and homogenized by pipetting with 1 ml of TRIzol reagent (Life Technologies, Grand Island, NY). Total RNA was isolated according to manufacturer's protocol. For cDNA synthesis, total RNA (1 μg) was subjected to reverse transcription in a reaction mixture containing dNTPs (0.5 mM), random hexamer primer (0.01 μg/μl), and 40 U of RNase inhibitor (Thermo Scientific, Waltham, MA) and RNasin (Promega Corporation, Madison, WI) for 45 min at 50 °C. Using premix PCR mixture (Thermo Scientific, Waltham, MA), PCR was performed in the presence of 0.33 μM of gene specific primers and 0.5 μl of cDNA in thermal cycler as follows; 95 °C × 1 min, followed by 35 cycles of 95 °C × 30 s, 61 °C × 30 s, 72 °C × 30 s, subsequently 72 °C × 5 min. Primers for GFAP were 5′-CTGGCTGCGTATAGACAGGA-3′ as forward, 5′-GAACTGGATCTCCTCCTCCA-3′ as reverse, and primers for *Tau* were 5′-GTGGAGGCAGTGTGCAAATA-3′ as forward, 5′-GCCAATCTTCGACTGGACTC-3′ as reverse. Aliquots were loaded and electrophoresed in 2% agarose gel. PCR product was visualized with ethidium bromide under UV illuminator and the image was captured using GeneSnap software (Syngene, Frederick, MD). Brain tissue from sham control mice was used as positive control.

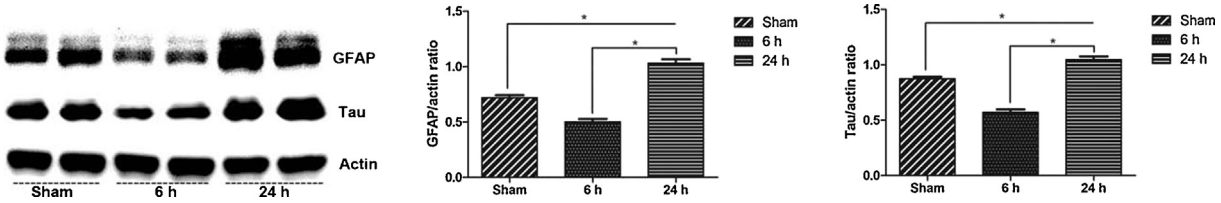

Fig. 1. Western blot analysis of the cerebellum showing the immediate decrease and later increase in the levels of GFAP and *Tau* proteins after repeated blast exposures. Representative blot from two out of four animals in each group is presented. Densitometry analysis was carried out as described in Section 2. $^{*}p < 0.01$ ($n = 4$).

2.5. Statistical analysis

Statistical analysis was carried out by analysis of variance (ANOVA) using SAS software version 9.3. Values were expressed as mean ± standard deviation (SD). A p value less than 0.01 was considered significant.

3. Results

3.1. Changes in GFAP and total Tau protein expression in the brain after blast exposure

Western blot analyses of the cerebellum revealed biphasic time-dependent changes in the expression of both GFAP and total *Tau* proteins after repeated blast exposures (Fig. 1). The levels of these proteins decreased significantly at 6 h and increased appreciably at 24 h after repeated blast exposures. Densitometry analysis indicated that the ratios of GFAP to actin as well as total *Tau* to actin were significantly reduced at 6 h and increased considerably at 24 h after repeated blast exposures.

3.2. Levels of GFAP and total Tau proteins in the plasma after blast exposure

Similar to the brain, biphasic changes in the levels of both GFAP and total *Tau* proteins were recorded in the plasma after repeated blast exposures (Fig. 2). Densitometry of the Western blot showed that plasma levels of GFAP as well as total *Tau* proteins were significantly reduced at 6 h and increased at 24 h after repeated blast exposures.

3.3. Levels of GFAP and total Tau proteins in the liver and spleen after blast exposure

GFAP and total *Tau* proteins were readily detected in the liver and spleen of sham control mice. Densitometry analysis and the ratios of GFAP to actin as well as total *Tau* protein to actin indicated a significant increase in the levels of both GFAP and total *Tau* proteins in the liver and spleen at 6 and 24 h after blast repeated exposures (Fig. 3). Compared to 6 h, the increase in the levels of both GFAP and total *Tau* proteins at 24 h was marginal and was not statistically significant in both tissues.

3.4. Expression of GFAP and Tau mRNA levels in the liver after blast exposure

To investigate whether the increase in GFAP and *Tau* proteins in the liver is due to increased synthesis, RT-PCR of liver tissue mRNA was performed and showed the presence of products with the same base pairs corresponding to GFAP and *Tau* proteins in the brain. Semi-quantitative RT-PCR analysis of liver tissues indicated that the levels of GFAP or *Tau* mRNAs were not increased significantly at 6 or 24 h after repeated blast exposures (Fig. 4).

4. Discussion

Our results showed for the first time that repeated blast exposures caused pronounced biphasic changes in two well-known biomarkers of TBI in the brain and plasma. In the brain and plasma, the levels of GFAP and total *Tau* proteins decreased significantly at 6 h after repeated blast exposures, whereas their levels were increased at 24 h post-blast exposures. The increase in the expression of GFAP at 24 h after blast exposure is in agreement with the previous preclinical studies [4,24]. To our knowledge, no studies have established this acute change in GFAP in the brain or plasma after single or repeated blast exposures. In the case of *Tau* protein, measured changes in total or phosphorylated *Tau* have been restricted to several days after single blast exposure [7,10].

The significant decrease in GFAP and Tau proteins in the brain at 6 h after repeated blast exposures was an unanticipated and somewhat paradoxical result. Since the turnover of GFAP and *Tau* proteins in the brain is very slow [6,16], the acute decrease in GFAP/Tau in the brain after blast exposure can most likely be interpreted as a blast-induced rapid disruption of glial/neuronal cell membranes and protein leakage across a disrupted blood–brain barrier into the circulation. However, Western blotting of plasma showed a similar significant decrease in the levels of both the proteins at 6 h after repeated blast exposures (Fig. 2). Parallel decreases of both putative biomarkers in brain and plasma shortly after blast exposure points to their rapid redistribution or elimination from the blood during this acute timeframe.

Using an *in vitro* model of blast-induced TBI, it has recently been shown that blast exposure causes transient disruption of neuronal cell membrane integrity leading to bidirectional movement of molecules across the cell membrane [1]. Rapid disruption of cell membrane integrity of liver cells and muscle fibers and the

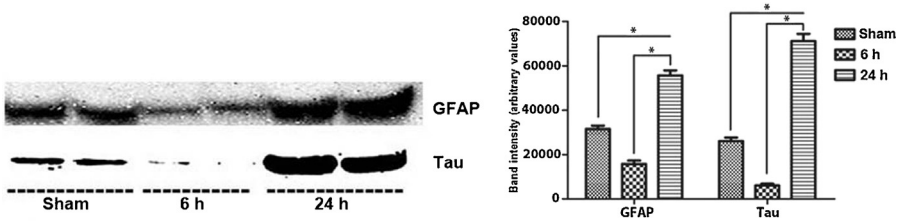

Fig. 2. Western blot analysis of plasma showing the immediate decrease and later increase in the levels of GFAP and *Tau* proteins after repeated blast exposures. Representative blot from two out of four animals in each group is presented. Densitometry analysis was carried out as described in Section 2.$^{*}p < 0.01$ ($n = 4$).

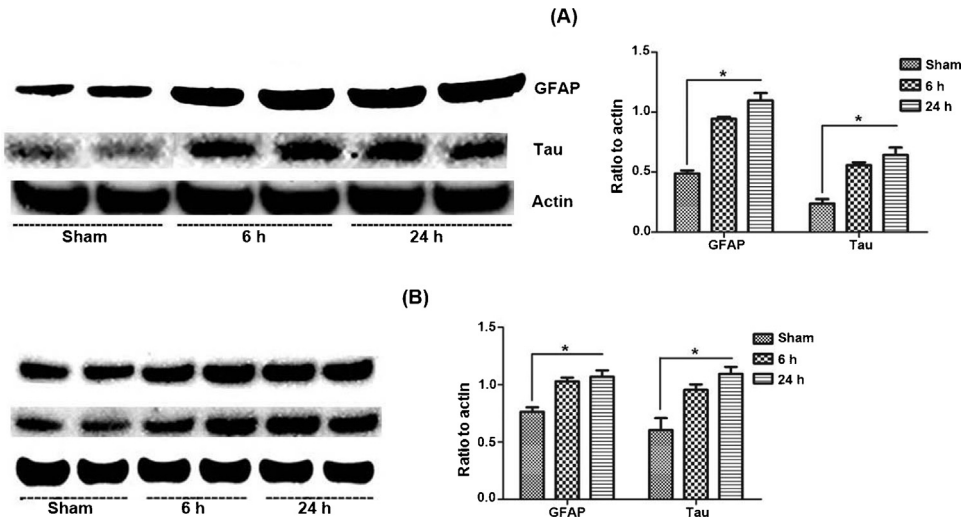

Fig. 3. Western blot analysis of liver (A) and spleen (B) showing the levels of GFAP and *Tau* proteins at 6 and 24 h after repeated blast exposures. Representative blots from two out of four animals in each group for liver and spleen are presented. Densitometry analysis was carried out as described in Section 2.*$p < 0.01$ ($n = 4$).

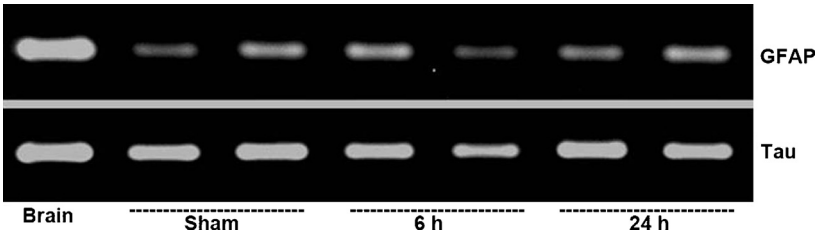

Fig. 4. Semi-quantitative RT-PCR analysis of liver showing the mRNA levels of GFAP and Tau proteins. Total RNA isolated from the brain of a sham control mice was used as positive control. RT-PCR was carried out as described in the methods section. Representative figure from two out of four animals in each group is presented.

subsequent release of organ specific cellular proteins into the circulation after repeated blast exposures have also been reported [2]. Collectively, these data suggest that blast exposure affects the cell membrane integrity of brain and peripheral organs which can lead to widespread bidirectional passage of molecules. The various potential mechanisms of cell membrane disruption after blast exposure have been described in detail by Nakagawa et al. [18].

The parallel decreased levels of GFAP/*Tau* proteins in the brain and plasma at 6 h after repeated blast exposures suggests a possible shift and accumulation of these proteins in peripheral organs. Liver is one of the largest organs of the body and it showed blast overpressure-dependent release of enzyme to circulation, revealing cell membrane disruption [2]. Based upon earlier studies of liver after blast exposure and the expression of GFAP and *Tau* proteins in this organ [2,8,17], we investigated blast-induced changes in the levels of these proteins in the liver. We also examined the spleen, which is a primary component of the reticuloendothelial system where the blood is being processed. Increased levels of GFAP and *Tau* in both the liver and spleen coincided with their simultaneously decreased levels in the brain and plasma at 6 h after repeated blast exposures. To investigate whether their increased levels resulted from locally increased synthesis, we measured the mRNA levels of GFAP and *Tau* proteins in the liver. The semi-quantitative RT-PCR analysis data showed no significant increase in the mRNA levels of GFAP and *Tau* proteins in the liver. These data reinforce the conclusion that these proteins transiently accumulate in these organs following passage from the circulation after repeated blast exposures.

Although GFAP and Tau proteins remained elevated in the liver and spleen after blast exposure, there was no significant difference in the levels at 24 h compared to 6 h, even though the levels of these proteins increased substantially in the plasma at 24 h after the blast exposure. Restoration of vascular, liver, and spleen cell membrane integrity may have prevented further passage of these proteins in these organs. Previous studies using *in vitro* and *in vivo* models of blast-induced TBI indicate that the cell membrane disruption after blast exposure is transient and the restoration of cell membrane integrity take place rapidly [1,2].

A potential pathophysiological consequence of transient disruption of cell membrane integrity after blast exposure is the transport of foreign molecules, including proteins, which can enter various cells of peripheral organs and brain from the blood circulation and may remain intracellularly for longer time leading to chronic pathological changes. Furthermore, the essential molecules rapidly released from the cells due to transient disruption of cell membrane after blast exposure can also affect cellular homeostasis. Thus, the rapid abnormal bidirectional movement of molecules in the brain and peripheral organs immediately after blast exposure may have the possibility to trigger long-term consequences, a potential mechanism contributing to blast-induced polytrauma. These time-dependent bidirectional changes also point to a fundamental issue complicating and potentially limiting the utility of these circulating proteins as acute biomarkers of blast injury.

Disclosure

The contents, opinions and assertions contained herein are private views of the authors and are not to be construed as official or reflecting the views of the Department of the Army or the Department of Defense. The authors report no conflict of interest.

Acknowledgements

Support from Mrs. Irene Gist and COL Paul Bliese are appreciated. We also gratefully acknowledge the technical guidance from Drs. Angela Boutte and Jitendra Dave.

References

[1] P. Arun, R. Abu-Taleb, M. Valiyaveettil, Y. Wang, J.B. Long, M.P. Nambiar, Transient changes in neuronal cell membrane permeability after blast exposure, NeuroReport 23 (2012) 342–346.
[2] P. Arun, S. Oguntayo, Y. Alamneh, C. Honnold, Y. Wang, M. Valiyaveettil, J.B. Long, M.P. Nambiar, Rapid release of tissue enzymes into blood after blast exposure: potential use as biological dosimeters, PLoS ONE 7 (2012) e33798.
[3] P. Arun, M. Valiyaveettil, L. Biggemann, Y. Alamneh, Y. Wei, S. Oguntayo, Y. Wang, J.B. Long, M.P. Nambiar, Modulation of hearing related proteins in the brain and inner ear following repeated blast exposures, Interventional Medicine and Applied Science 4 (2012) 125–131.
[4] I. Cernak, A.C. Merkle, V.E. Koliatsos, J.M. Bilik, Q.T. Luong, T.M. Mahota, L. Xu, N. Slack, D. Windle, F.A. Ahmed, The pathobiology of blast injuries and blast-induced neurotrauma as identified using a new experimental model of injury in mice, Neurobiology of Disease 41 (2011) 538–551.
[5] E. Czeiter, S. Mondello, N. Kovacs, J. Sandor, A. Gabrielli, K. Schmid, F. Tortella, K.K. Wang, R.L. Hayes, P. Barzo, E. Ezer, T. Doczi, A. Buki, Brain injury biomarkers may improve the predictive power of the IMPACT outcome calculator, Journal of Neurotrauma 29 (2012) 1770–1778.
[6] S.J.DeArmond, Y.L. Lee, H.A. Kretzschmar, L.F. Eng, Turnover of glial filaments in mouse spinal cord, Journal of Neurochemistry 47 (1986) 1749–1753.
[7] L.E. Goldstein, A.M. Fisher, C.A. Tagge, X.L. Zhang, L. Velisek, J.A. Sullivan, C. Upreti, J.M. Kracht, M. Ericsson, M.W. Wojnarowicz, C.J. Goletiani, G.M. Maglakelidze, N. Casey, J.A. Moncaster, O. Minaeva, R.D. Moir, C.J. Nowinski, R.A. Stern, R.C. Cantu, J. Geiling, J.K. Blusztajn, B.L. Wolozin, T. Ikezu, T.D. Stein, A.E. Budson, N.W. Kowall, D. Chargin, A. Sharon, S. Saman, G.F. Hall, W.C. Moss, R.O. Cleveland, R.E. Tanzi, P.K. Stanton, A.C. McKee, Chronic traumatic encephalopathy in blast-exposed military veterans and a blast neurotrauma mouse model, Science Translational Medicine 4 (2012) 134ra60.
[8] Y. Gu, F. Oyama, Y. Ihara, Tau is widely expressed in rat tissues, Journal of Neurochemistry 67 (1996) 1235–1244.
[9] M. Honda, R. Tsuruta, T. Kaneko, S. Kasaoka, T. Yagi, M. Todani, M. Fujita, T. Izumi, T. Maekawa, Serum glial fibrillary acidic protein is a highly specific biomarker for traumatic brain injury in humans compared with S-100B and neuron-specific enolase, Journal of Trauma 69 (2010) 104–109.
[10] E. Kovesdi, A.B. Gyorgy, S.K. Kwon, D.L. Wingo, A. Kamnaksh, J.B. Long, C.E. Kasper, D.V. Agoston, The effect of enriched environment on the outcome of traumatic brain injury; a behavioral, proteomics, and histological study, Frontiers in Neuroscience 5 (2011) 42.
[11] P.C. Liliang, C.L. Liang, H.C. Weng, K. Lu, K.W. Wang, H.J. Chen, J.H. Chuang, Tau proteins in serum predict outcome after severe traumatic brain injury, Journal of Surgical Research 160 (2010) 302–307.
[12] J.B. Long, T.L. Bentley, K.A. Wessner, C. Cerone, S. Sweeney, R.A. Bauman, Blast overpressure in rats: recreating a battlefield injury in the laboratory, Journal of Neurotrauma 26 (2009) 827–840.
[13] K.M. Lumpkins, G.V. Bochicchio, K. Keledjian, J.M. Simard, M. McCunn, T. Scalea, Glial fibrillary acidic protein is highly correlated with brain injury, Journal of Trauma 65 (2008) 778–782.
[14] J. Magnuson, F. Leonessa, G.S. Ling, Neuropathology of explosive blast traumatic brain injury, Current Neurology and Neuroscience Reports 12 (2012) 570–579.
[15] N. Marklund, K. Blennow, H. Zetterberg, E. Ronne-Engstrom, P. Enblad, L. Hillered, Monitoring of brain interstitial total tau and beta amyloid proteins by microdialysis in patients with traumatic brain injury, Journal of Neurosurgery 110 (2009) 1227–1237.
[16] J.Morales-Corraliza, M.J. Mazzella, J.D. Berger, N.S. Diaz, J.H. Choi, E. Levy, Y. Matsuoka, E. Planel, P.M. Mathews, In vivo turnover of tau and APP metabolites in the brains of wild-type and Tg2576 mice: greater stability of sAPP in the beta-amyloid depositing mice, PLoS ONE 4 (2009) e7134.
[17] S. Morini, S. Carotti, G. Carpino, A. Franchitto, S.G. Corradini, M. Merli, E. Gaudio, GFAP expression in the liver as an early marker of stellate cells activation, Italian Journal of Anatomy and Embryology 110 (2005) 193–207.
[18] A. Nakagawa, G.T. Manley, A.D. Gean, K. Ohtani, R. Armonda, A. Tsukamoto, H. Yamamoto, K. Takayama, T. Tominaga, Mechanisms of primary blast-induced traumatic brain injury: insights from shock-wave research, Journal of Neurotrauma 28 (2011) 1101–1119.
[19] K. Nylen, M. Ost, L.Z. Csajbok, I. Nilsson, K. Blennow, B. Nellgard, L. Rosengren, Increased serum-GFAP in patients with severe traumatic brain injury is related to outcome, Journal of the Neurological Sciences 240 (2006) 85–91.
[20] M. Ost, K. Nylen, L. Csajbok, A.O. Ohrfelt, M. Tullberg, C. Wikkelso, P. Nellgard, L. Rosengren, K. Blennow, B. Nellgard, Initial CSF total tau correlates with 1-year outcome in patients with traumatic brain injury, Neurology 67 (2006) 1600–1604.
[21] L.E. Pelinka, A. Kroepfl, R. Schmidhammer, M. Krenn, W. Buchinger, H. Redl, A. Raabe, Glial fibrillary acidic protein in serum after traumatic brain injury and multiple trauma, Journal of Trauma 57 (2004) 1006–1012.
[22] E. Rostami, J. Davidsson, K.C. Ng, J. Lu, A. Gyorgy, J. Walker, D. Wingo, S. Plantman, B.M. Bellander, D.V. Agoston, M. Risling, A model for mild traumatic brain injury that induces limited transient memory impairment and increased levels of axon related serum biomarkers, Frontiers in Neurology 3 (2012) 115.
[23] C. Smith, D.I. Graham, L.S. Murray, J.A. Nicoll, Tau immunohistochemistry in acute brain injury, Neuropathology and Applied Neurobiology 29 (2003) 496–502.
[24] S.I. Svetlov, V. Prima, D.R. Kirk, H. Gutierrez, K.C. Curley, R.L. Hayes, K.K. Wang, Morphologic and biochemical characterization of brain injury in a model of controlled blast overpressure exposure, Journal of Trauma 69 (2010) 795–804.
[25] H.T. Tran, L. Sanchez, T.J. Esparza, D.L. Brody, Distinct temporal and anatomical distributions of amyloid-beta and tau abnormalities following controlled cortical impact in transgenic mice, PLoS ONE 6 (2011) e25475.
[26] P.E. Vos, B. Jacobs, T.M. Andriessen, K.J. Lamers, G.F. Borm, T. Beems, M. Edwards, C.F. Rosmalen, J.L. Vissers, GFAP S100B are biomarkers of traumatic brain injury: an observational cohort study, Neurology 75 (2010) 1786–1793.
[27] Wang, Y. Wei, S. Oguntayo, W. Wilkins, P. Arun, M. Valiyaveettil, J. Song, J. Long, M.P. Nambiar, Tightly coupled repetitive blast-induced traumatic brain injury: development and characterization in mice, Journal of Neurotrauma 28 (2011) 2171–2183.
[28] J. Zurek, M. Fedora, The usefulness of S100B, NSE GFAP, NF-H, secretagogin and Hsp70 as a predictive biomarker of outcome in children with traumatic brain injury, Acta Neurochirurgica (Wien) 154 (2012) 93–103.

Neuroscience Research 76 (2013) 98–100

Contents lists available at SciVerse ScienceDirect

Neuroscience Research

journal homepage: www.elsevier.com/locate/neures

Rapid communication

Extracellular cyclophilin A protects against blast-induced neuronal injury☆

Peethambaran Arun*, Rania Abu-Taleb, Manojkumar Valiyaveettil, Ying Wang, Joseph B. Long, Madhusoodana P. Nambiar

Blast-Induced Neurotrauma Branch, Center for Military Psychiatry and Neuroscience, Walter Reed Army Institute of Research, 503 Robert Grant Ave, Silver Spring, MD 20910, USA

ARTICLE INFO

Article history:
Received 19 December 2012
Received in revised form 21 February 2013
Accepted 27 February 2013
Available online 17 March 2013

Keywords:
Traumatic brain injury
blast exposure
cyclophilin A
SH-SY5Y cells
neuroprotection

ABSTRACT

Blast-induced traumatic brain injury (TBI) and subsequent neurobehavioral deficits are major disabilities suffered by the military and civilian population worldwide. Rigorous scientific research is underway to understand the mechanism of blast TBI and thereby develop effective therapies for protection and treatment. By using an *in vitro* shock tube model of blast TBI with SH-SY5Y human neuroblastoma cells, we have demonstrated that blast exposure leads to neurobiological changes in an overpressure and time dependent manner. Paradoxically, repeated blast exposures resulted in less neuronal injury compared to single blast exposure and suggested a potential neuroprotective mechanism involving released cyclophilin A (CPA). In the present study, we demonstrate accumulation of CPA in the culture medium after repeated blast exposures supporting the notion of extracellular CPA mediated neuroprotection. Post-exposure treatment of the cells with purified recombinant CPA caused significant protection against blast-induced neuronal injury. Furthermore, repeated blast exposure was associated with phosphorylation of the proteins ERK1/2 and *Bad* suggesting a potential mechanism of neuroprotection by extracellular CPA and may aid in the development of targeted therapies for protection against blast-induced TBI.

Blast-induced traumatic brain injury (blast TBI) is a principal cause of major disabilities associated with the recent conflicts in Iraq and Afghanistan (Cernak, 2010; Ling et al., 2009; Magnuson et al., 2012; Wang et al., 2011). After more than a decade of rigorous research, still the mechanisms of blast TBI and associated neuropathological and neurobehavioral deficits are not well understood. In addition to understanding the mechanism of injury, identification of endogenous neuroprotective mechanisms against blast TBI is vital for developing therapies and strategies for rehabilitation and recovery.

In vitro models of blast TBI provide a powerful tool to investigate the cellular, biochemical and molecular mechanisms of injury and also to identify putative biomarkers and targeted therapies. Using a compressed air-driven shock tube with neuronal cells, we have developed an *in vitro* model of blast TBI (Arun et al., 2011, 2012). Repeated blast exposures of SH-SY5Y human neuroblastoma cells decreased intracellular levels of cyclophilin A (CPA) (Arun et al., 2011). Unexpectedly, repeated blast exposures also resulted in less neuronal injury than single blast exposure suggesting a possibility that CPA released after blast exposure exerting neuroprotective actions (Arun et al., 2011). In the present study, we have further explored this putative endogenous neuroprotective mechanism against blast injury and tried to validate that extracellular CPA offers neuroprotection against blast exposure.

SH-SY5Y cells, a thrice cloned subline of the neuroblastoma cells SK-N-SH which was isolated from a human brain tumor, was used for this study. Under cell culture conditions, these cells will differentiate into mature neuronal phenotype. The cells were grown in Dulbecco's modified Eagle's medium containing B-27 serum-free supplement and penicillin/streptomycin (Life Technologies, Grand Island, NY). The cells were kept at 37 °C in a CO_2 incubator with 5% CO_2 and 95% air in a humidified atmosphere. Cells (4×10^4 cells/well) were grown on 96 well tissue culture Plates 24 h before blast exposure. On the day of blast exposure, the medium was removed from the wells and 360 μl of fresh medium was added to completely fill the wells. The plates were then sealed with gas permeable Mylar plate seal and the edges of the plates and seal were secured using sterile tapes before blast exposure as described earlier (Arun et al., 2011, 2012).

Culture plates containing the cells were exposed to single or repeated blasts using a compressed air-driven shock tube as described earlier (Arun et al., 2011, 2012). The blast overpressure (21.05 psi) which resulted in significant neurobiological changes in SH-SY5Y cells in our earlier investigations was used for the study

Abbreviations: TBI, Traumatic brain injury; CPA, cyclophilin A; BOP, blast overpressure.

☆ *Disclaimer*: The contents, opinions and assertions contained herein are private views of the authors and are not to be construed as official or reflecting the views of the Department of the Army or the Department of Defense. The authors report no conflict of interest.

* Corresponding author. Tel.: +1 301 319 2009; fax: +1 301 319 9839.
E-mail addresses: peethambaran.arun@amedd.army.mil, arunpdr@gmail.com (P. Arun).

0168-0102/$ – see front matter © 2013 Elsevier Ireland Ltd and the Japan Neuroscience Society. All rights reserved.
http://dx.doi.org/10.1016/j.neures.2013.02.009

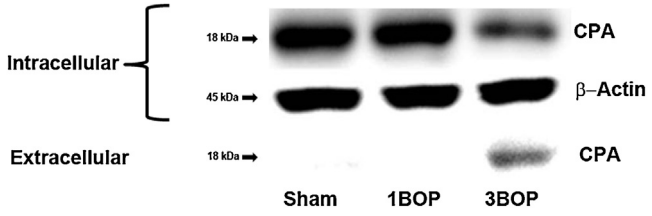

Fig. 1. Western blot analysis using CPA antibodies showing the decreased intracellular level of CPA and its accumulation in the culture medium after repeated blast exposures. 25 μg total protein was used for electrophoresis and Western blotting of the intracellular level of CPA. Volume corresponding to 360 μl culture medium was used for detecting the extracellular level of CPA. A representative figure from three different sets of experiments is shown. BOP – blast overpressure exposure.

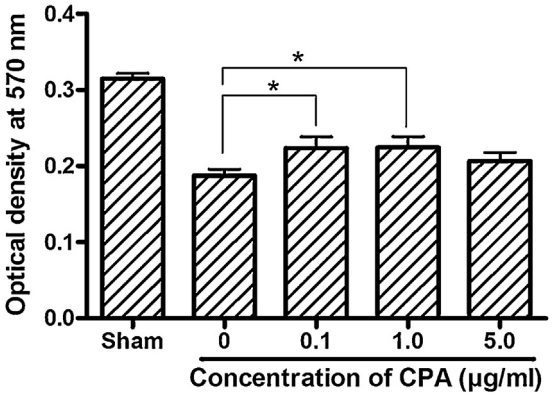

Fig. 2. MTT assay showing cellular injury after single blast exposure and protection by administration of purified recombinant CPA in the culture medium after blast exposure. Cells were exposed to single blast, treated with various doses of CPA after 15 min and MTT assay carried out at 24 h. Values of untreated cells were compared to those of CPA treated groups and expressed as mean ± standard deviation ($n = 12$). Statistical analysis was carried out using analysis of variance followed by Tukey's *post hoc* test. * $p < 0.05$.

(Arun et al., 2011, 2012). For repeated blast exposures, the cells were subjected to three blasts with 2 min intervals between each blast. For sham controls, cells were treated the same way as for blast exposure except that the plates containing the cells were not exposed to blast overpressure.

The SH-SY5Y cells and cell culture medium were collected from different wells of the plates subjected to single or repeated blasts along with sham controls at 24 h post-blast. The medium (9 ml from each group) was concentrated to 100 μl using 3000 MW cut off VIVASPIN 500 centrifugal filters (Sartorius Stedim, Bohemia, NY) according to manufacturer's instructions and 40 μl of the sample was used for polyacrylamide gel electrophoresis followed by Western blotting. The cells were suspended in M-PER mammalian protein extraction reagent (Pierce, Rockford, IL) and the total protein was extracted according to manufacturer's instructions and 25 μg total protein was used for Western blotting. Western blotting was carried out using rabbit polyclonal antibodies to CPA (1:1000 dilution) or mouse monoclonal antibodies to β-actin (1:50,000 dilution) (Sigma–Aldrich, St. Louis, MO), phosphorylated ERK1/2 or phosphorylated *Bad* (1:1000 dilution) (Cell signaling Technology, Danvers, MA).

At 15 min after single blast exposure, the medium was removed and fresh medium containing varying concentrations of purified recombinant CPA (Genway Biotech, San Diego, CA) was added and incubated for 24 h. After 24 h, the neuronal cell viability was assessed using MTT cell viability assay.

At 24 h after blast exposure, the medium was removed from each well and 100 μl fresh medium without CPA was added to conduct the cellular injury test using MTT cell proliferation assay kit (American Type Culture Collection, Manassas, VA, USA). Briefly, 10 μl of MTT reagent was added to each well and incubated in a CO_2 incubator for 2 h. One hundred micro liter detergent reagent was added to the wells and kept overnight at room temperature in dark. The optical density was measured at 570 nm using a SpectraMax M5 spectrophotometer (Molecular Devices, Sunnyvale, CA).

Western blot analysis data showed no significant changes in the level of CPA in SH-SY5Y cells at 24 h after single blast exposure. Also no detectable amount of CPA was found in the cell culture medium at 24 h after single blast exposure. On the other hand, repeated blast exposures resulted in a significant decrease in the level of CPA in SH-SY5Y cells and simultaneously CPA was detected in the culture medium (Fig. 1).

To further investigate the neuroprotective action of extracellular CPA, SH-SY5Y cells were incubated with various doses of CPA after single blast exposure and MTT cell viability assay was performed. The data showed that post-blast exposure treatment with purified recombinant CPA protein significantly protect against cellular injury in a dose-dependent manner (Fig. 2). Optimum protection against blast exposure was obtained at 0.1 μg/ml. At this dose, CPA treatment provided approximately 30% protection against blast-induced cellular injury. Higher concentrations of CPA decreased the degree of protection after blast exposure.

Using the *in vitro* blast TBI model, we have shown earlier that repeated blast exposures results in less cellular injury compared to single blast exposure and suggested the possibility of CPA release after blast exposure and the extracellular CPA playing a role in neuroprotection (Arun et al., 2011). In the present study, using the same model, we demonstrated for the first time that repeated blast exposures of human neuronal cells causes release of CPA. We also demonstrate that extracellular CPA can protect the cells from blast-induced cellular injury and the concentration of extracellular CPA seems to be critical for protection. Higher levels of extracellular CPA were less effective.

Neuroprotection induced by extracellular CPA has been demonstrated in different neuronal injury models. Administration of CPA was found to attenuate disrupted blood-brain barrier permeability and tissue damage in an *ex vivo* stab wound model of brain injury (Redell et al., 2007). The dose of CPA that showed protection in that study was in agreement with the doses used in the present study. Purified recombinant CPA administration to *in vitro* cortical neuronal cell models of ischemia and oxidative stress-induced neuronal injury showed significant neuroprotection supporting our observations (Boulos et al., 2007).

The precise mechanisms of neuroprotection triggered by extracellular CPA are still unresolved. It has been postulated that the neuroprotection induced by CPA involves its binding and signaling through CD147 receptors resulting in extracellular signal–regulated kinase (ERK1/2) activation (Boulos et al., 2007) and induction of anti-apoptotic protein Bcl2 (Seko et al., 2004). The activation of ERK1/2 by phosphorylation can stimulate anti-apoptotic proteins and inhibit pro-apoptotic proteins (Biswas and Greene, 2002; Riccio et al., 1999). In support of this notion, activation of ERK1/2 has been implicated in neuronal survival during excitotoxicity, oxidative injury and hypoxia (Adour et al., 1981; Hetman and Gozdz, 2004; Jin et al., 2002; Singer et al., 1999). To test whether phosphorylation of ERK1/2 occurs after repeated blast exposures due to the release of CPA, we tested phosphorylated ERK1/2 (p-ERK1/2) expression in SH-SY5Y cells at 1 h after repeated blast exposures. Activation of ERK1/2 can induce phosphorylation of the pro-apoptotic protein *Bad* and can inactive it (Jin et al., 2002). Our results indicate that repeated blast exposures result in the up-regulation of p-ERK1/2 and a simultaneous increase in phosphorylated *Bad* (p-*Bad*) suggesting a potential mechanism of neuroprotection (Fig. 3). Detailed studies are warranted to conclude

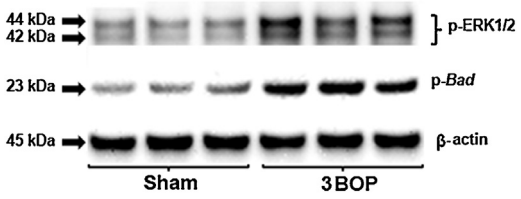

Fig. 3. Western blot analysis showing the expression of phosphorylated forms of ERK1/2 and *Bad* in SH-SY5Y cells at 1 h after repeated blast exposures.

that the extracellular CPA is solely responsible for these effects and also to demonstrate other neuroprotective effects of extracellular CPA.

Acknowledgements

Supports from Mrs. Irene Gist, Blast-induced Neurotrauma Branch and COL. Paul Bliese, Director, Center for Military Psychiatry and Neurosciences at Walter Reed Army Institute of Research are greatly acknowledged.

References

Adour, K.K., Sprague, M.A., Hilsinger Jr., R.L., 1981. Vestibular vertigo. A form of polyneuritis? JAMA 246, 1564–1567.

Arun, P., Spadaro, J., John, J., Gharavi, R.B., Bentley, T.B., Nambiar, M.P., 2011. Studies on blast traumatic brain injury using in-vitro model with shock tube. Neuroreport 22, 379–384.

Arun, P., Abu-Taleb, R., Valiyaveettil, M., Wang, Y., Long, J.B., Nambiar, M.P., 2012. Transient changes in neuronal cell membrane permeability after blast exposure. Neuroreport 23, 342–346.

Biswas, S.C., Greene, L.A., 2002. Nerve growth factor (NGF) down-regulates the Bcl-2 homology 3 (BH3) domain-only protein Bim and suppresses its proapoptotic activity by phosphorylation. J. Biol. Chem. 277, 49511–49516.

Boulos, S., Meloni, B.P., Arthur, P.G., Majda, B., Bojarski, C., Knuckey, N.W., 2007. Evidence that intracellular cyclophilin A and cyclophilin A/CD147 receptor-mediated ERK1/2 signalling can protect neurons against in vitro oxidative and ischemic injury. Neurobiol. Dis. 25, 54–64.

Cernak, I., 2010. The importance of systemic response in the pathobiology of blast-induced neurotrauma. Front. Neurol. 1, 151.

Hetman, M., Gozdz, A., 2004. Role of extracellular signal regulated kinases 1 and 2 in neuronal survival. Eur. J. Biochem. 271, 2050–2055.

Jin, K., Mao, X.O., Zhu, Y., Greenberg, D.A., 2002. MEK and ERK protect hypoxic cortical neurons via phosphorylation of Bad. J. Neurochem. 80, 119–125.

Ling, G., Bandak, F., Armonda, R., Grant, G., Ecklund, J., 2009. Explosive blast neurotrauma. J. Neurotrauma 26, 815–825.

Magnuson, J., Leonessa, F., Ling, G.S., 2012. Neuropathology of explosive blast traumatic brain injury. Curr. Neurol. Neurosci. Rep. 12, 570–579.

Redell, J.B., Zhao, J., Dash, P.K., 2007. Acutely increased cyclophilin a expression after brain injury: a role in blood-brain barrier function and tissue preservation. J. Neurosci. Res. 85, 1980–1988.

Riccio, A., Ahn, S., Davenport, C.M., Blendy, J.A., Ginty, D.D., 1999. Mediation by a CREB family transcription factor of NGF-dependent survival of sympathetic neurons. Science 286, 2358–2361.

Seko, Y., Fujimura, T., Taka, H., Mineki, R., Murayama, K., Nagai, R., 2004. Hypoxia followed by reoxygenation induces secretion of cyclophilin A from cultured rat cardiac myocytes. Biochem. Biophys. Res. Commun. 317, 162–168.

Singer, C.A., Figueroa-Masot, X.A., Batchelor, R.H., Dorsa, D.M., 1999. The mitogen-activated protein kinase pathway mediates estrogen neuroprotection after glutamate toxicity in primary cortical neurons. J. Neurosci. 19, 2455–2463.

Wang, Y., Wei, Y., Oguntayo, S., Wilkins, W., Arun, P., Valiyaveettil, M., Song, J., Long, J., Nambiar, M.P., 2011. Tightly Coupled repetitive blast-induced traumatic brain injury: development and characterization in mice. J. Neurotrauma 28, 2171–2183.

Farid A. Ahmed[1,2]
Alaa Kamnaksh[1,2]
Erzsebet Kovesdi[3]
Joseph B. Long[4]
Denes V. Agoston[1,2]

[1]Department of Anatomy, Physiology and Genetics, Uniformed Services University, Bethesda, MD, USA
[2]Center for Neuroscience and Regenerative Medicine, Uniformed Services University, Bethesda, MD, USA
[3]U.S. Department of Veterans Affairs, Veterans Affairs Central Office, Washington, DC, USA
[4]Blast-Induced Neurotrauma Branch, Center for Military Psychiatry and Neuroscience, Walter Reed Army Institute of Research, Silver Spring, MD, USA

Received February 6, 2013
Revised March 15, 2013
Accepted April 3, 2013

Short Communication

Long-term consequences of single and multiple mild blast exposure on select physiological parameters and blood-based biomarkers

Mild traumatic brain injury (mTBI), especially when it is repeated (rmTBI), can lead to progressive degenerative diseases and lasting neuropsychiatric abnormalities. To better understand the long-term pathobiological changes in mTBI and rmTBI, we exposed rats to single or repeated (5 total; administered on consecutive days) mild blast overpressure, monitored changes in physiological parameters, and determined the plasma levels of select biomarkers at 42 days post injury by proteomics. We unexpectedly found comparable changes in arterial oxygen saturation levels and heart rates of single-injured (SI) and multiple-injured (MI) rats throughout the observation period. Our analyses indicated lasting oxidative stress, vascular abnormalities, and neuronal and glial cell loss in both injured groups. However, MI rats exhibited a relatively more pronounced increase in the plasma levels of most of the tested markers—particularly those associated with inflammation—albeit the differences between the two injured groups were not statistically significant. Our findings indicate that the frequency of blast exposures is an important determinant of the resulting cumulative damage in rmTBI.

Keywords:
Animal models / Brain trauma / Experimental / Physiology / Proteomics
DOI 10.1002/elps.201300077

Mild traumatic brain injury (mTBI) accounts for the majority of civilian and military traumatic brain injury (TBI) cases [1, 2]. In both civilian and military environments, affected individuals (e.g. football players) often sustain additional mild injuries. mTBI symptoms are typically mild and transient, however, repeated mild TBIs (rmTBI) can result in disproportionately severe acute symptoms suggesting some sort of cumulative effect of repeated injuries [3]. rmTBIs also increase the risk of developing late onset, progressive degenerative conditions such as chronic traumatic encephalopathy [4]. Despite their high prevalence, the pathobiology and consequently the diagnosis and treatment of mTBI and rmTBI have not been adequately addressed.

In a previous study assessing some of the neurobehavioral, cellular, and molecular consequences of single and multiple mild blast exposure at an early (~2 h) and a later post injury time point (22 days), we unexpectedly found a mild cumulative effect following repeated injury [5]. Based on these findings, we hypothesized that the cumulative effect in rmTBI requires a longer post injury time period to manifest. To test this hypothesis, we extended our experimental timeline to 42 days post injury and utilized noninvasive, clinically relevant tools to follow long-term changes in basic physiological parameters and blood-based biomarkers.

A total of 30 Sprague Dawley male rats, weighing 245–265 g at arrival (Charles River Laboratories, Wilmington, MA, USA), were used in our study. Housing, handling, and experimental manipulations of animals have been described earlier [5]. After an acclimation and handling period of five days, animals were randomly assigned to the following groups: naïve ($N = 3$), single sham (SS; $N = 6$), single-injured (SI; $N = 7$), multiple sham (MS; $N = 6$), and multiple-injured (MI; $N = 8$). Naïve rats were kept in the Uniformed Services University (USU) animal facility for the duration of the study without any manipulation. SS rats were transported once from USU to Walter Reed Army Institute of Research (Silver Spring, MD, USA) and anesthetized in an induction chamber for

Correspondence: Dr. Denes V. Agoston, Department of Anatomy, Physiology and Genetics, School of Medicine, Uniformed Services University, 4301 Jones Bridge Road, Bethesda, MD 20814, USA
E-mail: vagoston@usuhs.edu
Fax: +1-301-295-1786

Abbreviations: CCR5, chemokine (C-C motif) receptor 5; **FPR1**, formyl peptide receptor 1; **GFAP**, glial fibrillary acidic protein; **HIF-1α**, hypoxia-inducible factor-1α; **HNE**, 4-hydroxynonenal; **MBP**, myelin basic protein; **MI**, multiple-injured; **MMP8**, matrix metalloproteinase 8; **MS**, multiple sham; **mTBI**, mild TBI; **NF-H**, neurofilament-heavy chain; **p38**, p38 mitogen-activated protein kinase; **rmTBI**, repeated mild TBI; **SI**, single-injured; **SS**, single sham; **TBI**, traumatic brain injury; **TLR9**, Toll-like receptor 9; **USU**, Uniformed Services University; **VEGF**, vascular endothelial growth factor; **vWF**, von Willebrand factor

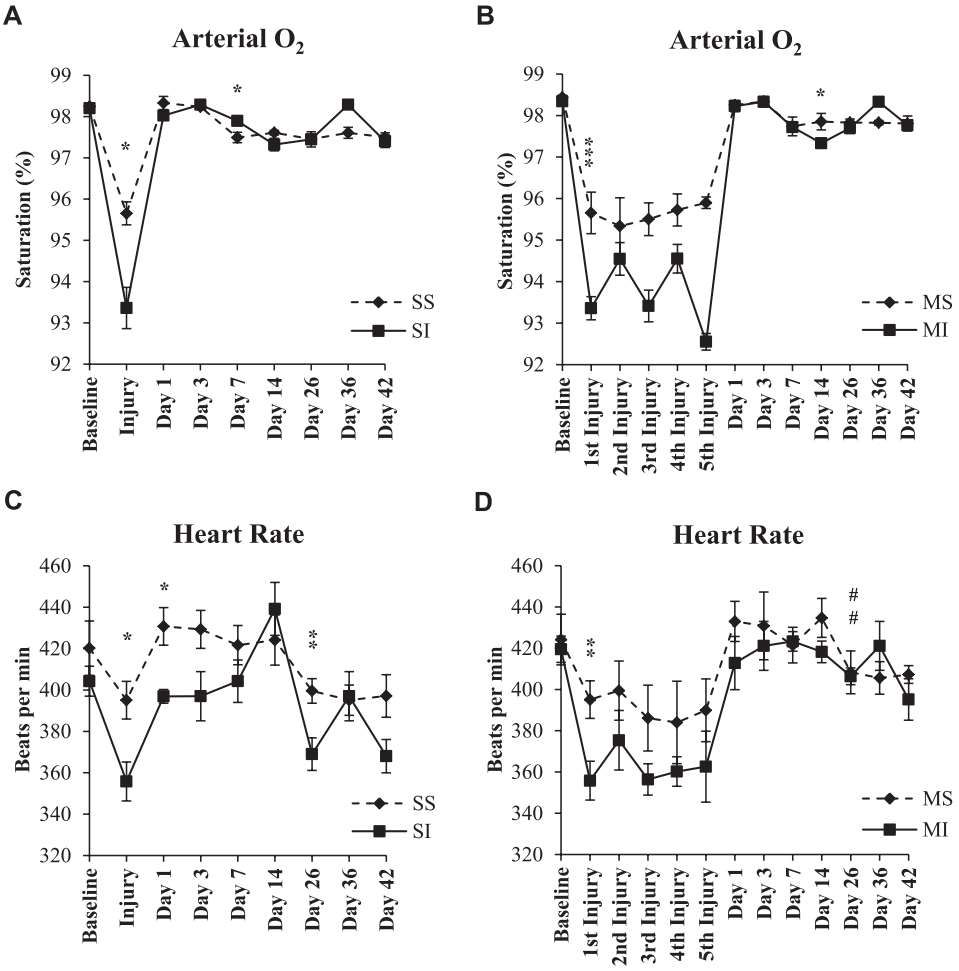

Figure 1. Arterial oxygen saturation levels (%) (A and B) and heart rates (beats per min) (C and D) of SS, SI, MS and MI rats. Measurements were obtained under isoflurane anesthesia at baseline, immediately following injury (5× for MI rats), and at days 1, 3, 7, 14, 26, 36, and 42 post injury. Data are presented as the mean ± SEM (*$p < 0.05$, **$p < 0.01$, and ***$p < 0.001$ sham versus injured; ##$p < 0.01$ SI versus MI).

6 min with 4% isoflurane (Forane; Baxter Healthcare Corporation, Deerfield, IL, USA). MS rats were similarly transported and anesthetized once per day for 5 consecutive days. SI and MI rats, weighing 300–330 g on injury day, underwent the same pre-injury procedures as their respective sham groups. SI and MI rats were then transferred to a compressed air-driven shock tube and exposed to a single or repeated (5 total administered on consecutive days) mild blast overpressure (average peak total pressure: ∼138 kPa) as described in detail [6, 7]. Mortality was: SI = 3 and MI = 4. Following the exposure(s), animals were transported back to the USU animal facility.

Arterial blood oxygen saturation (%), heart rate (beats per min), pulse distention (μm), and breath rate (breaths per min) were noninvasively monitored under light isoflurane anesthesia prior to injury (baseline), immediately after blast (or sham) exposure, and at days 1, 3, 7, 14, 26, 36, and 42 post injury using the MouseOx® Pulse Oximeter adopted for rats (Starr Life Sciences, Oakmont, PA, USA) [8]. At the termination of the experiment (day 42 post injury), rats (Naïve = 3, SS = 6, SI = 4, MS = 6, MI = 4) were deeply anesthetized in a bell jar with isoflurane inhalant until a tail or toe pinch produced no reflex movement. Blood was obtained by cardiac puncture, and samples were promptly centrifuged at 10 000 rpm for 15 min at 4°C; the supernatants (plasma) were then transferred into tubes, flash-frozen, and stored at −80°C until processing for reverse phase protein microarray [5].

Sample preparation, printing, scanning, and data analysis for reverse phase protein microarray were performed as described earlier in detail [9]. Primary antibodies were diluted to 10× the optimal Western analysis concentration in antibody incubation buffer and used in the following dilutions: 4-hydroxynonenal (HNE; 1:100) (Calbiochem, 393207), hypoxia-inducible factor-1α (HIF-1α; 1:20) (Santa Cruz, sc-53546), ceruloplasmin (1:20) (GeneTex, GTX28813), vascular endothelial growth factor (VEGF; 1:50) (Abcam, ab53465), von Willebrand factor (vWF; 1:20) (Santa Cruz, sc-8068), neurofilament-heavy chain (NF-H; 1:20) (Sigma–Aldrich, N4142), glial fibrillary acidic protein (GFAP; 1:500) (Abcam, ab7260), myelin basic protein (MBP; 1:20) (Santa Cruz, sc-13914), matrix metalloproteinase 8 (MMP8; 1:20) (Santa Cruz, sc-50384), formyl peptide receptor 1 (FPR1; 1:20) (Santa Cruz, sc-13198), p38 mitogen-activated protein kinase (p38; 1:20) (Cell Signaling Technology, 9212), chemokine (C-C motif) receptor 5 (CCR5; 1:20) (GeneTex, GTX61751), and toll-like receptor 9 (TLR9; 1:100) (Santa Cruz, sc-13218).

Table 1. Oxidative stress and vascular biomarker levels in the plasma at 42 days post injury

Marker	Group	Mean ± SEM	ANOVA		Comparison of means		
			F-value	*p*-value	2–3 (*p*)	4–5 (*p*)	3–5 (*p*)
4-Hydroxynonenal (HNE)	Naïve (1)	4.95 ± 0.17	7.89	0.000	− 0.39	− 0.48	− 0.03
	SS (2)	4.97 ± 0.04			**0.016**	**0.001**	0.999
	SI (3)	**5.37 ± 0.12**					
	MS (4)	4.91 ± 0.07					
	MI (5)	**5.40 ± 0.05**					
Hypoxia-inducible factor-1α (HIF-1α)	Naïve (1)	4.10 ± 0.59	4.53	0.005	− 0.56	− 1.09	− 0.91
	SS (2)	4.11 ± 0.17			0.474	**0.023**	0.137
	SI (3)	4.67 ± 0.18					
	MS (4)	4.48 ± 0.18					
	MI (5)	**5.58 ± 0.41**					
Ceruloplasmin	Naïve (1)	6.29 ± 0.08	10.87	0.000	− 0.41	− 0.51	− 0.06
	SS (2)	6.23 ± 0.05			**0.003**	**0.000**	0.980
	SI (3)	**6.64 ± 0.08**					
	MS (4)	6.20 ± 0.05					
	MI (5)	**6.71 ± 0.12**					
Vascular endothelial growth factor (VEGF)	Naïve (1)	4.29 ± 0.05	6.27	0.001	− 0.32	− 0.59	− 0.21
	SS (2)	4.36 ± 0.07			0.209	**0.001**	0.663
	SI (3)	4.68 ± 0.04					
	MS (4)	4.30 ± 0.06					
	MI (5)	**4.89 ± 0.19**					
von Willebrand Factor (vWF)	Naïve (1)	4.80 ± 0.09	22.74	0.000	− 0.60	− 0.63	− 0.07
	SS (2)	4.74 ± 0.04			**0.000**	**0.000**	0.951
	SI (3)	**5.34 ± 0.06**					
	MS (4)	4.78 ± 0.04					
	MI (5)	**5.41 ± 0.13**					

Mean protein values of naïve, SS, SI, MS and MI rats are log10. Tabulated results include the comparisons for blast injury, SS versus SI (2–3) and MS versus MI (4–5), and for the number of blast events, SI versus MI (3–5). Significant differences in biomarker levels are indicated in boldface.

Slides were incubated with the primary antibody solutions overnight at 4°C, then washed and incubated with the secondary antibodies Alexa Fluor® 633 donkey antisheep (A-21100), Alexa Fluor® 635 goat antimouse (A-31574), Alexa Fluor® 647 goat antirabbit (A-21245), or rabbit antigoat Immunoglobulin G (A-21446) (Molecular Probes®, Invitrogen) at 1:6000 dilution in antibody incubation buffer for 1 h at room temperature. Spot intensity data were imported into a Microsoft Excel-based bioinformatics program for analysis. The total amount of antigen is determined by the *Y*-axis intercept, that is by extrapolating the regression line to zero; reported protein values are log10 [9].

A total of 23 animals (Naïve = 3, SS = 6, SI = 4, MS = 6, MI = 4) were used for the statistical analyses. Student's *t*-test followed by a one-way ANOVA was used to analyze differences in the measured physiological parameters between injured groups and their respective sham groups at baseline, immediately after injury (5 consecutive days for MI rats), and days 1, 3, 7, 14, 26, 36, and 42 post injury. The SI and MI groups were compared on injury day (first injury for MI rats to correspond with SI rats) and each subsequent post injury time point. Statistical significance was reported for blast injury (SS versus SI and MS versys MI*) and for the number of blast events (SI versus MI#). A p value of < 0.05 is depicted by one special character, $p < 0.01$ by two, and $p < 0.001$ by three. Differences in the mean protein biomarker levels measured in plasma were analyzed with ANOVA followed by Tukey's HSD Test. All statistical analyses were performed using IBM SPSS Statistics 20 software. Tests were two tailed using $\alpha = 0.05$; data are presented as the mean ± SEM.

Consistent with our previous findings, the exposure to experimental manipulations alone (i.e. handling, transportation, and anesthesia) can elicit physiological changes as seen in sham animals on the injury day(s) (Fig. 1A–D) [6]. For logistical reasons we were not able to measure the immediate pre and post injury values of the selected physiological parameters, thus the extent and temporal pattern of acute changes remain unknown. However, the restoration of O_2 saturation levels to pre-injury values within a day after a single blast exposure (Fig. 1A) suggests that MI rats similarly recover after each daily exposure (Fig. 1B).

Of the four physiological parameters, only arterial O_2 saturation levels and heart rate changed significantly in response to either type of injury; the detected changes were transient over the length of the experiment (Fig. 1A–D). No significant injury-induced changes (i.e. sham versus injured) were measured in pulse distension and breath rate at any of the time points (data not shown). Importantly, we did not

Table 2. Neuronal, glial, and inflammatory biomarker levels in the plasma at 42 days post injury

Marker	Group	Mean ± SEM	ANOVA		Comparison of means		
			F-value	*p*-value	2–3 (*p*)	4–5 (*p*)	3–5 (*p*)
Neurofilament-heavy chain (NF-H)	Naïve (1)	5.94 ± 0.06	6.29	0.001	−0.37	−0.24	0.06
	SS (2)	5.83 ± 0.05			**0.002**	**0.049**	0.975
	SI (3)	**6.21 ± 0.13**					
	MS (4)	5.90 ± 0.03					
	MI (5)	**6.15 ± 0.04**					
Glial fibrillary acidic protein (GFAP)	Naïve (1)	2.55 ± 0.23	8.87	0.000	−0.98	−1.25	−0.09
	SS (2)	2.94 ± 0.16			**0.038**	**0.000**	0.999
	SI (3)	**3.92 ± 0.39**					
	MS (4)	2.75 ± 0.14					
	MI (5)	**4.01 ± 0.21**					
Myelin basic protein (MBP)	Naïve (1)	4.59 ± 0.14	6.45	0.001	−0.63	−0.7	−0.12
	SS (2)	4.64 ± 0.06			**0.013**	**0.012**	0.984
	SI (3)	**5.28 ± 0.24**					
	MS (4)	4.70 ± 0.07					
	MI (5)	**5.40 ± 0.15**					
Matrix metalloproteinase 8 (MMP8)	Naïve (1)	5.27 ± 0.10	3.24	0.022	−0.12	−0.27	−0.12
	SS (2)	5.25 ± 0.07			0.659	**0.016**	0.720
	SI (3)	5.37 ± 0.04					
	MS (4)	5.21 ± 0.04					
	MI (5)	**5.49 ± 0.07**					
Formyl peptide receptor 1 (FPR1)	Naïve (1)	4.96 ± 0.07	4.02	0.009	−0.33	−0.44	−0.06
	SS (2)	5.00 ± 0.06			0.175	**0.034**	0.996
	SI (3)	5.34 ± 0.04					
	MS (4)	4.95 ± 0.05					
	MI (5)	**5.39 ± 0.09**					
P38 mitogen-activated protein kinase (p38)	Naïve (1)	3.10 ± 0.22	5.26	0.002	−0.56	−0.73	−0.02
	SS (2)	2.97 ± 0.05			0.091	**0.008**	0.999
	SI (3)	3.52 ± 0.15					
	MS (4)	2.80 ± 0.13					
	MI (5)	**3.53 ± 0.12**					
Chemokine (C-C motif) receptor 5 (CCR5)	Naïve (1)	2.56 ± 0.12	5.08	0.003	−0.85	−0.48	0.41
	SS (2)	3.05 ± 0.10			**0.041**	0.33	0.697
	SI (3)	**3.90 ± 0.11**					
	MS (4)	3.01 ± 0.12					
	MI (5)	3.50 ± 0.07					
Toll-like receptor 9 (TLR9)	Naïve (1)	4.00 ± 0.06	0.82	0.523	−0.29	0.53	−0.08
	SS (2)	4.01 ± 0.39			0.987	0.876	0.999
	SI (3)	4.30 ± 0.17					
	MS (4)	3.95 ± 0.74					
	MI (5)	4.38 ± 0.48					

Mean protein values of naïve, SS, SI, MS and MI rats are log10. Tabulated results include the comparisons for blast injury, SS versus SI (2–3) and MS versus MI (4–5), and for the number of blast events, SI versus MI (3–5). Significant differences in biomarker levels are indicated in boldface.

detect any lasting changes between SI and MI animals in any of the measured vitals.

Forty-two days post injury, it appears that repeated exposure to mild blast overpressure resulted in hypoxia and oxidative stress as reflected in significantly increased plasma levels of oxidative stress markers HNE, HIF-1α, and ceruloplasmin (Table 1). At this late time point, HNE and ceruloplasmin levels were also increased in SI animals albeit to a lesser degree than in MI animals. These changes indicate a potential role for hypoxia and oxidative stress in the pathobiology of blast-induced TBI [10]. An increase in HNE levels during periods of oxidative stress is due to an increase in the lipid peroxidation chain reaction that affects a variety of biological pathways, including the cell cycle and cellular adhesion. Elevated ceruloplasmin levels are another indication of oxidative stress triggered by hypoxia [11]. As well demonstrated in stroke models, hypoxia can cause lasting increases in HIF-1α levels [12]. HIF-1α plays a crucial role in the adaptive and restorative response of organisms following neuronal insults (e.g. stroke and TBI) as it coordinates the expression of numerous genes to cope with noxious conditions thus mitigating the effects of ischemic conditions.

TBI also adversely affects several vascular functions including blood brain barrier permeability [13]. VEGF along with vWF is a key regulator of vascular permeability and other endothelial functions [14, 15]. The more robust increase in VEGF levels in MI rats suggests that VEGF may be involved in mediating the cumulative, more severe outcomes of rmTBI (Table 1). While VEGF levels were only significantly elevated at 42 days post injury in MI rats, vWF plasma levels remained significantly elevated in response to both types of injury. These findings implicate long-term alterations in endothelial functions after TBI including increased blood brain barrier permeability, which enables large molecules such as neuron- and glia-specific proteins to cross into the systemic circulation.

Consistent with our previous findings, even a single mild blast exposure significantly increased NF-H, GFAP, and MBP levels in the plasma (Table 2). Unlike the neuronal marker NF-H, GFAP, and MBP concentrations were relatively higher in MI animals than in SI animals as observed in the majority of the tested protein markers. Increased NF-H and MBP concentrations reflect damage to axons and their myelin sheaths as a result of the physical forces of the blast. Damage to axons and white matter tracts have been identified both clinically and experimentally as hallmarks of blast TBI along with damage to astroglia reflected in increased GFAP levels [16, 17].

Of the markers associated with various aspects of inflammation, MMP8, FPR1, and p38 were only elevated in MI animals suggesting greater damage accumulation and/or a more severe outcome in rmTBI. Given the role of these markers in the mediation of the neuroinflammatory process in several central nervous system disorders [18], it is not surprising that rmTBIs increase the risk for debilitating conditions like chronic traumatic encephalopathy. At this late time point, CCR5 levels were significantly elevated in SI animals alone while TLR9 was relatively unchanged in both injured groups. A potential explanation for the insignificant CCR5 response in MI rats is the late sampling time after injury. This can also account for the insignificant TLR9 levels in both injured groups due to the protein's rapid elevation and decline after injury.

In conclusion, the exposure to single and repeated mild blast at this frequency of insults triggers lasting changes in the form of oxidative stress, vascular abnormalities, and neuronal and glial cell damage/death. The chronic nature of these changes is particularly important considering that a rat week is the equivalent of 6–8 human months. However, we found no increase in the magnitude of the cumulative effect at this late time point suggesting that the frequency of the repetitive insults plays a critical role in determining the extent of the damage accumulation in rmTBI.

We thank the Neurotrauma Team at the Walter Reed Army Institute of Research for their technical help during the exposures. This work was supported by the Center for Neuroscience and Regenerative Medicine grant number G1703F. The views, opinions, and/or findings contained herein are those of the authors and should not be construed as an official position, policy, or decision of the Department of the Army or the Department of Defense. The authors have no financial disclosures. Animal handling and treatments were conducted in compliance with the Animal Welfare Act and other Federal statutes and regulations related to animals and experiments involving animals, and adhered to principles stated in the Guide to the Care and Use of Laboratory Animals, National Research Council. The facilities are fully accredited by the Association for Assessment and Accreditation of Laboratory Animal Care International.

The authors have declared no conflict of interest.

References

[1] Elder, G. A., Mitsis, E. M., Ahlers, S. T., Cristian, A., *Psychiatr. Clin. North Am.* 2010, *33*, 757–781.

[2] Laker, S. R., *PM R* 2011, *3*, S354–358.

[3] Hayes, J. P., Morey, R. A., Tupler, L. A., *Neurocase* 2012, *18*, 258–269.

[4] Stern, R. A., Riley, D. O., Daneshvar, D. H., Nowinski, C. J., Cantu, R. C., McKee, A. C., *PM R* 2011, *3*, S460–467.

[5] Kamnaksh, A., Kwon, S. K., Kovesdi, E., Ahmed, F., Barry, E. S., Grunberg, N. E., Long, J., Agoston, D., *Electrophoresis* 2012, *24*, 3680–3690.

[6] Kamnaksh, A., Kovesdi, E., Kwon, S. K., Wingo, D., Ahmed, F., Grunberg, N. E., Long, J., Agoston, D. V., *J. Neurotrauma* 2011, *28*, 2145–2153.

[7] Long, J. B., Bentley, T. L., Wessner, K. A., Cerone, C., Sweeney, S., Bauman, R. A., *J. Neurotrauma* 2009, *26*, 827–840.

[8] Cernak, I., Merkle, A. C., Koliatsos, V. E., Bilik, J. M., Luong, Q. T., Mahota, T. M., Xu, L., Slack, N., Windle, D., Ahmed, F. A., *Neurobiol. Dis.* 2011, *41*, 538–551.

[9] Gyorgy, A. B., Walker, J., Wingo, D., Eidelman, O., Pollard, H. B., Molnar, A., Agoston, D. V., *J. Neurosci. Methods* 2010, *192*, 96–101.

[10] Readnower, R. D., Chavko, M., Adeeb, S., Conroy, M. D., Pauly, J. R., McCarron, R. M., Sullivan, P. G., *J. Neurosci. Res.* 2010, *88*, 3530–3539.

[11] Dash, P. K., Redell, J. B., Hergenroeder, G., Zhao, J., Clifton, G. L., Moore, A., *J. Neurosci. Res.* 2010, *88*, 1719–1726.

[12] Yeh, S. H., Ou, L. C., Gean, P. W., Hung, J. J., Chang, W. C., *Brain Pathol.* 2011, *21*, 249–262.

[13] Schoknecht, K., Shalev, H., *Epilepsia* 2012, *53*(Suppl 6), 7–13.

[14] De Oliveira, C. O., Reimer, A. G., Da Rocha, A. B., Grivicich, I., Schneider, R. F., Roisenberg, I., Regner, A., Simon, D., *J. Neurotrauma* 2007, *24*, 1331–1338.

[15] Ferrara, N., *Curr. Opin. Biotechnol.* 2000, *11*, 617–624.

[16] Agoston, D. V., Elsayed, M., *Front Neurol.* 2012, *3*, 107.

[17] Matthews, S. C., Strigo, I. A., Simmons, A. N., O'Connell, R. M., Reinhardt, L. E., Moseley, S. A., *Neuroimage* 2011, *54(Suppl 1)*, S69–75.

[18] Barone, F. C., Parsons, A. A., *Expert Opin. Investig. Drugs* 2000, *9*, 2281–2306.

